

# Structural and functional characterization of the mycobacterial ESX-1 secretion system

THÈSE N° 7093 (2016)

PRÉSENTÉE LE 31 AOÛT 2016

À LA FACULTÉ DES SCIENCES DE LA VIE

UNITÉ DU PROF. COLE

PROGRAMME DOCTORAL EN APPROCHES MOLÉCULAIRES DU VIVANT

ÉCOLE POLYTECHNIQUE FÉDÉRALE DE LAUSANNE

POUR L'OBTENTION DU GRADE DE DOCTEUR ÈS SCIENCES

PAR

Ye LOU

acceptée sur proposition du jury:

Prof. N. Harris, présidente du jury

Prof. S. Cole, directeur de thèse

Prof. R. Brosch, rapporteur

Prof. M. Basler, rapporteur

Prof. A. Ablasser, rapporteuse



ÉCOLE POLYTECHNIQUE  
FÉDÉRALE DE LAUSANNE

Suisse  
2016



## Table of Contents

<b>Abstract .....</b>	<b>I</b>
<b>Résumé .....</b>	<b>III</b>
<b>List of abbreviations .....</b>	<b>V</b>
<b>Chapter 1 General introduction .....</b>	<b>1</b>
<b>1.1 Tuberculosis .....</b>	<b>1</b>
<b>1.2 Prevention, diagnosis, and treatment of TB.....</b>	<b>2</b>
<b>1.3 Mycobacteria .....</b>	<b>7</b>
1.3.1 <i>Mycobacterium tuberculosis</i> ( <i>M. tb</i> ) .....	7
1.3.2 Other pathogenic mycobacterial species .....	10
1.3.3 Non-pathogenic mycobacteria .....	11
<b>1.4 Bacterial secretion systems .....</b>	<b>12</b>
<b>1.5 Type VII / ESX secretion systems in mycobacteria .....</b>	<b>15</b>
<b>1.6 ESX-1 secretion system .....</b>	<b>17</b>
1.6.1 <i>esx-1</i> locus and RD1 .....	17
1.6.2 <i>espACD</i> operon .....	21
1.6.3 Current model of ESX-1 secretion system .....	23
<b>1.7 Research scope and objective .....</b>	<b>25</b>
<b>References .....</b>	<b>28</b>
<b>Chapter 2 EspC forms a filamentous structure in the cell envelope of Mycobacterium tuberculosis and effects ESX-1 secretion .....</b>	<b>38</b>
<b>2.1 Abstract .....</b>	<b>38</b>
<b>2.2 Introduction .....</b>	<b>39</b>
<b>2.3 Results.....</b>	<b>40</b>
Purification, oligomerization and filament formation of recombinant EspC.....	40
EspC is not membranolytic .....	40
EspC polymerizes upon secretion from <i>M. tb</i> .....	41
EspC interacts with EspA in the cytosol and cell envelope .....	42
YxxxD motif impacts EspC secretion and ESX-1 function .....	43
The C-terminal domain is critical for polymer formation and stability.....	43
EspC spans the capsule and is surface-exposed.....	44
<b>2.4 Discussion.....</b>	<b>46</b>
<b>2.5 Materials and Methods.....</b>	<b>49</b>

2.6 Figures and Tables.....	55
References .....	70
Supplementary.....	73
Full-length EspC is a highly immunodominant antigen .....	73
Plasmids, primers and bacterial strains .....	75
<b>Chapter 3 Characterization of EccCb1 as an ATPase .....</b>	<b>77</b>
3.1 Abstract .....	77
3.2 Introduction .....	78
3.3 Results.....	80
Overexpression of EccCa1 and EccCb1 in <i>E.coli</i> .....	80
Purification of EccCb1 .....	80
Recombinant EccCb1 is hexameric.....	81
EccCb1 is an essential energizing component of ESX-1 secretion system .....	82
3.4 Discussion.....	83
3.5 Materials and Methods.....	84
3.6 Figures and Tables.....	86
References .....	93
<b>Chapter 4 Calcium deprivation promotes ESX-1 secretion and persistence of <i>M. tb</i></b> .....	<b>95</b>
4.1 Introduction .....	95
4.2 Results.....	96
Calcium stress blocks ESX-1 secretion .....	96
Effect of calcium stress on <i>M. tb</i> growth.....	96
Calcium stress repressed DevR regulon.....	97
4.3 Discussion.....	98
4.4 Materials and Methods.....	99
4.5 Figures and Tables.....	102
References .....	106
<b>Chapter 5 Discussion and Perspective.....</b>	<b>110</b>
<b>Appendix.....</b>	<b>117</b>
<b>Acknowledgement.....</b>	<b>130</b>
<b>CV.....</b>	<b>132</b>



## Abstract

Human tuberculosis (TB) is a frequently fatal lung disease mostly caused by *Mycobacterium tuberculosis* (*M. tb*), a slow-growing intracellular pathogen. *M. tb* utilizes the ESX-1 secretion system, classified as type VII, to export the virulence factors needed for host infection and pathogenesis. A functional ESX-1 pathway largely involves the proteins encoded by two gene clusters, *esx-1* and *espACD*. These proteins are diverse in functions, such as cytolysis, immunogenicity, pore forming, stabilization and energization. Although many of the ESX-1 associated proteins were characterized individually, the overall mechanism of ESX-1 secretion is still far from clear.

The main objective of my thesis is to better understand the structure and function of the ESX-1 secretion system in *M. tb*. To achieve this, an integrated approach which combines biochemistry, biophysics and genetics was applied. The experimental results are organized into three parts, in which I investigated EspC, EccCb1 and the effect of calcium on ESX-1 secretion.

Firstly, the focus of this thesis is EspC, a secreted protein encoded in the *espACD* operon which is not linked to the *esx-1* locus, but mediates ESX-1-associated virulence. Based on what I observed from a series of experiments, we propose a novel working model of the ESX-1 apparatus, in which EspC interacts with EspA in the cytosol and then translocates across the membrane to assemble into a channel in the outer membrane and spans the capsular layer of *M. tb*. This model could explain the mechanism by which the major virulence factors EsxA and EsxB (also named ESAT-6 and CFP-10) rely on EspC for secretion. Moreover, EspC is a potential outer membrane pore protein which has not been previously identified in *M. tb*.

Secondly, the putative ATPase EccCb1 is another protein that was studied. EccCb1 is predicted as an ATPase that targets the EsxA/EsxB heterodimer during

translocation. EccCb1 was overexpressed and purified in the form of a NusA-EccCb1 fusion protein due to its low stability. The protein was characterized as a hexamer with an ATPase activity. This result confirms that EccCb1 belongs to the FtsK/SpoIIIE ATPase family.

Thirdly, we observed that ESX-1 secretion can be inhibited by a high concentration of calcium (~500  $\mu$ M) in the culture medium. Moreover, bacterial persistence, rather than growth rate, decreased with the elevated calcium. RNA-seq was performed to evaluate the changes of global gene expression of *M. tb* in the presence of high calcium levels. Surprisingly, calcium dramatically repressed hypoxia response genes in the DevRS regulon, leading to reduced persistence.

I also include a section that describes the additional work I was involved with, in which we investigated the activation of cGAS-dependent host response by ESX-1.

Taken together, these findings provide new insights into the structural and functional aspects of ESX-1 secretion system, and will contribute to discovery of ESX-1 inhibitors with potential applications in TB therapy.

**Key words:** Tuberculosis, *Mycobacterium tuberculosis*, ESX-1 secretion system, type VII secretion system, EspC, EccCb1

## Résumé

La tuberculose humaine (TB) est une des maladies infectieuses les plus meurtrières au monde. Touchant principalement les poumons, elle est majoritairement causée par *Mycobacterium tuberculosis* (*M. tb*), une mycobactérie intracellulaire à croissance très lente. *M. tb* utilise le système de sécrétion ESX-1, un des cinq systèmes de sécrétion de type VII, pour le transport des facteurs de virulence nécessaires à la pathogénicité et l'invasion de l'hôte. Le système ESX-1 implique les protéines sécrétées par deux groupes de gènes, *esx-1* et *espACD*. Ces protéines ont diverses fonctions incluant la cytolysse, l'immunogénicité, la formation de pores, la stabilisation et l'apport d'énergie. Bien que plusieurs de ces protéines aient été caractérisées individuellement, le mécanisme général du système de sécrétion ESX-1 n'est pas complètement élucidé.

L'objectif principal de ma thèse est d'étudier la structure et la fonction du système de sécrétion ESX-1 chez *M. tb* en utilisant une approche intégrée combinant la biochimie, la biophysique et la génétique. Les résultats obtenus sont organisés en trois parties, dans lesquelles j'ai étudié EspC, EccCb1 et l'effet du calcium sur la sécrétion d'ESX-1.

Tout d'abord, le sujet principal de cette thèse est EspC, une protéine sécrétée codée par l'opéron *espACD*, non associé au locus *esx-1*, mais qui régule la virulence d'ESX-1. D'après les résultats obtenus, nous proposons ici un nouveau modèle du système ESX-1, dans lequel ESX-1 interagit avec EspA dans le cytosol pour ensuite être transloquée jusqu'à la membrane externe où ils forment un canal traversant ainsi la capsule de *M. tb*. Ce modèle pourrait expliquer le mécanisme par lequel les facteurs majeurs de virulence tels que EsxA et EsxB (aussi connus sous les noms de ESAT-6 et CFP-10) dépendent de EspC pour la sécrétion. De plus, nous montrons ici que EspC peut former un pore dans la membrane externe, ceci n'ayant jamais été observé précédemment chez *M. tb*.

Dans un second temps, je me suis concentrée sur la protéine EccCb1. Cette protéine est décrite comme une probable ATPase qui cible l'hétérodimère EsxA/EsxB pendant la translocation. Afin de confirmer sa fonction, EccCb1 a été surexprimée et purifiée sous la forme d'une protéine de fusion NusA-EccCb1 en raison de sa faible stabilité. La protéine a ensuite pu être caractérisée comme un hexamère ayant une activité ATPase. Ces résultats confirment que EccCb1 appartient à la famille FtsK/SpoIIIE des ATPases.

Puis, dans la troisième partie, nous avons observé que le système de sécrétion ESX-1 pouvait être inhibé en présence d'une concentration importante de calcium ( $\sim 500 \mu\text{M}$ ) dans le milieu de culture. De plus, la persistance bactérienne, et non le taux de croissance, est diminuée pour une concentration élevée de calcium. Nous avons alors comparé les modifications de l'expression génique chez *M. tb* en présence de hautes concentrations de calcium en utilisant la technologie de séquençage de l'ARN. Étonnamment, nous avons observé que le calcium inhibe considérablement les gènes du régulon DevRS, impliqués dans la réponse à l'hypoxie et conduisant à la réduction de la persistance.

Enfin, j'inclus une quatrième section qui décrit le travail supplémentaire dans lequel nous avons étudié l'activation de la réponse de l'hôte dépendant du signal cGAS par ESX-1.

Pris ensemble, ces résultats améliorent notre compréhension sur les aspects structuraux et fonctionnels du système de sécrétion ESX-1, et ont permis la découverte d'inhibiteurs d'ESX-1 avec des applications potentielles dans le traitement de la tuberculose.

**Mots clefs:** Tuberculose, *Mycobacterium tuberculosis*, système de sécrétion ESX-1, système de sécrétion de type VII, EspC, EccCb1

## List of abbreviations

<b>ADC</b>	albumin/dextrose/catalase	<b>LTBI</b>	latent tuberculosis infection
<b>AIDS</b>	acquired immune deficiency syndrome	<b>MDR</b>	multi-drug resistance
<b>ATP</b>	adenosine triphosphate	<b>MTBC</b>	mycobacterium tuberculosis complex
<b>BCG</b>	Bacillus Calmette–Guérin	<b>MycP1</b>	mycosin protease-1
<b>BME</b>	$\beta$ -mercaptoethanol	<b>OADC</b>	oleic acid/albumin/dextrose/catalase
<b>bp</b>	base pair	<b>OD</b>	optical density
<b>BSA</b>	bovine serum albumin	<b>PBS</b>	phosphate-buffered saline
<b>CD</b>	circular dichroism	<b>PCR</b>	polymerase chain reaction
<b>CFP-10</b>	10 kDa culture filtrate protein	<b>PZA</b>	pyrazinamide
<b>CF</b>	culture filtrate	<b>RD</b>	region of difference
<b>cGAS</b>	cyclic GMP-AMP synthase	<b>RIF</b>	rifampicin
<b>CL</b>	cell lysate	<b>RNA-seq</b>	RNA sequencing
<b>DTT</b>	Dithiothreitol	<b>SCID</b>	severe combined immunodeficiency
<b>Ecc</b>	ESX conserved components	<b>Sec</b>	general secretion
<b>EDTA</b>	Ethylenediaminetetraacetic acid	<b>Tat</b>	twin arginine translocation
<b>ESAT-6</b>	6 kDa early secretory antigenic target	<b>TB</b>	tuberculosis
<b>Esp</b>	ESX secretion-associated proteins	<b>TCA</b>	trichloroacetic acid
<b>EM</b>	electron microscopy	<b>TCSS</b>	two-component signaling system
<b>FPLC</b>	fast protein liquid chromatography	<b>TEM</b>	transmission electron microscopy
<b>GTP</b>	guanosine-5'-triphosphate	<b>TPR</b>	tetratricopeptide repeat
<b>HA</b>	hemagglutinin	<b>TST</b>	tuberculin skin test
<b>HIV</b>	human immunodeficiency virus	<b>TxSS</b>	type x secretion system
<b>IF</b>	immunofluorescence	<b>XDR</b>	extensively drug resistance
<b>IGRA</b>	interferon gamma release assay	<b>WHO</b>	world health organization
<b>IPTG</b>	isopropyl $\beta$ -D-1-thiogalactopyranoside	<b>wt</b>	wildtype
<b>INH</b>	isoniazid		
<b>LC/MS</b>	liquid chromatography-mass spectrometry		



## **Chapter 1**

### **General introduction**





## 1.1 Tuberculosis

Tuberculosis (TB) is a chronic lung disease caused by *Mycobacterium tuberculosis* (*M. tb*). Around 1.5 million annual deaths from TB were reported by the World Health Organization (WHO) in 2014. One third of the world's population are estimated to be latently infected [1], making the disease a global public health challenge. In fact, TB has plagued the human population since prehistoric times and throughout much of known human history. It is suspected that *M. tb* has killed more people than any other microbial pathogens during its long-term co-existence with humans [2]. Hershkovitz *et al.* reported their detection of mycobacterial DNA in human bone samples from Eastern Mediterranean as long as ~9000 years ago. According to the authors, it is the earliest report of the disease in humans that has been confirmed by molecular means [3]. "Phthisis", the early term for tuberculosis, was firstly described around 460 BC by Hippocrates, a physician from ancient Greece [4]. The patients who suffered from phthisis were described to have fever and cough, and it became the most common disease of the time. During the 18<sup>th</sup> and 19<sup>th</sup> century, TB, also known as "white death", "the great white plague" and some other names derived from its symptoms, was an epidemic in Europe. Millions of people died from TB, until the late 19<sup>th</sup> centuries, when Dr. Robert Koch discovered the "*Tubercle bacillus*" as the bacterium causing weakness of the lung. He provided many evidences that TB is an airborne infectious disease. Koch won the Nobel Prize for Physiology (Medicine) in 1905 for his significant contributions, and since then the term "tuberculosis" or "TB" has become well accepted. The history of TB was changed, and the number of deaths gradually declined thereafter [2,4].

In the modern world, although TB is still the second biggest infectious killer after HIV, it has been clearly studied. Tubercle bacilli are transmitted in tiny microscopic droplets through the air from the lungs of TB patients when they cough. Only 5% to 10% of the infected people develop an active disease over their lifetime [5]. Normally, the infection can be cleared by a healthy immune system. Incomplete elimination of the bacilli by the immune system can lead to a

latent infection (LTBI), due to the presence of viable bacilli in the granulomatous tissues. People with LTBI are asymptomatic carriers and are not able to spread the disease. However, when the immune system is weakened by aging, stress, or co-infection with HIV, the host cannot effectively control the *M. tb* bacillus any longer. In 2012, 24% of deaths in HIV-infected patients were due to active TB [6]. The situation of TB in recent years was worsened by the emergence of extensively drug resistant (XDR) and multi-drug resistant (MDR) *M. tb* strains, which has become another major concern [7]. In this regard, the history of human understanding and controlling TB is still far from ending.

## **1.2 Prevention, diagnosis, and treatment of TB**

Currently, Bacille Calmette-Guérin (BCG) is the only vaccine available against TB with more than 4 billion people having been immunized with BCG [8]. It is an attenuated vaccine strain that was isolated by Calmette and Guérin from *Mycobacterium bovis* and has been used since the early 1900s [9]. Despite being protective for tuberculous meningitis in children, the efficacy of BCG against adult pulmonary disease varies dramatically (0 to 80%) and is therefore inadequate [10]. The reasons for the variation are unclear and under debate. A high-fidelity vaccination could be developed either by genetically attenuating mycobacterium or by introducing immunodominant *M. tb* specific antigens, such as ESAT-6 (Early secreted antigenic target of 6 kDa, or EsxA) which was found to confer an enhanced protection [11]. As WHO reported in 2015, sixteen different TB vaccine candidates are in clinical phase-I/II trials and many more are in preclinical development. One of the promising cases is Ag85 (antigen 85)-ESAT-6 fusion protein formulated with the adjuvant IC31, which boosted the BCG-primed individuals to develop a better protection [12-14]. Furthermore, new *M. tb* specific antigens are being identified, including EspC ([15] and Supplementary section in Chapter 2). These achievements may lead to more effective global TB control.

TB is primarily an airborne disease. When a person has been in contact with a patient with active TB, he was at risk of being infected. The symptoms of active TB may be fever, weight loss, cough, haemoptysis and chest pain, but additional tests are required for correct diagnosis. The tuberculin skin test (TST), a 100-year-old diagnostic tool for TB is still commonly used for TB detection. This test is simple but often gives false-positive results. Another common TB test is based on the detection of interferon-gamma released (IFN- $\gamma$ ) by T-cells when exposed to specific TB antigens in the blood (named IGRA assay)[16]. The advantage of IGRA over TST is that IGRA is unaffected by prior BCG vaccination. In addition to the conventional assays, a new and advanced test for TB, GeneXpert, has been available for clinical diagnosis since 2008. It is able to detect the presence of tubercle bacillus and drug-resistant bacterium in the sputum through DNA analyses within two hours, which is more accurate and faster [17]. If the person is suspected to have an active infection based on the diagnostic test, a chest X-ray or CT scan could be further conducted for confirmation. However, a more effective approach for clinical diagnosis of LTBI is still under development [18].

Although TB can be fatal, anti-TB treatments are available nowadays. The first antibiotic effective against TB, streptomycin, was discovered by Selman Waksman in 1943 and saved many lives at that time [2,19,20]. However, it was soon realized that although streptomycin reduced mortality initially, drug resistance was rapidly acquired during monotherapy, indicating that TB is not easily curable by monotherapy. Since then, research was carried out to understand the mechanisms of drug resistance and to develop combined anti-TB drug chemotherapy. In the following years' efforts to improve anti-TB regimens resulted in the discovery of aminosalicylic acid, isoniazid, pyrazinamide, cycloserine and ethambutol, which paved the way for combination therapy [21]. A big event in the history of anti-TB drug discovery occurred in the 1960s, when rifampicin, an antibiotic with a new mechanism of action against TB, was discovered. This breakthrough shortened the treatment duration dramatically from ~18 months to ~9 months. Nowadays, there are more than 20 drugs available for TB treatment, which are used in various combinations under different circumstances [22,23] (Table 1.1). Using rifampicin as the key

component, the first-line oral drug therapy is a combination of rifampicin, isoniazid, pyrazinamide and ethambutol. This regimen is effective against drug-sensitive *M. tb* because each component has a different mode of action (Fig.1.1).

**Table 1.1 Main anti-TB drugs and their target (adapted from [23])**

Drug (year of discovery)	Target	Effect
<b>First-line drugs</b>		
Isoniazid (1952)	Enoyl-[acyl-carrier-protein] reductase	Inhibits mycolic acid synthesis
Rifampicin (1963)	RNA polymerase, beta subunit	Inhibits transcription
Pyrazinamide (1954)	S1 component of 30S ribosomal subunit	Inhibits translation and <i>trans</i> -translation, acidifies cytoplasm
Ethambutol (1961)	Arabinosyl transferases	Inhibits arabinogalactan biosynthesis
<b>Second-line drugs</b>		
<i>Para</i> -amino salicylic acid (1948)	Dihydropteroate synthase	Inhibits folate biosynthesis
Streptomycin (1944)	S12 and 16S rRNA components of 30S ribosomal subunit	Inhibits protein synthesis
Ethionamide (1961)	Enoyl-[acyl-carrier-protein] reductase	Inhibits mycolic acid biosynthesis
Ofloxacin (1980)	DNA gyrase and DNA topoisomerase	Inhibits DNA supercoiling
Capreomycin (1963)	Interbridge B2a between 30S and 50S ribosomal subunits	Inhibits protein synthesis
Kanamycin (1957)	30S ribosomal subunit	Inhibits protein synthesis
Amikacin (1972)	30S ribosomal subunit	Inhibits protein synthesis
Cycloserine (1955)	D-alanine racemase and ligase	Inhibits peptidoglycan synthesis

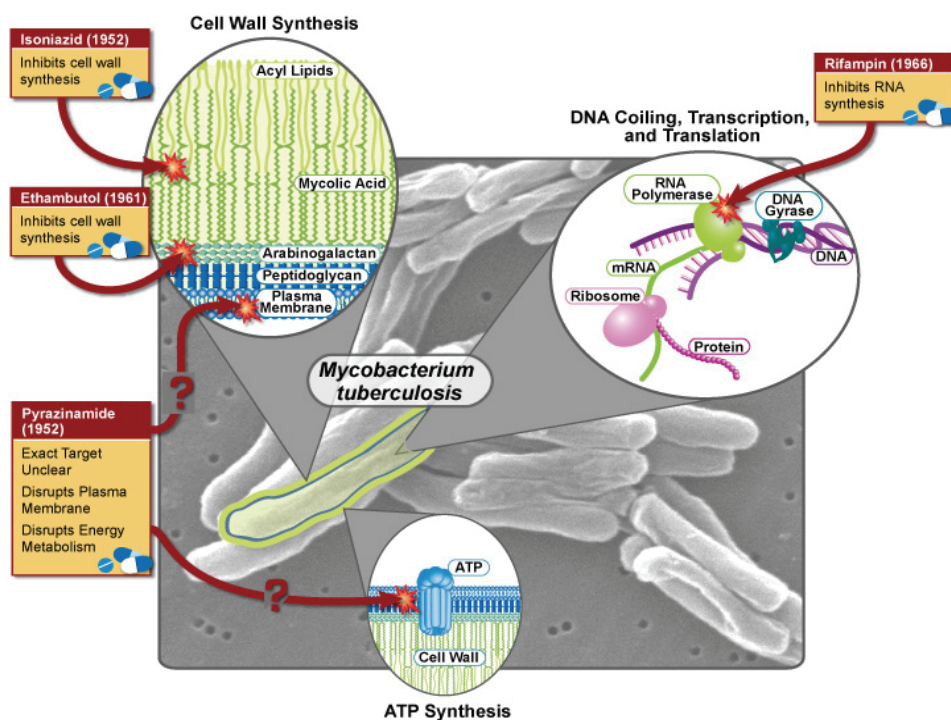


**Fig.1.1** Different modes of action of first-line TB drugs for the treatment of drug-sensitive TB (National Institute of Allergy and Infectious Diseases and [24]).

**Isoniazid (INH)** inhibits the biosynthesis of mycolic acids at the mycobacterial cell wall, thereby leading to increased susceptibility of the mycobacterium to reactive oxygen radicals and other environmental factors. **Rifampicin (RIF)** targets the RNA polymerase and kills the bacteria by inhibiting RNA synthesis. **Ethambutol** interferes with cell wall synthesis like INH, but via inactivation of arabinogalactan synthesis. **Pyrazinamide** has strong synergy with INH and RIF. The cellular target has not been identified. It potentially disrupts membrane energetics, thereby inhibiting membrane transport function.

Although many lives were saved by this therapy, the long treatment time, side effects and co-infection with HIV post a challenge to successful treatment.

Serious challenges are emerging, such as MDR-TB and XDR-TB. First-line drugs are less effective in patients who suffer from drug-resistant TB than those who have drug-sensitive TB [25]. An effective treatment for MDR-TB needs individualized regimens on the basis of drug-susceptibility test. More seriously, XDR-TB, a relatively rare type of MDR-TB, is resistant to the potent anti-TB drugs, including the first-line drugs rifampicin and isoniazid, as well as the best second-line drugs fluoroquinolone and at least one of the three injectable second-line drugs: amikacin, kanamycin and capreomycin [23]. In 1993, WHO declared TB as a global public health emergency since TB drug resistance was widespread throughout the world [26]. Novel drugs, which are more effective, better tolerated, affordable, and with a shorter time course, are in urgent need for the treatment of MDR-TB and XDR-TB. Promising new candidates are bedaquiline and delamanid [23].

The history of TB control has entered into a post-antibiotic era. Targeting bacterial secretion system to inhibit export of the virulence factors, is an alternative strategy for new drug discovery. The anti-virulence drug which allows elimination of the pathogen by the immune system, rather than direct killing, can be a supplement to antibiotic therapy. In the past years, more and more bacterial virulence inhibitors have been screened as potential therapeutics [27]. A whole-cell-based high-throughput screen (HTS) identified two molecules that inhibit secretion of the major *M. tb* virulence factor EsxA. These two molecules have distinct mechanisms of action on the virulence-associated proteins, leading to reduced bacterial survival in the macrophages [28]. Apart from the cell-based HTS approach, several core components of the mycobacterial ESX-1 secretion, a protein transport pathway mainly utilized to secrete EsxA, are potentially targetable by drugs to attenuate the *M. tb* virulence. In this respect, to understand the structure of the ESX-1 apparatus can help us to screen for or design anti-virulence compounds, which can be used in combination with the conventional multidrug regimens to improve the treatment.

Hence, toward new drug discovery is the ultimate goal of the ESX-1 research. Being the topic of my thesis, the details of the ESX-1 secretion system will be further described in the following sections.

## 1.3 Mycobacteria

### 1.3.1 *Mycobacterium tuberculosis* (*M. tb*)

The development of novel anti-TB drugs requires a deep knowledge of the mechanism of the disease, the pathogen itself, and the interaction between host and pathogen. Species belonging to the *Mycobacterium tuberculosis* complex (MTBC), which comprises *M. tb*, *M. bovis*, *M. bovis* BCG, *M. africanum* and *M. microti*, are the causative agent of most cases of TB in mammals. These subspecies share 99% nucleotide sequence similarity, but have some phenotypic properties that differentiate them [29,30]. Basically, the tubercle bacillus is a small, rod-shaped prokaryote of the Actinomycetes family with a high GC content (58% to 69%) of the genome, and is closely related to the Streptomyces, Nocardia and Corynebacteria groups [29,31]. The mycobacterial cell envelope comprises a regular phospholipid bilayer plasma membrane, a lipid-rich cell wall and an outer capsule [32-34]. Compared to other bacteria, mycobacteria have an atypical dual layer of peptidoglycan and arabinogalactan covalently linked to a long and branched (C60-C90) fatty acid chain (known as mycolic acid) associated with free intercalating glycolipids (Fig.1.2). This thick and hydrophobic cell wall, also called the mycomembrane, is much less penetrable than the Gram-positive cell wall, forming a double protective permeability barrier to polar molecules and antibiotics, which plays an important role for drug resistance and survival of mycobacteria in harsh environments [35,36]. While the architecture of the mycomembrane partly resembles a Gram-positive cell wall, electron microscopic analysis demonstrated that the structural organization also has a Gram-negative morphology [37,38]. Because of the unique composition of its cell wall, a mycobacterium is identified by the acid-fast stain (Ziehl-Neelsen stain) instead of the typical Gram-stain. At the extremity of the cell, a thick capsular layer is surrounding the cell wall, which contains polysaccharides (glycan and



arabinomannan), proteins and a small amount of lipid [38,39]. The capsule was shown to promote binding of macrophages and dampen pro-inflammatory cytokine response [38]. It can be removed when the bacteria are grown in the liquid media by the addition of a detergent, such as Tween-80. This also prevents the clumping of the bacteria when they are growing in liquid media [40].

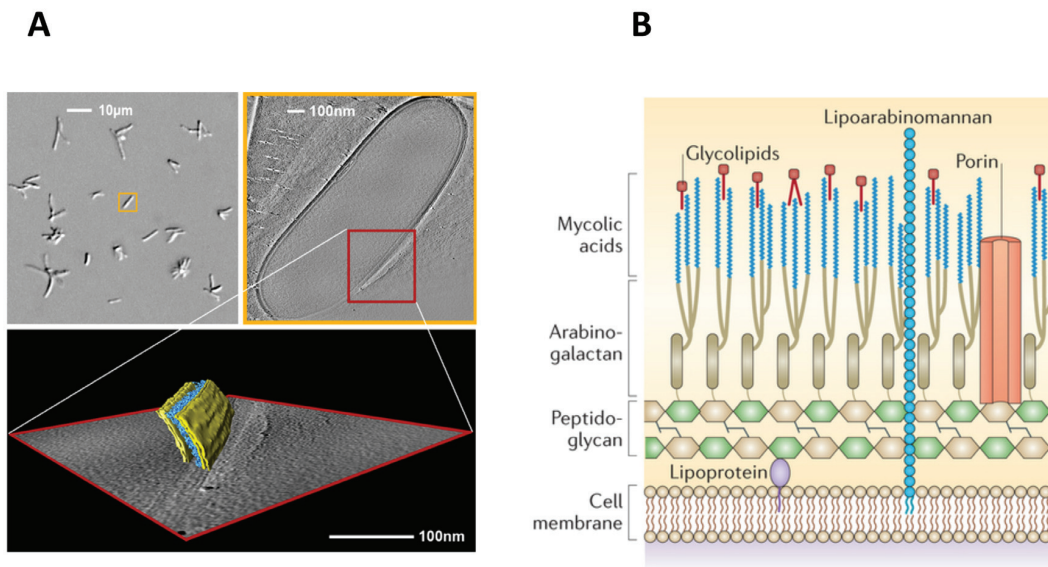


**Fig.1.2 Organization of the mycobacterial cell wall (adapted from [33] [34])**

**(A)** Mycobacterium (*M. bovis* BCG shown here) is a rod-shaped prokaryote. Cryo-electron tomography enables visualization of the inner membrane and mycomembrane of the mycobacterial cell wall (in yellow), between which is the periplasmic space containing the layers of the arabinogalactan-peptidoglycan polymer (in blue) [34]. **(B)** Mycobacterial cell wall is mainly composed of a layer of peptidoglycan-arabinogalactan, and a layer of mycolic acids associated with free lipids such as glycolipids that is referred to as the mycomembrane. Lipoproteins, porins and cell membrane-anchored lipoarabinomannans are also present in the cell wall [33].



In addition to the GC-rich genome and complicated cell envelope, the other characteristic features of pathogenic mycobacteria are their slow growth rate and longevity. *M. tb* divides every 20 to 24 hours in synthetic medium or infected animals, and takes weeks to form colonies on agar plates. When the gene encoding MspA, a porin that only exists in the outermembrane of fast-growing mycobacteria, was introduced to a slow-growing mycobacterium, the growth rate found to be accelerated [41]. Therefore, the slow generation time may be partly due to a low rate of nutrient uptake, which is a consequence of the low permeability of the thick cell wall.

*M. tb*, responsible for the majority of human TB cases, is a facultative intracellular pathogen. Upon entry into the host by aerosol transmission, *M. tb* goes through its pathogenic life cycle as shown in Fig.1.3. The infection is initiated with phagocytosis, a receptor-dependent process during which the pathogens are taken up by macrophages. The *M. tb* residing in the phagosomes is then targeted to be degraded. However, *M. tb* manages to escape degradation by means of specific strategies, including activating the ESX-1 secretion system as described in the following sections, to arrest phago-lysosomal fusion, lyse the membrane of vesicle and escape into the macrophage's cytosol. Survival and replication of *M. tb* in the macrophage lead to pro-inflammatory responses, recruitment of innate immune systems, and formation of a granuloma- a hallmark pathological structure of TB. The granuloma plays an important role in maintaining latent TB infection as the bacilli can persist for a long period of time in it with little or no replication. When the immune system is weakened, a necrotic granuloma core develops and then ruptures. As a consequence, the bacteria that replicate extracellularly are released into the airways and transmitted to the new host [42-45].

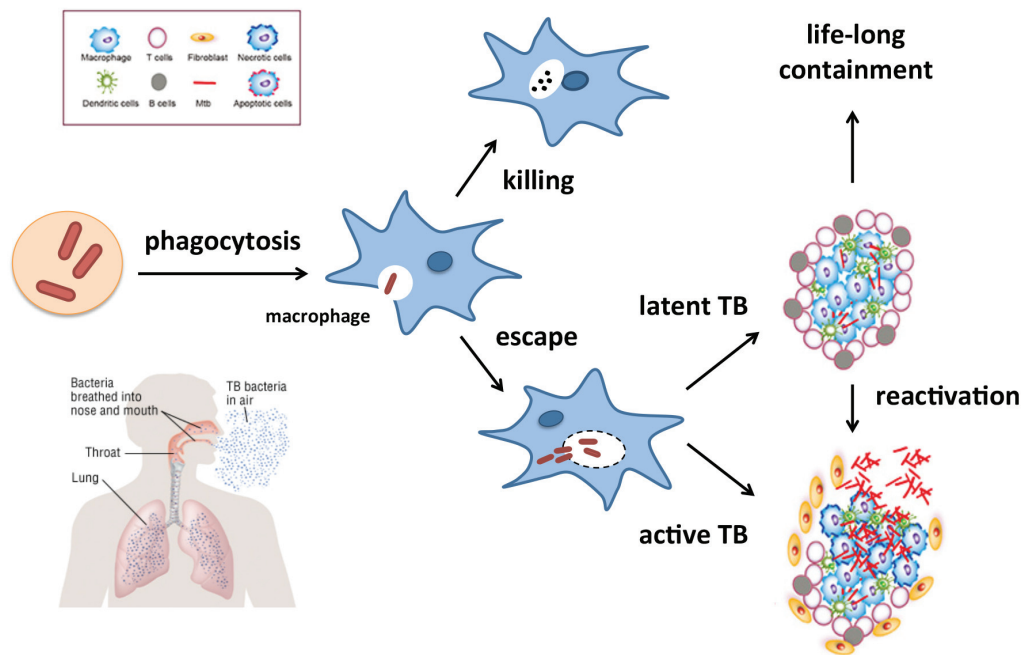


**Fig.1.3 Pathogenic life cycle of *M. tb* (adapted from [46]) .**

Upon inhalation of aerosol particles containing *M. tb*, the infection is initiated with phagocytosis by alveolar macrophages. The internalized bacteria are able to escape from the phagosome and replicate in the macrophage's cytosol, including the formation of granulomas- organized aggregates of macrophages and other immune cells. A granuloma restricts bacterial growth, in which the dominant bacteria can persist for a long period of time without causing disease. However, the bacteria are not cleared within the granuloma. When the host's immune system is suppressed, the granuloma can undergo necrosis, forming a necrotic caseous center that allows bacterial re-activation and growth, and eventual spread to a new host.

### 1.3.2 Other pathogenic mycobacterial species

Alternative models were used in the past years to study mycobacterial pathogenesis. Although these models do not mimic certain aspects of human *M.*

*tb* infection, the obvious advantages over utilizing *M. tb* are faster growth and lower pathogenicity, which makes these models not restricted to biosafety level-3 laboratory. *Mycobacterium marinum* is one of the important alternative models in TB research. It is genetically closely related to *M. tb* [47], infecting fish and amphibians as its natural hosts and occasionally causing granulomatous skin lesions in humans [48]. The generation time of *M. marinum* is 4-6 hrs at 25°C-35°C and 14 hrs at 37°C [39], which is between *M. tb* and the fast-growing, non-pathogenic mycobacteria [49]. *M. bovis* is a member of the MTBC with a broader host range than *M. tb*. It not only infects domesticated animals, but can also cause TB in humans albeit with a low risk of infection [50]. The only available TB vaccine, BCG, is derived from *M. bovis*. By comparative genomic analyses with *M. tb* H37Rv strain, 14 regions of difference (RD) were found missing [51,52]. Among these, RD1 (*rv3871* to *rv3879c* in *M. tb*) plays an essential role in virulence [50,53-55]. Thus, *M. bovis* BCG strain has been used to investigate the mechanism of attenuation and to identify mycobacterial virulence factors [50,56,57]. *Mycobacterium leprae* is a causative agent of leprosy, a disease affecting superficial tissues such as skin and nasal mucosa. *M. leprae* has a reduced genome (3.2 Mbp), grows extremely slowly with the longest doubling time of all known bacteria (14 days in mice), and is uncultivable *in vitro* [58]. Because *M. leprae* contains a substantial number of pseudogenes, comparing its genome to that of *M. tb* and other mycobacterial pathogens helps to understand the minimal gene set required by a pathogenic mycobacterium.

### 1.3.3 Non-pathogenic mycobacteria

Apart from *M. chelonae*, *M. fortuitum* and *M. phlei*, the best known non-pathogenic mycobacterium is *M. smegmatis*, an environmental mycobacterium species defined as a fast-growing mycobacterium [59]. Due to its rapid growth and absence of virulence to humans, *M. smegmatis* is widely used in genetic studies, as well as an overexpression tool of mycobacterial proteins [60]. The information provided by comparative genomics and proteomics illustrates the adaptation of pathogenic and non-pathogenic species to their respective niches [50,61].

## 1.4 Bacterial secretion systems

Present at the cytoplasmic membrane of bacteria and archaea, two distinct pathways, namely the general secretion pathway (Sec pathway) and the twin arginine pathway (Tat pathway), are utilized to translocate intracellular proteins and to insert them into or across the membrane. While the Sec pathway transports proteins in their unfolded state, the Tat system exports fully folded proteins harboring a twin arginine motif at the N-terminal signal sequence, as indicated by the name [62-64].

In addition to the universal secretory pathways, bacteria have evolved a series of specialized secretion systems to interact with the hosts. Seven types of secretion system have been defined as types I-VII (T1SS-T7SS). The substrates of these secretion systems include proteins, DNA, small molecules and lipids, which are translocated via the specific secretion system from the bacterial cytosol to the extracellular environment, or are directed into the target cell [65,66]. The secretion processes can consist of a single step, in which the secretory apparatus extends from the cytosol through the entire cell envelope without periplasmic intermediates (e.g. T3SS); or two steps (e.g. T2SS), in which the substrates are firstly exported through the cytoplasmic membrane following a second translocation across the outer membrane to the outside (Fig.1.4). Of the seven secretion systems, T3SS, T4SS and T6SS are actively studied by many research groups around the world. T3SS present in various pathogenic Gram-negative bacteria, is composed of approximately thirty different proteins. The structural components assemble into a needle-like structure (termed injectisome) to translocate effector proteins from the bacterial cytoplasm into the host cell, thereby modulating host cellular functions during infection, such as gene expression, signal transduction and immune response [67,68]. Similarly, T4SS is also a single-step translocation, directly delivering the substrates into the target cell in a contact-dependent process. It comprises ~12 core proteins, forming a scaffold and translocation apparatus spanning the double-membrane, as well as a pilus extending into the extracellular space [69,70]. The versatile T4SS is not only involved in secretion of virulence proteins, but also mediates DNA

conjugation and contributes to the spread of antibiotic resistance genes among the pathogenic bacteria. In this regard, T4SS can be divided into conjugation system, DNA uptake/release system, and effector translocator system [71]. T6SS is utilized to inhibit or kill bacterial and eukaryotic target host cells through export of toxins, therefore, it functions in pathogenesis and inter-bacterial competition [72,73]. T6SS consists of two complexes: a baseplate at the membrane and a tube wrapped by an exterior sheath [74,75]. The components of T6SS are homologous to those of T4 phage tail in structure. Moreover, the secretory apparatus is also mechanistically analogous to the phage tail, displaying a dynamic activity of sheath extension, contraction and disassembly cycle [73].

Although these specialized secretion systems are distinct in function and structural arrangement, they all require ATPases and pore forming proteins as the mandatory components. The export of substrates is not a spontaneous process but consumes energy. ATP is the main source of energy to drive export, therefore, targeting the substrates to an ATPase is critical for a secretion pathway. This is followed by translocation of the substrate through a pore forming protein, which is usually a protein with multi-transmembrane domains embedded in the cell membrane. Together with the core components and other accessory proteins, a dedicated secretory nanomachine is assembled at the bacterial cell envelope, playing an essential role in pathogenesis and physiology [65,69,76-80]. Deeper knowledge about bacterial secretion systems is invaluable for antibiotic development strategies.

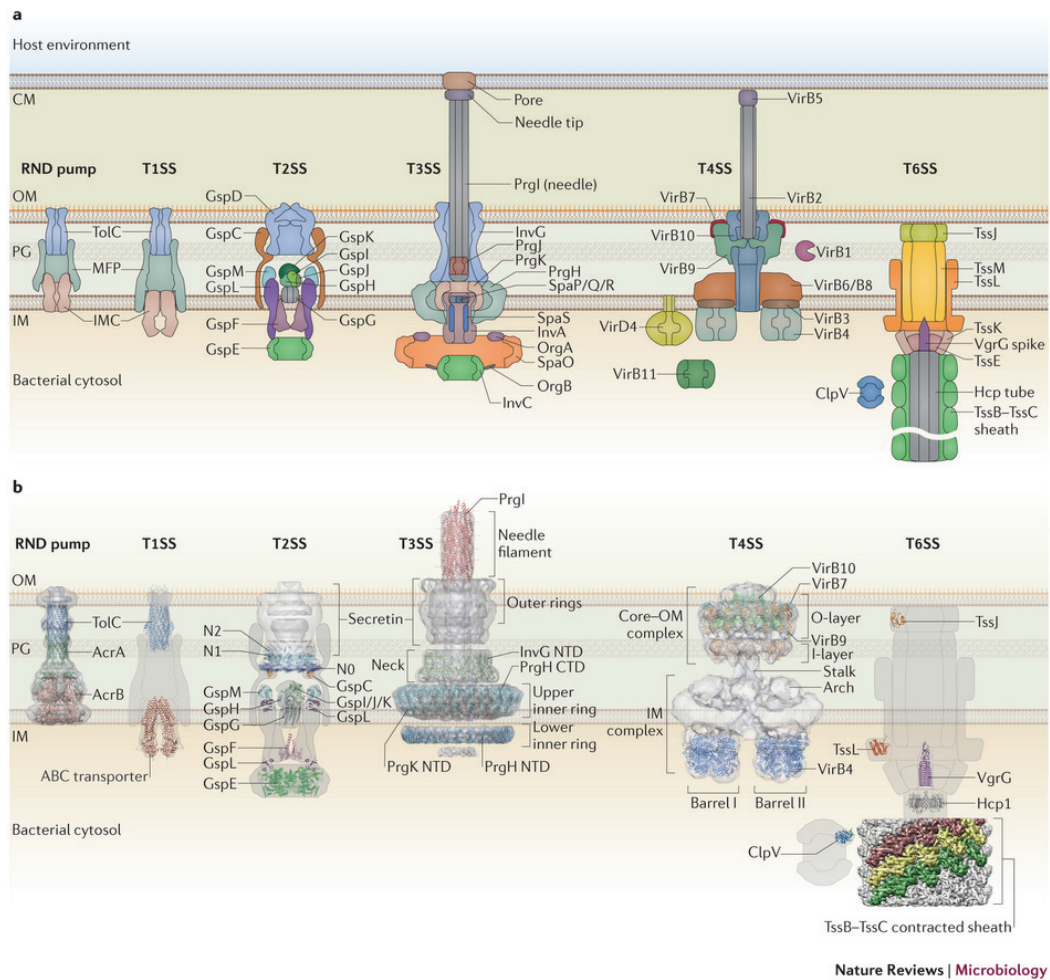


**Fig.1.4 Bacterial secretion systems [65].**

Bacterial secretion systems with diverse structures and functions have been defined as type I-VII. The image shows the secretion systems of Gram-negative bacteria, which span the double membrane. The putative locations and the solved structures of individual proteins are demonstrated.

## 1.5 Type VII / ESX secretion systems in mycobacteria

Type VII secretion system, also referred to as the ESX secretion system, is required for virulence and growth of mycobacteria. It is sub-categorized into ESX-1 to ESX-5 which vary in function and the number of genes in the corresponding loci (Fig.1.5). In the early 2000s, the ESX-1 secretion system was discovered as the first T7SS which is closely linked to virulence. It is named after the secreted protein EsxA (ESAT-6, 6-kDa early secretory antigenic target), which is encoded in the RD1 region within the *esx-1* locus [81]. Along with its chaperone EsxB (CFP-10, 10-kDa culture filtrate protein), EsxA is a major virulence factor essential for the survival of *M. tb* within the host cell. On the other hand, in the fast-growing, non-pathogenic *M. smegmatis*, ESX-1 is involved in conjugal DNA transfer [82]. The ESX-3 secretion system which secretes EsxG/EsxH heterodimer, is responsible for iron and zinc uptake, and it is negatively regulated by the availability of these ions [83,84]. Therefore, ESX-3 may function to maintain iron and zinc homeostasis in *M. tb*. The ESX-5 secretion system mediates the export of PE/PPE proteins, some of which are virulent and immunogenic [29,85,86]. Restricted to slow-growing mycobacteria, ESX-5 plays a role not only in pathogenesis, but also in bacterial growth through nutrient acquisition [87], suggesting a possible effect on the slow-growing phenotype. While ESX-1, ESX-3 and ESX-5 have been well studied in the past years, the function of ESX-2 and ESX-4 are still unclear. So far, they have not been found to be actively involved in protein secretion. The functions of the five ESXs are summarized in Table 1.2.



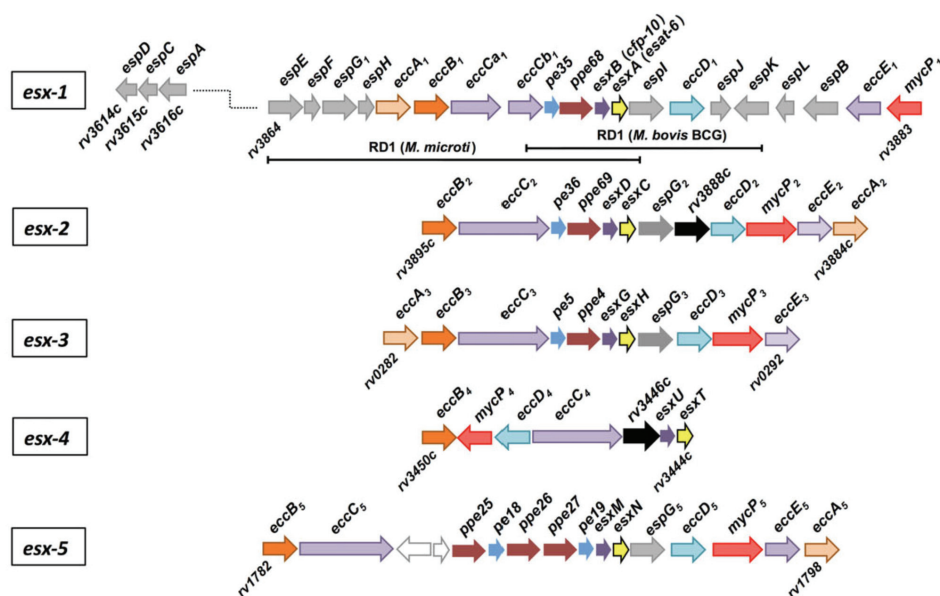


**Fig.1.5 Genetic organization of mycobacterial ESX secretion systems [88]**

Five *esx* clusters are present in *M. tb*, encoding Esx, Esp, Ecc and PE/PPE proteins of the ESX-1 to ESX-5 secretion systems. Respective RD1 deletions of *M. bovis* BCG and *M. microti* are indicated.

**Table 1.2 Function of ESX secretion systems in mycobacteria**

System	Function
ESX-1	Virulence (pathogenic mycobacteria), conjugation ( <i>M. smegmatis</i> )
ESX-2	Unknown
ESX-3	Acquisition and homeostasis of zinc and iron
ESX-4	Unknown
ESX-5	Immune modulation, virulence, nutrient uptake, PE-PGRS export



Most of the T7SS substrates contain a consensus secretion signal sequence “YxxxD/E” which is usually present at the flexible C-terminus of secreted proteins, such as EsxB of ESX-1, EsxG of ESX-3 and PE25 of ESX-5 [89]. They usually form a pair with a WxG100-family protein, using the C-terminal signal to target the heterodimer (EsxA/EsxB, EsxG/EsxH, PE25/PPE41, etc) to the secretory apparatus for translocation [90,91]. In many cases, the signal-harboring protein itself also belongs to the WxG100 family. WxG100 (Trp-x-Gly) protein family is a class of effector proteins widely present in Gram-positive bacterial and mycobacterial secretion systems. These proteins with a conserved WxG motif are characterized by their small size (~100 residues), having hairpin folds and having a tendency to form a heterodimer with another WxG protein. As such, a helix bundle seems to be a common folding pattern for T7 substrates.

## 1.6 ESX-1 secretion system

### 1.6.1 *esx-1* locus and RD1

ESX-1 is of the most interesting ESX secretion systems, because it is linked to mycobacterial virulence. The *esx-1* locus spans over 20 genes, encoding core components (Ecc), substrates, ESX secretion-associated proteins (Esp) and a mycosin protease (MycP1) (Fig.1.5). A 9.5 kb gene cluster spanning from *rv3871* to *rv3879c* within *esx-1* loci, known as RD1, is missing in the BCG vaccine strain [92], and the RD1 was found to present in all the pathogenic mycobacterial species [52]. The virulence of BCG can be largely restored by complementation with RD1, indicating the crucial role of RD1 and the ESX-1 secretion system in *M. tb* pathogenesis. This is supported by a number of experiments showing attenuation of ESX-1 mutant strains in infected macrophages and SCID mice [92-96]. In the following sections, some essential proteins of the ESX-1 secretion system will be described in detail.

#### 6.1.1.1 The virulence factors

The secreted proteins EsxA and EsxB, encoded in the RD1 cluster, are the major mycobacterial virulence factors. Interruption of either *esxA* or *esxB* resulted in a similar attenuated phenotype as a mutant strain deficient for RD1 ( $\Delta$ RD1) in growth and virulence within macrophages [97]. Due to a sensitive and highly specific induction of T-cell response, EsxA and EsxB have a long history of being used for T-cell based TB diagnosis such as skin test and IFN- $\gamma$  release assays [98,99], and are potential candidates for vaccine development [100]. As members of the WxG100 family, EsxA and EsxB associate to form a 1:1 tight heterodimer *in vitro*, where the two proteins adopt a hairpin structure antiparallel to each other [101,102]. The complex was found to dissociate in the sample buffer with acidic pH [103]. Since the two proteins are co-secreted in mycobacteria, EsxA and EsxB are thought to be exported as a pair as well [104]. Disruption of an artificial membrane by purified EsxA suggests a possible role in cytolysis [81,105]. In agreement with this, when the *esxA esxB* operon was interrupted, host cell lytic activity of *M. tb* was compromised, resulting in a reduction of bacterial invasion of lung interstitial tissue [81]. It was also reported that a *M. marinum* mutant strain defective in EsxA/EsxB secretion failed to escape from the phagosome and was delivered to the phagolysosomal compartment for degradation [106]. Taken together, these findings support a hypothesis for an intracellular survival mechanism, in which the secreted EsxA/EsxB complex dissociates in the acidic environment of the phagosome, resulting in membrane damage due to cytolytic activity of the released EsxA and subsequent phagosome maturation arrest.

EspB is another well-characterized ESX-1-specific virulence factor. It is encoded in the region outside RD1, termed extended RD1 (extRD1). The essentiality of EspB to mycobacterial pathogenesis was highlighted, as a strain with inactivated EspB was attenuated *in vivo* and in macrophages [107]. Further assays showed that EspB is required for EsxA secretion [97,108]. In fact, EspB is similar to EsxA in the sense that it is an ESX-1 secreted protein with membranolytic ability, which is demonstrated by the induction of THP-1 cytotoxicity in the presence of

the affinity-purified protein alone [109]. Therefore, EspB is involved in intracellular survival, and not only promotes EsxA export but also directly contributes to membranolytic capabilities of *M. tb*. Intriguingly, EspB is cleaved at the C-terminus by the protease MycP1 during secretion, resulting in a 50 kDa mature isoform [110]. As shown by X-ray crystallization and electron microscopy studies, EspB has a propensity to associate into a heptameric structure with a pore at the center [90]. Therefore, it is plausible that EspB might be a surface-exposed component of the ESX-1 nanomachine that facilitates EsxA translocation.

Investigation of extRD1 upstream of the 5' region of the *esx-1* cluster revealed the presence of genes for EsxA-independent virulence factors EspF and EspG1. Loss of *espF* and part of *espG1* resulted in reduced virulence in the SCID mouse model and macrophages, whereas EsxA secretion and specific T-cell responses were not compromised [94,111]. In a *M. microti*  $\Delta rv3860-3866$  strain where RD1 is missing (Fig.1.5), complementation of RD1 led to EsxA secretion but the bacterial growth in mice was not enhanced, again highlighting the plausible role of EspF and EspG1 in virulence [94]. EspGs in ESX-1, ESX-3 and ESX-5 were found to interact with a variety of PPE proteins, thereby functioning to stabilize and mediate secretion of the PE/PPE complex [111-113]. Therefore, EspG is a specific chaperone for T7SS [114]. Although exactly how EspF affects virulence remains unknown, bioinformatic analyses revealed that the sequence of EspF is highly similar to that of EspC, an ESX-1 substrate encoded in a remote *espACD* operon that is required for EsxA/EsxB secretion (described in Section 1.6.2). The similarity between EspE and EspA, the two proteins respectively adjacent to EspF and EspC in the genome, was also identified. In this regard, an overlap in function cannot be excluded until further clarification.

#### **1.6.1.2 PE/PPE proteins**

PE/PPE gene families are quite abundant in pathogenic mycobacteria, and account for ~10% of the *M. tb* genome [29]. While the non-pathogenic *M. smegmatis* has a genome more than 50% larger than that of *M. tb*, it only has

two pairs of putative PE and PPE genes [115]. They are named after the characteristic proline-glutamic acid (PE) or proline-proline-glutamic acid (PPE) motifs near the N-terminus. Similar to EsxA/ EsxB, the PE/PPE proteins usually form a helical bundle complex, with the assistance from the chaperone EspG, for translocation [112,114,116]. The complex is exported to the cell surface and interacts with the host immune system. In the ESX-1 secretion system, PE35 and PPE68 are T-cell antigens with their genes adjacent to *esxA* within the RD1 cluster. Inactivation of these genes affects intracellular growth [117], but does not inhibit the secretion level of EsxA [118]. Therefore, PE35/PPE68 plays an immunomodulatory role in *M. tb* pathogenesis.

#### **1.6.1.3 Ecc proteins in ESX-1 secretion system**

Ecc proteins are the fundamental components of the ESX secretory architecture. Using the ESX-5 secretion system as a model, the conserved EccB, EccC, EccD and EccE were co-purified from the cell envelope. Thus, they are thought to form a central channel at the cytoplasmic/inner membrane [119]. While the roles of EccB1 and EccE1 are unclear, EccD1 is predicted to be a pore forming protein at the inner membrane because it contains a multi-transmembrane domain.

Unique to the ESX-1 secretion system of *M. tb*, EccC1 comprises two separate proteins- EccCa1 and EccCb1. EccCa1 contains a FtsK/SpoIIIE ATPase domain at the C-terminus, and a transmembrane domain at its N-terminus that anchors the protein to the cell membrane. EccCb1, bound to EccCa1 [95], has two FtsK/SpoIIIE ATPase domains. The EccCa1-EccCb1 complex is predicted to be the putative molecular motor for protein translocation. A yeast two-hybrid assay demonstrated an interaction of EccCb1 with the C-terminal signal sequence of EsxB, indicating that the EsxA/EsxB heterodimer is recognized by EccC1 during secretion. A recent study using EccC of *Thermomonospora curvata* revealed that while the functionality of EccC as a molecular motor was triggered upon contact to EsxB, it was inactivated when the EsxA/EsxB complex forms [120]. This substrate-controlled activation suggests that T7SS activity might be partly regulated at the post-translational level when substrates are targeted to the

ATPase for export. Apart from EccCa1-EccCb1, ESX-1 recruits a third ATPase EccA1 to provide energy. This cytosolic ATPase harbors a N-terminal TPR motif that is involved in cargo interaction, and a C-terminal AAA+ (ATPase associated with various cellular activities) domain that possesses ATPase activity and mediates protein hexamerization [121,122]. A yeast two-hybrid assay showed that the ESX-1 substrate EspC is targeted to EccA1 for secretion. Although containing the same C-terminal secretion signal YxxxD/E, swapping the C-termini of EsxB with that of EspC disrupted ESX-1 secretion, indicating that the ATPases EccA1 and EccC1 are functionally distinct [123].

#### **1.6.1.4 Protease MycP1**

MycP1 is a serine protease localized at the inner membrane, playing a dual role in regulation of protein secretion and virulence. Lack of MycP1 abolishes EsxA secretion, suggesting an important role in ESX-1 secretion. Intriguingly, mutation at the MycP1 proteolytic site results in an immature EspB without cleavage of its C-terminus, and an increased secretion of EsxA [110]. It appears that the protease activity of MycP1 inhibits its function in the ESX-1 pathway. The two faces of MycP1 remain a secret to be uncovered.

#### **1.6.2 *espACD* operon**

In addition to the proteins encoded in the *esx-1* cluster, the *espACD* operon (*rv3614c-rv3616c*) is critical for ESX-1 secretion and function [124]. The *espACD* operon is positively controlled by the regulatory protein EspR at the transcriptional level [125,126]. Two of the products, EspA and EspC, are ESX-1-dependent substrates of particular interest. Fortune *et al.* found that deletion of either *espA*, *esxA* or *esxB* blocks the secretion of the others, revealing a mutual dependency of secretion as a characteristic feature of ESX-1 [104]. EspA contains the conserved WxG motif at the linker of the two predicted helices, but lacks a secretion signal. On the other hand, EspC, which is predicted to possess a hairpin structure, has YxxxD/E signal at the C-terminus. It is likely that EspA/C forms a typical helix bundle that is common in T7SS as described previously in Section

1.5. Moreover, due to co-secretion of EspA/C and EsxA/EsxB, these two heterodimers are thought to further associate into a complex during translocation, although there are no experimental data supporting this hypothesis so far [127]. On the other hand, EspD translocation is independent from the ESX-1 secretion system, and secretion of EspD and EsxA is not coupled [128].

The roles of EspA/C/D in ESX-1 remain undefined. In addition to the fact that EspA is necessary for the secretion of the virulence factors EsxA/EsxB, it was shown to directly affect mycobacterial cell wall integrity [129]. The functional integrity can be altered by disruption of the disulfide bond (Cys-138) in EspA, which led to reduced virulence *in vivo* [129]. However, this model is under debate due to irreproducibility of the results [130]. The EspC protein is predicted to adopt a helix-turn-helix structure, which harbors the general secretion signal that is recognized by the ATPase EccA1. The similarities of EspC to EsxA and EsxB are not only in size and sequence, but also in cellular immune response. The high specificity and immunodominance to induce T-cell response make EspC a TB vaccine candidate [15]. EspD appears to modulate ESX-1 through maintaining the intracellular levels of EspA and EspC. The mechanism is not well understood [128].

Remarkably, the *espACD* operon is missing from the non-pathogenic mycobacteria, such as *M. smegmatis*. Based on the distinct functions of ESX-1 between pathogenic and non-pathogenic mycobacterial species, e.g. virulence for the former and conjugative DNA transfer for the latter, it is speculated that *espACD* genes might have been evolved from or transferred into slow-growing mycobacteria, which are then recruited by the ESX-1 secretion system to further develop the functions related to virulence.

**Table 1.3 Roles of ESX-1-associated proteins**

<b>Protein</b>	<b>Gene</b>	<b>(Predicted) Roles/Functions</b>
EspE	<i>rv3864</i>	Unknown
EspF	<i>rv3865</i>	Contributes to EsxA-independent virulence
EspG1	<i>rv3866</i>	Chaperone
EspH	<i>rv3867</i>	Unknown
EccA1	<i>rv3868</i>	Cytosolic AAA+ ATPase, interacts with EspC
EccB1	<i>rv3869</i>	Component of cell membrane complex
EccCa1	<i>rv3870</i>	Membrane bound FtsK/SpoIIIE ATPase
EccCb1	<i>rv3871</i>	Cytosolic FtsK/SpoIIIE ATPase bound to EccCa1, interacts with EsxB
PE35	<i>rv3872</i>	Has immunomodulatory effect
PPE68	<i>rv3873</i>	Has immunomodulatory effect, interacts with PE35
EsxB	<i>rv3874</i>	Major virulence factor, chaperone of EsxA, interacts with ATPase EccCb1
EsxA	<i>rv3875</i>	Major virulence factor with cytolytic activity
EspI	<i>rv3876</i>	Mediates the response of low cellular ATP level
EccD1	<i>rv3877</i>	Pore forming protein at the inner membrane
EspJ	<i>rv3878</i>	Unknown
EspK	<i>rv3879c</i>	Unknown, interacts with EspB
EspL	<i>rv3880c</i>	Unknown
EspB	<i>rv3881c</i>	Virulence factor with cytolytic activity, required for EsxA/EsxB secretion
EccE1	<i>rv3882c</i>	Component of cell membrane complex
MycP1	<i>rv3883c</i>	Serine protease, cleaves EspB; negatively regulates ESX-1
EspA	<i>rv3616c</i>	Co-secreted with EsxA/EsxB, affects cell wall integrity
EspC	<i>rv3615c</i>	Unknown, T-cell antigen
EspD	<i>rv3614c</i>	Stabilize cellular levels of EspA and EspC

### 1.6.3 Current model of ESX-1 secretion system

Although plenty of ESX-1 components have been individually investigated, the overall mechanism of translocation is still unclear. Based on the evidence from

experimental data and bioinformatic analyses, Majlessi *et al.* have proposed a model of ESX-1 machinery, which is the most informative to date describing the ESX-1 pathway (Fig.1.6) [88].

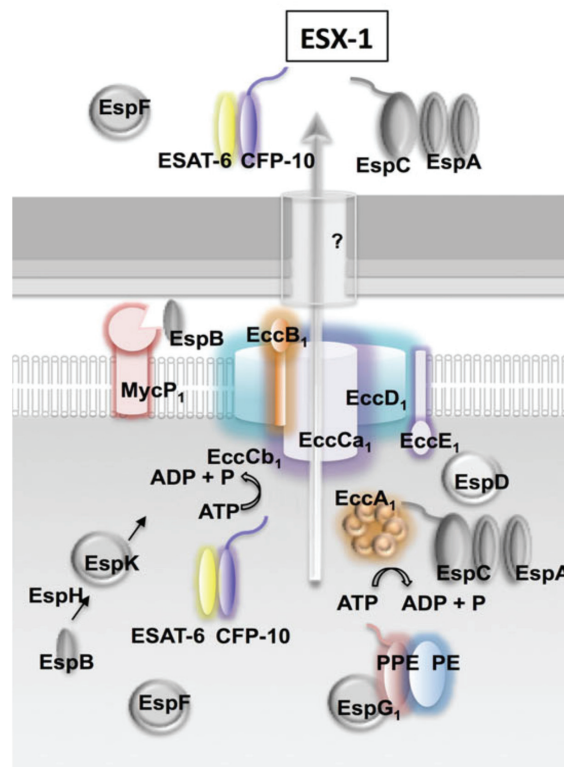


**Fig.1.6 Schematic representation of the ESX-1 secretory apparatus [88].**

EsxA/EsxB (ESAT-6/CFP-10) and EspA/C complexes are secreted by the ESX-1 machinery in a two-step process. The translocation is initiated with substrate recognition by the respective ATPases (EccCb1 or EccA1) via the C-terminal secretion motif YxxxD/E. Subsequently, the substrates are targeted to the putative inner membrane channel comprising EccD, ATPases EccCa1-EccCb1, EccB and EccE. EspF, EspB and PE/PPE are also exported across the cell membrane via an undefined mechanism. During secretion, EspB is cleaved by protease MycP1 in the periplasmic space. The pore protein in the outer membrane has not yet been identified.



## 1.7 Research scope and objective

The ESX-1 secretion system is the principal TB virulence determinant that mediates intracellular spread of pathogenic mycobacteria, such as *M. tb*. As it is essential for pathogenesis, ESX-1 is a potential target for novel anti-TB drug discovery. However, we are still far from the complete understanding of the role of each protein comprising the apparatus as well as their assembly mechanism. The main objective of my thesis is to provide deeper functional and mechanistic insight into the ESX-1-mediated translocation.

In the past years, although more and more clues about the functioning of the ESX-1 system were uncovered by combining genetic approaches and structure-based function studies, a question that still remains to be answered is which is the protein that functions as an outer membrane pore specifically serving for ESX-1 secretion (Fig.1.6). One of the obstacles in addressing this question is the complexity of the mycomembrane where the ESX-1 apparatus is embedded. In contrast to the Gram-negative bacteria (e.g. *E. coli* containing more than 60 integral outer membrane proteins), few outer membrane proteins have been identified in mycobacteria. Only two porins, MctB and OmpATb, were found in *M. tb* [131]. One reason for this is the technical difficulty in isolating the outer membrane protein from the cell wall of mycobacteria. Moreover, genome comparison was not able to find a candidate for the outer membrane pore protein that is related to ESX-1 secretion [34,132]. Adding to the challenge, the cell surface of *M. tb* is covered with a glycan-rich capsular layer. Several ESX-1-associated proteins were identified in the capsule extracts, which proves that ESX-1 apparatus is surface-exposed [38]. However, this also highlights the difficulty in direct visualization. It was noticed that the outer membrane channel of T4SS are formed by a ring of two-helix bundles [133], which is a structure without a typical feature of a porin. Therefore, if a channel is formed by such proteins having this atypical pattern, it would be likely overlooked by current prediction strategies. Similar to the assembly of T4SS, the major part of the injectisome in the T3SS is assembled by multiple copies of hairpin-structured proteins called needle proteins [134], hinting that such structures could be

common in the paralogous systems such as ESX-1. This background knowledge provided a new research direction which eventually led us to identify EspC, a self-polymerizing protein encoded in the *espACD* cluster. As the putative pore protein at the outer membrane of *M. tb*, it is critical for ESX-1 secretion. The results from this project will be described in Chapter 2.

In addition to the research on EspC, Chapters 3 and 4 demonstrate some of the minor findings throughout my PhD period, which are also related to ESX-1. In Chapter 3, I describe the purification of the potential ATPase EccCb1 of *M. tb*, and the determination of ATPase activity. The ability of ATP hydrolysis, which dramatically decreased when a mutation was introduced to the conserved Walker A motif, confirms that EccCb1 belongs to FtsK/SpoIIIE ATPase family as previously predicted. This observation is controversial to what another group reported using EccC of *Thermomonospora curvata* (*T. curvata*) as the model, in which EccC activity was triggered only in the presence of the substrate. Interestingly, the EccC architecture of ESX-1 in *M. tb* is unique as the protein is split into EccCa1 and EccCb1, which would explain the interspecies difference.

*M. tb* is a facultative intracellular pathogen of humans, whose growth and virulence are controlled in response to a multiplicity of environmental factors. Similar facultative pathogens that are Gram-negative, such as *Shigella*, *Salmonella* and *Yersinia*, have been deeply studied with respect to their regulation of virulence factor/effector protein translocation achieved via T3SS. It was reported that these species sense divalent cations such as magnesium and calcium to control T3SS, either in the natural settings inside the host or in the laboratory culture medium. In Chapter 4, we show that “a low calcium response” which exists in *Yersinia* is also found in *M. tb* [135]. Experimentally, the elevated concentrations of calcium in the medium blocked EsxA and EspC secretion, and inhibited bacterial persistence. This suggests that a low intracellular calcium environment is essential for *M. tb* survival, because it promotes ESX-1 secretion as well as bacterial viability in the host cell. The global gene expression in the presence of high concentration of calcium was investigated using RNA-seq analysis. We found that hypoxia response genes in the DevRS regulon were

significantly down-regulated by calcium, which could be the reason for the observed reduced persistence. On the other hand, how exactly calcium inhibits ESX-1 secretion system is not clear from our RNA-seq experiment, indicating that the regulation of ESX-1 may occur at the post-transcriptional level.

Finally in Chapter 5, I critically address the results of my work and present future perspectives for the ESX-1 secretion system research.

## References

1. Zumla A, George A, Sharma V, Herbert RHN, Masham Ilton B, et al. (2015) The WHO 2014 Global tuberculosis report-further to go. *Lancet Global Health* 3: E10-E12.
2. Daniel TM (2006) The history of tuberculosis. *Respir Med* 100: 1862-1870.
3. Hershkovitz I, Donoghue HD, Minnikin DE, Besra GS, Lee OYC, et al. (2008) Detection and Molecular Characterization of 9000-Year-Old *Mycobacterium tuberculosis* from a Neolithic Settlement in the Eastern Mediterranean. *Plos One* 3.
4. Hardy A (1999) Captain of death: the story of tuberculosis. *Medical History* 43: 149-149.
5. Thakur M (2001) Global tuberculosis control report. *Natl Med J India* 14: 189-190.
6. Korenromp EL, Glaziou P, Fitzpatrick C, Floyd K, Hosseini M, et al. (2012) Implementing the global plan to stop TB, 2011-2015--optimizing allocations and the Global Fund's contribution: a scenario projections study. *PLoS One* 7: e38816.
7. Zignol M, Hosseini MS, Wright A, Lambregts-van Weezenbeek C, Nunn P, et al. (2006) Global incidence of multidrug-resistant tuberculosis. *Journal of Infectious Diseases* 194: 479-485.
8. Horwitz MA, Harth G, Dillon BJ, Maslesa-Galic S (2005) Enhancing the protective efficacy of *Mycobacterium bovis* BCG vaccination against tuberculosis by boosting with the *Mycobacterium tuberculosis* major secretory protein. *Infect Immun* 73: 4676-4683.
9. Luca S, Mihaescu T (2013) History of BCG Vaccine. *Maedica (Buchar)* 8: 53-58.
10. Andersen P, Doherty TM (2005) The success and failure of BCG - implications for a novel tuberculosis vaccine. *Nat Rev Microbiol* 3: 656-662.
11. Pym AS, Brodin P, Majlessi L, Brosch R, Demangel C, et al. (2003) Recombinant BCG exporting ESAT-6 confers enhanced protection against tuberculosis. *Nat Med* 9: 533-539.
12. Ottenhoff THM, Kaufmann SHE (2012) Vaccines against Tuberculosis: Where Are We and Where Do We Need to Go? *Plos Pathogens* 8.
13. van Dissel JT, Soonawala D, Joosten SA, Prins C, Arend SM, et al. (2011) Ag85B-ESAT-6 adjuvanted with IC31(R) promotes strong and long-lived *Mycobacterium tuberculosis* specific T cell responses in volunteers with previous BCG vaccination or tuberculosis infection. *Vaccine* 29: 2100-2109.
14. Brandt L, Elhay M, Rosenkrands I, Lindblad EB, Andersen P (2000) ESAT-6 subunit vaccination against *Mycobacterium tuberculosis*. *Infect Immun* 68: 791-795.

15. Millington KA, Fortune SM, Low J, Garces A, Hingley-Wilson SM, et al. (2011) Rv3615c is a highly immunodominant RD1 (Region of Difference 1)-dependent secreted antigen specific for Mycobacterium tuberculosis infection. *Proceedings of the National Academy of Sciences of the United States of America* 108: 5730-5735.
16. Halevy S, Cohen AD, Grossman N (2005) Clinical implications of in vitro drug-induced interferon gamma release from peripheral blood lymphocytes in cutaneous adverse drug reactions. *J Am Acad Dermatol* 52: 254-261.
17. Evans CA (2011) GeneXpert-A Game-Changer for Tuberculosis Control? *Plos Medicine* 8.
18. Berry MP, Graham CM, McNab FW, Xu Z, Bloch SA, et al. (2010) An interferon-inducible neutrophil-driven blood transcriptional signature in human tuberculosis. *Nature* 466: 973-977.
19. Schatz A, Bugie E, Waksman SA (1944) Streptomycin, a substance exhibiting antibiotic activity against gram positive and gram-negative bacteria. *Proceedings of the Society for Experimental Biology and Medicine* 55: 66-69.
20. Wassersug JD (1946) Pulmonary tuberculosis. *N Engl J Med* 235: 220-229.
21. Fox W, Sutherland I (1959) A five-year assessment of patients in a controlled trial of streptomycin with different doses of para-aminosalicylic acid in pulmonary tuberculosis. *Q J Med* 28: 77-95.
22. WHO (2010). *Treatment of Tuberculosis: Guidelines*. 4th ed. Geneva.
23. Zumla A, Nahid P, Cole ST (2013) Advances in the development of new tuberculosis drugs and treatment regimens. *Nat Rev Drug Discov* 12: 388-404.
24. Rattan A, Kalia A, Ahmad N (1998) Multidrug-resistant Mycobacterium tuberculosis: molecular perspectives. *Emerg Infect Dis* 4: 195-209.
25. Centers for Disease C, Prevention (2006) Emergence of Mycobacterium tuberculosis with extensive resistance to second-line drugs--worldwide, 2000-2004. *MMWR Morb Mortal Wkly Rep* 55: 301-305.
26. (1995) TB. A global emergency, WHO, July 1994. *Lepr Rev* 66: 270-271.
27. Barczak AK, Hung DT (2009) Productive steps toward an antimicrobial targeting virulence. *Curr Opin Microbiol* 12: 490-496.
28. Rybniker J, Chen JM, Sala C, Hartkoorn RC, Vocat A, et al. (2014) Anticytolytic screen identifies inhibitors of mycobacterial virulence protein secretion. *Cell Host Microbe* 16: 538-548.
29. Cole ST, Brosch R, Parkhill J, Garnier T, Churcher C, et al. (1998) Deciphering the biology of Mycobacterium tuberculosis from the complete genome sequence. *Nature* 393: 537-544.
30. Brosch R, Gordon SV, Pym A, Eiglmeier K, Garnier T, et al. (2000) Comparative genomics of the mycobacteria. *International Journal of Medical Microbiology* 290: 143-152.

31. Parish T, Stoker NG (1998) Mycobacteria. Bugs and bugbears. *Methods Mol Biol* 101: 1-13.
32. Brennan PJ (2003) Structure, function, and biogenesis of the cell wall of *Mycobacterium tuberculosis*. *Tuberculosis (Edinb)* 83: 91-97.
33. Brown L, Wolf JM, Prados-Rosales R, Casadevall A (2015) Through the wall: extracellular vesicles in Gram-positive bacteria, mycobacteria and fungi. *Nat Rev Microbiol* 13: 620-630.
34. Niederweis M, Danilchanka O, Huff J, Hoffmann C, Engelhardt H (2010) Mycobacterial outer membranes: in search of proteins. *Trends Microbiol* 18: 109-116.
35. Brennan PJ, Nikaido H (1995) The envelope of mycobacteria. *Annu Rev Biochem* 64: 29-63.
36. Brennan PJ, Crick DC (2007) The cell-wall core of *Mycobacterium tuberculosis* in the context of drug discovery. *Current Topics in Medicinal Chemistry* 7: 475-488.
37. Hoffmann C, Leis A, Niederweis M, Plitzko JM, Engelhardt H (2008) Disclosure of the mycobacterial outer membrane: cryo-electron tomography and vitreous sections reveal the lipid bilayer structure. *Proc Natl Acad Sci U S A* 105: 3963-3967.
38. Sani M, Houben EN, Geurtsen J, Pierson J, de Punder K, et al. (2010) Direct visualization by cryo-EM of the mycobacterial capsular layer: a labile structure containing ESX-1-secreted proteins. *PLoS Pathog* 6: e1000794.
39. Daffe M, Etienne G (1999) The capsule of *Mycobacterium tuberculosis* and its implications for pathogenicity. *Tuber Lung Dis* 79: 153-169.
40. Wright EL, Pourshafie M, Barrow WW (1992) *Mycobacterium-Avium* Rough-to-Smooth Colony Conversion Resulting from Growth in Tween 80 without Presence of Type-Specific Glycopeptidolipid Antigens. *Fems Microbiology Letters* 98: 209-216.
41. Mailaender C, Reiling N, Engelhardt H, Bossmann S, Ehlers S, et al. (2004) The MspA porin promotes growth and increases antibiotic susceptibility of both *Mycobacterium bovis* BCG and *Mycobacterium tuberculosis*. *Microbiology-Sgm* 150: 853-864.
42. Cambier CJ, Falkow S, Ramakrishnan L (2014) Host evasion and exploitation schemes of *Mycobacterium tuberculosis*. *Cell* 159: 1497-1509.
43. de Chastellier C (2009) The many niches and strategies used by pathogenic mycobacteria for survival within host macrophages. *Immunobiology* 214: 526-542.
44. Russell DG (2007) Who puts the tubercle in tuberculosis? *Nat Rev Microbiol* 5: 39-47.
45. Rayasam GV, Balganes TS (2015) Exploring the potential of adjunct therapy in tuberculosis. *Trends Pharmacol Sci* 36: 506-513.

46. Yuk JM, Jo EK (2014) Host immune responses to mycobacterial antigens and their implications for the development of a vaccine to control tuberculosis. *Clin Exp Vaccine Res* 3: 155-167.
47. Tonjum T, Welty DB, Jantzen E, Small PL (1998) Differentiation of *Mycobacterium ulcerans*, *M. marinum*, and *M. haemophilum*: Mapping of their relationships to *M. tuberculosis* by fatty acid profile analysis, DNA-DNA hybridization, and 16S rRNA gene sequence analysis. *Journal of Clinical Microbiology* 36: 918-925.
48. Primm TP, Lucero CA, Falkinham JO (2004) Health impacts of environmental mycobacteria. *Clinical Microbiology Reviews* 17: 98-+.
49. Clark HF, Shepard CC (1963) Effect of Environmental Temperatures on Infection with *Mycobacterium Marinum* (Balnei) of Mice and a Number of Poikilothermic Species. *J Bacteriol* 86: 1057-1069.
50. Brosch R, Pym AS, Gordon SV, Cole ST (2001) The evolution of mycobacterial pathogenicity: clues from comparative genomics. *Trends Microbiol* 9: 452-458.
51. Behr MA, Wilson MA, Gill WP, Salamon H, Schoolnik GK, et al. (1999) Comparative genomics of BCG vaccines by whole-genome DNA microarray. *Science* 284: 1520-1523.
52. Gordon SV, Brosch R, Billault A, Garnier T, Eiglmeier K, et al. (1999) Identification of variable regions in the genomes of tubercle bacilli using bacterial artificial chromosome arrays. *Molecular Microbiology* 32: 643-655.
53. Mahairas GG, Sabo PJ, Hickey MJ, Singh DC, Stover CK (1996) Molecular analysis of genetic differences between *Mycobacterium bovis* BCG and virulent *M. bovis*. *Journal of Bacteriology* 178: 1274-1282.
54. Mattow J, Jungblut PR, Schaible UE, Mollenkopf HJ, Lamer S, et al. (2001) Identification of proteins from *Mycobacterium tuberculosis* missing in attenuated *Mycobacterium bovis* BCG strains. *Electrophoresis* 22: 2936-2946.
55. Brosch R, Gordon SV, Marmiesse M, Brodin P, Buchrieser C, et al. (2002) A new evolutionary scenario for the *Mycobacterium tuberculosis* complex. *Proc Natl Acad Sci U S A* 99: 3684-3689.
56. Gunawardena HP, Feltcher ME, Wrobel JA, Gu S, Braunstein M, et al. (2013) Comparison of the membrane proteome of virulent *Mycobacterium tuberculosis* and the attenuated *Mycobacterium bovis* BCG vaccine strain by label-free quantitative proteomics. *J Proteome Res* 12: 5463-5474.
57. Jungblut PR, Schaible UE, Mollenkopf HJ, Zimny-Arndt U, Raupach B, et al. (1999) Comparative proteome analysis of *Mycobacterium tuberculosis* and *Mycobacterium bovis* BCG strains: towards functional genomics of microbial pathogens. *Molecular Microbiology* 33: 1103-1117.
58. Brosch R, Gordon SV, Eiglmeier K, Garnier T, Cole ST (2000) Comparative genomics of the leprosy and tubercle bacilli. *Res Microbiol* 151: 135-142.



59. Gordon RE, Smith MM (1953) Rapidly growing, acid fast bacteria. I. Species' descriptions of *Mycobacterium phlei* Lehmann and Neumann and *Mycobacterium smegmatis* (Trevisan) Lehmann and Neumann. *J Bacteriol* 66: 41-48.
60. Noens EE, Williams C, Anandhakrishnan M, Poulsen C, Ehebauer MT, et al. (2011) Improved mycobacterial protein production using a *Mycobacterium smegmatis* groEL1 Delta C expression strain. *Bmc Biotechnology* 11.
61. Wang R, Prince JT, Marcotte EM (2005) Mass spectrometry of the *M. smegmatis* proteome: protein expression levels correlate with function, operons, and codon bias. *Genome Res* 15: 1118-1126.
62. Park E, Rapoport TA (2012) Mechanisms of Sec61/SecY-mediated protein translocation across membranes. *Annu Rev Biophys* 41: 21-40.
63. Palmer T, Berks BC (2012) The twin-arginine translocation (Tat) protein export pathway. *Nat Rev Microbiol* 10: 483-496.
64. Frobel J, Rose P, Muller M (2012) Twin-arginine-dependent translocation of folded proteins. *Philos Trans R Soc Lond B Biol Sci* 367: 1029-1046.
65. Costa TR, Felisberto-Rodrigues C, Meir A, Prevost MS, Redzej A, et al. (2015) Secretion systems in Gram-negative bacteria: structural and mechanistic insights. *Nat Rev Microbiol* 13: 343-359.
66. Tseng TT, Tyler BM, Setubal JC (2009) Protein secretion systems in bacterial-host associations, and their description in the Gene Ontology. *BMC Microbiol* 9 Suppl 1: S2.
67. Galan JE, Wolf-Watz H (2006) Protein delivery into eukaryotic cells by type III secretion machines. *Nature* 444: 567-573.
68. Raymond B, Young JC, Pallett M, Endres RG, Clements A, et al. (2013) Subversion of trafficking, apoptosis, and innate immunity by type III secretion system effectors. *Trends Microbiol* 21: 430-441.
69. Christie PJ, Whitaker N, Gonzalez-Rivera C (2014) Mechanism and structure of the bacterial type IV secretion systems. *Biochim Biophys Acta* 1843: 1578-1591.
70. Low HH, Gubellini F, Rivera-Calzada A, Braun N, Connery S, et al. (2014) Structure of a type IV secretion system. *Nature* 508: 550-553.
71. Alvarez-Martinez CE, Christie PJ (2009) Biological diversity of prokaryotic type IV secretion systems. *Microbiol Mol Biol Rev* 73: 775-808.
72. Suarez G, Sierra JC, Sha J, Wang S, Erova TE, et al. (2008) Molecular characterization of a functional type VI secretion system from a clinical isolate of *Aeromonas hydrophila*. *Microb Pathog* 44: 344-361.
73. Basler M, Ho BT, Mekalanos JJ (2013) Tit-for-tat: type VI secretion system counterattack during bacterial cell-cell interactions. *Cell* 152: 884-894.
74. Kudryashev M, Wang RY, Brackmann M, Scherer S, Maier T, et al. (2015) Structure of the type VI secretion system contractile sheath. *Cell* 160: 952-962.



75. Basler M, Pilhofer M, Henderson GP, Jensen GJ, Mekalanos JJ (2012) Type VI secretion requires a dynamic contractile phage tail-like structure. *Nature* 483: 182-186.
76. Delepelaire P (2004) Type I secretion in gram-negative bacteria. *Biochim Biophys Acta* 1694: 149-161.
77. Filloux A (2004) The underlying mechanisms of type II protein secretion. *Biochim Biophys Acta* 1694: 163-179.
78. Cornelis GR (2006) The type III secretion injectisome. *Nat Rev Microbiol* 4: 811-825.
79. Henderson IR, Navarro-Garcia F, Desvaux M, Fernandez RC, Ala'Aldeen D (2004) Type V protein secretion pathway: the autotransporter story. *Microbiol Mol Biol Rev* 68: 692-744.
80. Coulthurst SJ (2013) The Type VI secretion system - a widespread and versatile cell targeting system. *Res Microbiol* 164: 640-654.
81. Hsu T, Hingley-Wilson SM, Chen B, Chen M, Dai AZ, et al. (2003) The primary mechanism of attenuation of bacillus Calmette-Guerin is a loss of secreted lytic function required for invasion of lung interstitial tissue. *Proc Natl Acad Sci U S A* 100: 12420-12425.
82. Coros A, Callahan B, Battaglioli E, Derbyshire KM (2008) The specialized secretory apparatus ESX-1 is essential for DNA transfer in *Mycobacterium smegmatis*. *Molecular Microbiology* 69: 794-808.
83. Ilghari D, Lightbody KL, Veverka V, Waters LC, Muskett FW, et al. (2011) Solution structure of the *Mycobacterium tuberculosis* EsxG.EsxH complex: functional implications and comparisons with other *M. tuberculosis* Esx family complexes. *J Biol Chem* 286: 29993-30002.
84. Serafini A, Pisu D, Palu G, Rodriguez GM, Manganelli R (2013) The ESX-3 Secretion System Is Necessary for Iron and Zinc Homeostasis in *Mycobacterium tuberculosis*. *Plos One* 8.
85. Sayes F, Sun L, Di Luca M, Simeone R, Degaiffier N, et al. (2012) Strong immunogenicity and cross-reactivity of *Mycobacterium tuberculosis* ESX-5 type VII secretion: encoded PE-PPE proteins predicts vaccine potential. *Cell Host Microbe* 11: 352-363.
86. Strong M, Sawaya MR, Wang S, Phillips M, Cascio D, et al. (2006) Toward the structural genomics of complexes: crystal structure of a PE/PPE protein complex from *Mycobacterium tuberculosis*. *Proc Natl Acad Sci U S A* 103: 8060-8065.
87. Ates LS, Ummels R, Commandeur S, van de Weerd R, Sparrius M, et al. (2015) Essential Role of the ESX-5 Secretion System in Outer Membrane Permeability of Pathogenic *Mycobacteria*. *PLoS Genet* 11: e1005190.
88. Majlessi L, Prados-Rosales R, Casadevall A, Brosch R (2015) Release of mycobacterial antigens. *Immunol Rev* 264: 25-45.

89. Daleke MH, Ummels R, Bawono P, Heringa J, Vandenbroucke-Grauls CM, et al. (2012) General secretion signal for the mycobacterial type VII secretion pathway. *Proc Natl Acad Sci U S A* 109: 11342-11347.
90. Solomonson M, Setiাপutra D, Makepeace KAT, Lameignere E, Petrotchenko EV, et al. (2015) Structure of EspB from the ESX-1 Type VII Secretion System and Insights into its Export Mechanism. *Structure* 23: 571-583.
91. Houben EN, Korotkov KV, Bitter W (2014) Take five - Type VII secretion systems of Mycobacteria. *Biochim Biophys Acta* 1843: 1707-1716.
92. Pym AS, Brodin P, Brosch R, Huerre M, Cole ST (2002) Loss of RD1 contributed to the attenuation of the live tuberculosis vaccines *Mycobacterium bovis* BCG and *Mycobacterium microti*. *Mol Microbiol* 46: 709-717.
93. Stoop EJM, Bitter W, van der Sar AM (2012) Tubercle bacilli rely on a type VII army for pathogenicity. *Trends in Microbiology* 20: 477-484.
94. Brodin P, Majlessi L, Marsollier L, de Jonge MI, Bottai D, et al. (2006) Dissection of ESAT-6 system 1 of *Mycobacterium tuberculosis* and impact on immunogenicity and virulence. *Infect Immun* 74: 88-98.
95. Stanley SA, Raghavan S, Hwang WW, Cox JS (2003) Acute infection and macrophage subversion by *Mycobacterium tuberculosis* require a specialized secretion system. *Proc Natl Acad Sci U S A* 100: 13001-13006.
96. Lewis KN, Liao R, Guinn KM, Hickey MJ, Smith S, et al. (2003) Deletion of RD1 from *Mycobacterium tuberculosis* mimics bacille Calmette-Guerin attenuation. *J Infect Dis* 187: 117-123.
97. Guinn KM, Hickey MJ, Mathur SK, Zakel KL, Grotzke JE, et al. (2004) Individual RD1-region genes are required for export of ESAT-6/CFP-10 and for virulence of *Mycobacterium tuberculosis*. *Molecular Microbiology* 51: 359-370.
98. Gey van Pittius N, Warren RM, van Helden PD (2002) ESAT-6 and CFP-10: What is the diagnosis? *Infection and Immunity* 70: 6509-6510.
99. Brandt L, Oettinger T, Holm A, Andersen AB, Andersen P (1996) Key epitopes on the ESAT-6 antigen recognized in mice during the recall of protective immunity to *Mycobacterium tuberculosis*. *Journal of Immunology* 157: 3527-3533.
100. van Dissel JT, Arend SM, Prins C, Bang P, Tingskov PN, et al. (2010) Ag85B-ESAT-6 adjuvanted with IC31 promotes strong and long-lived *Mycobacterium tuberculosis* specific T cell responses in naive human volunteers. *Vaccine* 28: 3571-3581.
101. Renshaw PS, Panagiotidou P, Whelan A, Gordon SV, Hewinson RG, et al. (2002) Conclusive evidence that the major T-cell antigens of the *Mycobacterium tuberculosis* complex ESAT-6 and CFP-10 form a tight, 1 : 1 complex and characterization of the structural properties of ESAT-6, CFP-10, and the ESAT-6-CFP-10 complex - Implications for pathogenesis and virulence. *Journal of Biological Chemistry* 277: 21598-21603.

102. Renshaw PS, Lightbody KL, Veverka V, Muskett FW, Kelly G, et al. (2005) Structure and function of the complex formed by the tuberculosis virulence factors CFP-10 and ESAT-6. *EMBO J* 24: 2491-2498.
103. de Jonge MI, Pehau-Arnaudet G, Fretz MM, Romain F, Bottai D, et al. (2007) ESAT-6 from *Mycobacterium tuberculosis* dissociates from its putative chaperone CFP-10 under acidic conditions and exhibits membrane-lysing activity. *J Bacteriol* 189: 6028-6034.
104. Fortune SM, Jaeger A, Sarracino DA, Chase MR, Sasseti CM, et al. (2005) Mutually dependent secretion of proteins required for mycobacterial virulence. *Proc Natl Acad Sci U S A* 102: 10676-10681.
105. Simeone R, Bottai D, Brosch R (2009) ESX/type VII secretion systems and their role in host-pathogen interaction. *Current Opinion in Microbiology* 12: 4-10.
106. Tan T, Lee WL, Alexander DC, Grinstein S, Liu J (2006) The ESAT-6/CFP-10 secretion system of *Mycobacterium marinum* modulates phagosome maturation. *Cell Microbiol* 8: 1417-1429.
107. Gao LY, Guo S, McLaughlin B, Morisaki H, Engel JN, et al. (2004) A mycobacterial virulence gene cluster extending RD1 is required for cytolysis, bacterial spreading and ESAT-6 secretion. *Molecular Microbiology* 53: 1677-1693.
108. Xu J, Laine O, Masciocchi M, Manoranjan J, Smith J, et al. (2007) A unique *Mycobacterium* ESX-1 protein co-secretes with CFP-10/ESAT-6 and is necessary for inhibiting phagosome maturation. *Molecular Microbiology* 66: 787-800.
109. Chen JM, Zhang M, Rybniker J, Boy-Rottger S, Dhar N, et al. (2013) *Mycobacterium tuberculosis* EspB binds phospholipids and mediates EsxA-independent virulence. *Mol Microbiol* 89: 1154-1166.
110. Ohol YM, Goetz DH, Chan K, Shiloh MU, Craik CS, et al. (2010) *Mycobacterium tuberculosis* MycP1 protease plays a dual role in regulation of ESX-1 secretion and virulence. *Cell Host Microbe* 7: 210-220.
111. Bottai D, Majlessi L, Simeone R, Frigui W, Laurent C, et al. (2011) ESAT-6 secretion-independent impact of ESX-1 genes *espF* and *espG1* on virulence of *Mycobacterium tuberculosis*. *J Infect Dis* 203: 1155-1164.
112. Ekiert DC, Cox JS (2014) Structure of a PE-PPE-EspG complex from *Mycobacterium tuberculosis* reveals molecular specificity of ESX protein secretion. *Proc Natl Acad Sci U S A* 111: 14758-14763.
113. Korotkova N, Freire D, Phan TH, Ummels R, Creekmore CC, et al. (2014) Structure of the *Mycobacterium tuberculosis* type VII secretion system chaperone EspG5 in complex with PE25-PPE41 dimer. *Mol Microbiol* 94: 367-382.
114. Daleke MH, van der Woude AD, Parret AH, Ummels R, de Groot AM, et al. (2012) Specific chaperones for the type VII protein secretion pathway. *J Biol Chem* 287: 31939-31947.

115. Gey van Pittius NC, Sampson SL, Lee H, Kim Y, van Helden PD, et al. (2006) Evolution and expansion of the *Mycobacterium tuberculosis* PE and PPE multigene families and their association with the duplication of the ESAT-6 (*esx*) gene cluster regions. *BMC Evol Biol* 6: 95.
116. Sampson SL (2011) Mycobacterial PE/PPE Proteins at the Host-Pathogen Interface. *Clinical & Developmental Immunology*.
117. Sassetti CM, Rubin EJ (2003) Genetic requirements for mycobacterial survival during infection. *Proc Natl Acad Sci U S A* 100: 12989-12994.
118. Demangel C, Brodin P, Cockle PJ, Brosch R, Majlessi L, et al. (2004) Cell envelope protein PPE68 contributes to *Mycobacterium tuberculosis* RD1 immunogenicity independently of a 10-kilodalton culture filtrate protein and ESAT-6. *Infect Immun* 72: 2170-2176.
119. Houben EN, Bestebroer J, Ummels R, Wilson L, Piersma SR, et al. (2012) Composition of the type VII secretion system membrane complex. *Mol Microbiol* 86: 472-484.
120. Rosenberg OS, Dovala D, Li X, Connolly L, Bendebury A, et al. (2015) Substrates Control Multimerization and Activation of the Multi-Domain ATPase Motor of Type VII Secretion. *Cell* 161: 501-512.
121. Wagner JM, Evans TJ, Korotkov KV (2014) Crystal structure of the N-terminal domain of EccA(1) ATPase from the ESX-1 secretion system of *Mycobacterium tuberculosis*. *Proteins* 82: 159-163.
122. Luthra A, Mahmood A, Arora A, Ramachandran R (2008) Characterization of Rv3868, an essential hypothetical protein of the ESX-1 secretion system in *Mycobacterium tuberculosis*. *J Biol Chem* 283: 36532-36541.
123. Champion PA, Champion MM, Manzanillo P, Cox JS (2009) ESX-1 secreted virulence factors are recognized by multiple cytosolic AAA ATPases in pathogenic mycobacteria. *Mol Microbiol* 73: 950-962.
124. MacGurn JA, Raghavan S, Stanley SA, Cox JS (2005) A non-RD1 gene cluster is required for *Snm* secretion in *Mycobacterium tuberculosis*. *Molecular Microbiology* 57: 1653-1663.
125. Blasco B, Chen JM, Hartkoorn R, Sala C, Uplekar S, et al. (2012) Virulence Regulator *EspR* of *Mycobacterium tuberculosis* Is a Nucleoid-Associated Protein. *Plos Pathogens* 8.
126. Cao GX, Howard ST, Zhang PP, Hou GH, Pang XH (2013) Functional Analysis of the *EspR* Binding Sites Upstream of *espR* in *Mycobacterium tuberculosis*. *Current Microbiology* 67: 572-579.
127. Das C, Ghosh TS, Mande SS (2011) Computational analysis of the ESX-1 region of *Mycobacterium tuberculosis*: insights into the mechanism of type VII secretion system. *PLoS One* 6: e27980.
128. Chen JM, Boy-Rottger S, Dhar N, Sweeney N, Buxton RS, et al. (2012) *EspD* is critical for the virulence-mediating ESX-1 secretion system in *Mycobacterium tuberculosis*. *J Bacteriol* 194: 884-893.

129. Garces A, Atmakuri K, Chase MR, Woodworth JS, Krastins B, et al. (2010) EspA Acts as a Critical Mediator of ESX1-Dependent Virulence in *Mycobacterium tuberculosis* by Affecting Bacterial Cell Wall Integrity. *Plos Pathogens* 6.
130. Chen JM, Zhang M, Rybniker J, Bastera L, Dhar N, et al. (2013) Phenotypic profiling of *Mycobacterium tuberculosis* EspA point mutants reveals that blockage of ESAT-6 and CFP-10 secretion in vitro does not always correlate with attenuation of virulence. *J Bacteriol* 195: 5421-5430.
131. van der Woude AD, Mahendran KR, Ummels R, Piersma SR, Pham TV, et al. (2013) Differential Detergent Extraction of *Mycobacterium marinum* Cell Envelope Proteins Identifies an Extensively Modified Threonine-Rich Outer Membrane Protein with Channel Activity. *Journal of Bacteriology* 195: 2050-2059.
132. Mah N, Perez-Iratxeta C, Andrade-Navarro MA (2010) Outer membrane pore protein prediction in mycobacteria using genomic comparison. *Microbiology-Sgm* 156: 2506-2515.
133. Chandran V, Fronzes R, Duquerroy S, Cronin N, Navaza J, et al. (2009) Structure of the outer membrane complex of a type IV secretion system. *Nature* 462: 1011-1015.
134. Demers JP, Habenstein B, Loquet A, Kumar Vasa S, Giller K, et al. (2014) High-resolution structure of the *Shigella* type-III secretion needle by solid-state NMR and cryo-electron microscopy. *Nat Commun* 5: 4976.
135. Fowler JM, Brubaker RR (1994) Physiological basis of the low calcium response in *Yersinia pestis*. *Infect Immun* 62: 5234-5241.



## Chapter 2

**EspC forms a filamentous structure in the cell envelope of *Mycobacterium tuberculosis* and effects ESX-1 secretion**





## 2.1 Abstract

Pathogenicity of *M. tb* is mediated by the ESX-1 system, which secretes the major virulence factors, EsxA and EsxB. Functional information about ESX-1 components is scarce. Here, we show purified EspC to homodimerize *via* disulfide bond formation and self-assemble into long filaments. EspC associates with EspA in the cytoplasm and membrane, then polymerizes during export to form filaments in *M. tb*. The C-terminal domain is required for multimerization as truncation and selected point mutations therein impact EspC filament formation, thus reducing secretion of EsxA and causing complete or partial attenuation of *M. tb*. EspC was localized by immunogold electron microscopy in whole cells or cryo-sections as an ~50 nm long filamentous structure that is attached to the plasma membrane, spans the capsule layer and is surface-exposed. Our data support a model in which EspC contributes to a channel used to secrete EsxA/B and cause disease.

## 2.2 Introduction

In this chapter, we investigated the role of EspC in the ESX-1 secretion system. Most mycobacteria contain an *esx-1* locus located near *oriC*, the chromosomal origin of replication, but only the pathogens possess the distally located *espACD* gene cluster (Fig.2.1a). EspC (Rv3615c), encoded in *espACD* cluster, is a small protein with a YxxxD motif, which is also a highly specific T-cell antigen [1]. Secondary structure predictions indicate that EspC, like the cytolytic EsxA and other Esx-family proteins, comprises two alpha helices connected by a short loop (Fig.2.1b). An alignment of the EspC proteins revealed strict conservation of 45 of the 103 amino acid residues (Fig.2.1b). Prominent among these were the YxxxD/E motif (Y87-D91) and a single cysteine residue (Cys-48). A second paralogous copy of this cluster, comprising *espEFG<sub>1</sub>H*, occurs at the 5'-end of the *esx-1* locus in *M. tb* and *M. marinum*. In *M. leprae*, the *espEFG<sub>1</sub>* genes have undergone pseudogenization so cannot contribute to EsxA/B secretion. In *M. tb*, EspF is also 103 amino acids long, shares 37 identical residues, including the YxxxD motif, with EspC and is also predicted to contain two alpha helices (Fig.2.1c). Both the *espC* and *espF* genes are transcribed and their proteins have been detected by proteomics [2]. Therefore, overlap function cannot be excluded.

Given the co-dependent manner of secretion of EsxA/EsxB, and EspA/EspC, it is likely that these proteins interact or form a complex during translocation [3,4]. Our functional investigation of EspC provides new insight into the ESX-1 secretion mechanism. We reveal that EspC interacts initially with EspA in the cytoplasm and then the cell membrane before polymerizing during export into a filament that spans the capsule of *M. tb*. Filament formation is essential for ESX-1 secretion and pathogenesis and EspC functionally resembles the needle proteins of T3SS, which form a conduit through the cell wall of pathogenic Gram-negative bacteria [5-8].

## 2.3 Results

### Purification, oligomerization and filament formation of recombinant EspC

To investigate the function of EspC, we initially overexpressed and purified an N-terminally His-tagged form from *Escherichia coli* (*E. coli*) (Fig.2.2a,b). However, since the solubility was low we adopted a mycobacterial expression system, based on the *M. smegmatis* groEL1ΔC strain [9,10], thereby improving solubility and enabling purification to homogeneity.

During purification we noticed that the solubility of EspC was salt-dependent and therefore used 500 mM NaCl. Surprisingly, this small protein was predominantly expressed as a polymer with an estimated molecular weight of >100 kDa according to size exclusion chromatography (Fig.2.3a). Circular dichroism (CD) spectroscopy indicated that the polymer was mainly composed of  $\alpha$ -helices (Fig.2.3b). Urea-denatured EspC could refold and self-associate into a polymer of similar size to the native state (Fig.2.3a). As noted above, EspC has a single cysteine residue, Cys-48, that contributes to homo-dimerization; the dimer of purified EspC, visible by SDS-PAGE, was converted to a monomer when treated with the reducing agents  $\beta$ -mercapto-ethanol (BME) or dithiothreitol (DTT), implying the presence of intermolecular disulfide bonds in the EspC polymer (Fig.2.3c). Lowering the NaCl concentration caused purified EspC to further self-assemble into filaments *in vitro*. Transmission electron micrographs of negatively stained EspC revealed that the filaments elongate over time (Fig.2.3d). After 5 days, EspC existed predominantly as needle-like filaments of >100 nm length and around 15 nm in diameter.

### EspC is not membranolytic

Secreted EsxA damages the phagosomal membrane thereby enabling *M. tb* to escape from the phagosome [11-13]. To establish whether EspC, which resembles EsxA in length and predicted structure, can lyse membranes, or make pores, we performed a macrophage cytotoxicity assay in which the intracellular potassium

level was used to monitor the viability of RAW 264.7 cells after exposure to purified EspC for 2 h. Unlike EsxA, which caused massive potassium efflux, EspC had no detectable cytolytic activity (Fig.2.4).

### **EspC polymerizes upon secretion from *M. tb***

Since EspC overexpressed by *M. smegmatis* was polymeric it was important to analyze its oligomeric state in *M. tb*. However, as all our attempts to raise specific EspC antibodies were unsuccessful, we produced a hemagglutinin (HA) epitope-tagged form by inserting the HA coding sequence after the start codon of EspC. To ensure that the resultant HA-tagged EspC, which was readily detected by the cognate murine monoclonal antibody, retained full activity a complementation experiment was undertaken with an *espC* transposon insertion mutant (*espC::Tn*) of *M. tb*. We introduced the pMD31-*espAC<sub>HA</sub>D* construct into the *espC::Tn* mutant (Fig.2.5a) in order to test for ESX-1 function. Use of the entire *espACD* cluster was required since the three genes are co-transcribed [10]; transformants bearing the empty vector pMD31 failed to produce EspC (Fig.2.5c) or to secrete EsxA (Fig.2.5b). By contrast, the ESX-1 secretion system of the *espC::Tn+espAC<sub>HA</sub>D* strain was fully functional since EsxA was detected in the culture filtrate in normal amounts (Fig.2.5b). Thus, HA-tagging did not noticeably affect function and allowed for further characterization of EspC.

Given that disulfide bond formation is important for assembly of the purified protein, we assessed the effect of DTT on the multimeric state of EspC produced in *M. tb*. Cell lysates and culture filtrates were analyzed by SDS-PAGE and immunoblotting. In the cell lysate of *M. tb*, EspC was monomeric, irrespective of the presence of DTT, whereas in the culture filtrate, EspC appeared as multiple SDS-stable high molecular weight species thereby implying that EspC polymerization occurs during secretion (Fig.2.5c). Notably, the polymeric forms in the culture filtrate were reduced by DTT treatment to lower molecular weight forms, including the monomer, which again indicates the role of disulfide bond formation in polymer assembly. Stabilization of EspC by Cys-48 is supported by our finding that

its replacement by serine in strain *espC::Tn+espAC<sup>C48S</sup>D* decreased the amount of EspC to below the level of detection thereby ablating EsxA secretion (Fig.2.6).

### **EspC interacts with EspA in the cytosol and cell envelope**

YxxxD proteins are expected to interact with a WxG100 partner protein and in the case of EspC the likely candidate is EspA [3,14]. To identify potential partners, we exploited the ability of beads coated with HA-antibodies to capture the HA-tagged form of EspC present in cell lysates. On analysis of the silver-stained proteins bound to such beads, a single 40 kDa species was present when HA-tagged EspC was used but not when native EspC was employed (Fig.2.5d). This species was identified by LC-MS/MS analysis, after trypsin digestion, as EspA (Spectrum count: 18; Sequence coverage: 37%). These results were confirmed by immunoblotting using HA-antibodies and EspA-specific antibodies (Fig.2.5e). This demonstrated a specific interaction between EspA and EspC in cell lysates but not between EspC and EsxA or EsxB. To establish whether EspA interacts with EspC in the cytosol, cell membrane fraction or both, the immunoprecipitation experiment was repeated with sub-cellular fractions of the cell lysate. EspA co-precipitated with HA-tagged EspC from both the cytosolic and membrane fractions (Fig.2.7a,b), and EspA and EspC appeared to be more abundant in the latter (Fig.2.7c,d).

Like EspC, EspA forms disulfide-bonded homodimers via Cys-138. To explore the possibility of heterodimeric disulfide bond formation, we repeated the pull-down experiment in the presence of excess DTT but found the EspA-EspC interaction to be unaffected (data not shown). Consequently, we constructed and tested an EspA variant where Cys-138 was replaced by alanine. Again, EspC interacted normally with EspA<sup>C138A</sup> implying that this residue does not contribute to the EspA/C association in *M. tb* (Fig.2.8). In the same experiment, we also tested if EspA<sup>W55R</sup> mutant would dissociate the heterodimer. The Trp-55 (W55) in the WxG motif of EspA is a conserved amino acid localized in the region between two predicted helices. The replacement of the Trp-55 to Arg was found to disrupt the secretion of EspA and EsxA/B, and attenuate the virulence of *M. tb* in cellular model of infection [20]. It turned out that EspC level in the cell lysate of the EspA<sup>W55R</sup> variant was

significantly reduced, while EspA level was not changed by the mutation (Fig.2.8a). As EspA may be required to stabilize EspC intracellularly [20], we speculate that the EspC reduction might attribute to the disruption of the EspA/C interaction. Thus, Trp-55 of EspA is likely to mediate formation of the heterodimer, thereby affecting the ESX-1 secretion.

#### **YxxxD motif impacts EspC secretion and ESX-1 function**

To establish whether the YxxxD motif is required for EspC secretion, site-directed mutagenesis was used to replace Tyr-87 and Asp-91 by alanine. EspC abundance was greatly affected by the Tyr87Ala substitution and the protein was only detected in the cell lysates. By contrast, although wild type levels of the Asp91Ala variant of EspC were found in the cells, none was detected in the culture filtrate. Both mutations also led to a complete block in EsxA secretion and cytotoxicity (Fig.2.6).

#### **The C-terminal domain is critical for polymer formation and stability**

Since the EspC polymer exported from *M. tb* was not fully disrupted by DTT, and purified EspC<sup>C48S</sup> still polymerizes (Fig.2.9), we reasoned that additional features might be essential for EspC assembly. There are functional and structural similarities between EspC and certain T3SS needle proteins, such as MxiH of *Shigella* and PrgI of *Salmonella*, as their N-termini can be modified without affecting the activity of the respective secretion systems. The C-terminus of PrgI is important for polymerization and deletion of the last five amino acid residues from MxiH causes polymerization and needle formation defects [7,15]. This region contains an IxxxF motif that is also present in EspC (Ile-98xxxPhe-102, Fig.2.10a). Consequently, the role of the corresponding region of EspC was investigated.

A C-terminally truncated form, lacking the last six amino acid residues, EspC<sup>Δ6</sup>, was constructed together with derivatives in which residues Ile-98 and Phe-102 were replaced, either singly or together, by Ala. The corresponding His-tagged proteins were overexpressed in *M. smegmatis*, purified and characterized by gel

filtration chromatography. In contrast to EspC<sup>wt</sup>, the EspC<sup>CA6</sup> protein was predominantly monomeric (Fig.2.10b), while the EspC<sup>I98A</sup> variant exhibited a profile containing a mixture of monomeric and multimeric forms. EspC<sup>F102A</sup> behaved like wild type protein (data not shown). The combined results indicate that the C-terminal region of EspC contributes to polymer formation like its counterpart in the T3SS needle proteins.

To gain deeper functional insight into this region a further six mutations were introduced into *espC* and the resultant HA-tagged proteins expressed in the *espC::Tn* mutant of *M. tb* then assessed for multimerization, export and impact on EsxA secretion (Fig.2.10, Fig.2.11). Of the eight point mutants tested, two exhibited striking phenotypes: EspC<sup>R95A</sup> and EspC<sup>I98A</sup>. The EspC<sup>R95A</sup> protein was present in slightly reduced amounts in cell lysates, but almost absent from the culture filtrate, where EsxA was not detected (Fig.2.11). Compared to wild type EspC, the EspC<sup>I98A</sup> protein occurred in reduced amounts in the culture filtrate, where less EsxA was present. The EspC<sup>CA6</sup> protein was scarcely detectable in cell lysates, consequently, EsxA was not secreted (Fig.2.10c,d).

To assess the impact of these C-terminal EspC modifications on ESX-1-mediated cytotoxicity selected mutants were used to infect THP-1 cells. This revealed that the C-terminal truncation, as well as mutation of R95A, caused severe attenuation of *M. tb* compared to the *espC::Tn+espAC<sup>wt</sup>D* strain. By contrast, expression of the EspC<sup>I98A</sup> protein led to an intermediate level of virulence (Fig.2.10e and Fig.2.11).

In Table 2.1, we summarize phenotypes of all EspC variants constructed in this study and their impact on protein stability, export, ability to multimerize *in vitro* (C48, I98, F102, EspC<sup>CA6</sup>) or in the cell envelope (D75, R95, K96, I98, D99, L101, F102, T103, EspC<sup>CA6</sup>) and affect on cytotoxicity leading to attenuation.

### **EspC spans the capsule and is surface-exposed**

In Gram-negative bacteria T3SS needle proteins are surface exposed. To establish whether this were also true for EspC, we investigated its subcellular localization in

*M. tb.* ESX-1 substrates have been detected in the capsular layer of *M. marinum* [16], consequently, we examined this cellular compartment for EspC. The capsule of mycobacteria can be removed by extraction with a detergent such as Tween-80 that is usually added to cultures to prevent clumping [16]. The matched strains, *espC::Tn+espAC<sub>HAD</sub>* and *espC::Tn+pMD31*, were grown in Sauton's medium with or without Tween-80 to mid-log phase. After extraction with the mild detergent Genapol X-080, capsular proteins were TCA-precipitated and analyzed by immunoblotting. HA-tagged EspC was clearly detectable in the *M. tb* capsule extract from *espC::Tn+espAC<sub>HAD</sub>* cells grown without Tween-80 but was completely absent when these cells had been grown with Tween-80 or when the *espC::Tn+pMD31* mutant was used (Fig.2.12a and data not shown). The capsular EspC was still present in SDS-resistant multimeric form despite the Genapol extraction and TCA-precipitation. Furthermore, like the form present in the culture filtrate, capsular EspC was mainly reduced to the monomer by DTT treatment. By comparing the respective band intensities in culture filtrates (Fig.2.5b,c), EspC was much more abundant in the capsule of *M. tb*, where EsxA was undetectable.

Immunogold-labeling was then employed to visualize EspC on the surface of intact *M. tb* cells by transmission electron microscopy (TEM). When both the *espC::Tn+espAC<sub>HAD</sub>* and *espC::Tn+pMD31* strains were grown in Sauton's medium lacking Tween-80, the capsular layers were clearly seen as a transparent zone outside the cell (Fig.2.12b). EspC labeling was randomly distributed along the cell surface of the *espC::Tn+espAC<sub>HAD</sub>* strain and present in clusters or as a filament (Fig.2.12b inset), whereas the *espC::Tn+pMD31* mutant showed no labeling (Fig.2.12b). Independent confirmation of this finding was obtained by immunofluorescence microscopy using secondary antibodies labeled with the fluorescent dye Alexa-488 (Fig.2.12c).

Next, most of the capsule was removed from intact cells by treatment with diluted Genapol X-080 and immunogold localization of EspC was performed. This revealed gold beads in a filamentous arrangement on the cell surface (Fig.2.13a). TEM analysis of HA-antibody stained cryo-sections of cells also revealed EspC filaments within (Fig.2.13b) and beyond (Fig.2.13c) the capsule layer. Taken together, the EM



results indicate that EspC spans the capsule and is exposed on the surface of *M. tb*.

## 2.4 Discussion

It has long been known that the EsxA/EsxB heterodimer and the EspA and EspC proteins of the *M. tb* ESX-1 secretion system are mutually co-dependent for their secretion [17]. A partial explanation for this codependency was provided by a recent investigation of the structure of the EccC multidomain ATPase in complex with EsxB [18]. Binding of EsxB triggered multimerization and activation of EccC that then became functionally competent for type VII secretion. However, while this finding accounts for an early stage in the co-dependent secretion it does not explain the roles of EspA and EspC. Here, we have studied the functions of EspC, and to a lesser extent EspA, which has previously been hampered by difficulty in overexpression and purification of the recombinant proteins. Highly pure EspC protein was obtained by using an *M. smegmatis* expression system thus enabling downstream biochemical and biophysical characterization.

Bioinformatic and CD analyses predict EspC to fold into a predominantly  $\alpha$ -helical structure reminiscent of those of the EsxA-like WxG100 proteins but unlike EsxA, EspC had no cytolytic activity. During purification from *M. smegmatis*, EspC behaved as a polymer with a helical structure that assembled into long filaments. Importantly, EspC detected in the culture filtrate of *M. tb* also assembled into large SDS-resistant polymers showing that the affinity purified protein behaved similarly to native EspC. There are interesting similarities between the higher order structures of EspC and the EspB protein, another ESX-1 substrate, whose crystal structure was recently solved [14,19]. Unusually, EspB contains both YxxxD and WxG motifs. From a cytoplasmic protomer, EspB appears to form a heptameric, all-helical, donut-shaped barrel that then oligomerizes during the secretion process in *M. tb* [19], as we report here for EspC.

During secretion from *M. tb*, Cys-48 appeared to be involved in intermolecular disulfide bond formation between EspC protomers and replacement of this residue

by serine severely destabilizes EspC. This contrasts with the situation inside *M. tb* cells where EspC is predominantly monomeric (Fig.2.5c) and associated with EspA (Fig.2.5d,e). The latter protein also contains a single, phylogenetically conserved cysteine residue, Cys-138 [20]. Like EspC, EspA also forms disulfide-bonded homodimers on secretion [21]. Replacement of Cys-138 in EspA by alanine, while abrogating disulfide-bond formation, does not impact ESX-1 secretion or the cognate innate and adaptive immune responses, but did result in a notable degree of attenuation in SCID mice [21]. Our data indicate that EspA and EspC do not heterodimerize *via* disulfide bond in the cytoplasm but that disulfide bonded-homodimers may form after export. Evidence for EspA-EspC interaction in the cell envelope was also obtained (Fig.2.7).

These intriguing findings prompted us to investigate whether EspC might be a structural component of the ESX-1 secretion system located beyond the plasma membrane. We noted many common features between EspC and the needle protein of the multi-subunit T3SS employed by Gram-negative pathogens to export their exotoxins and effector proteins across the bacterial cell wall and into host cells. The needle component protein of the T3SS apparatus is usually small ( $\approx 9$  kDa) and composed of two  $\alpha$ -helices linked by a loop. It is highly immunogenic and the C-terminus is essential for polymer/needle formation upon secretion from the cytosol [5-8,22,23]. Like the N-terminus of T3SS needle proteins, the N-terminus of EspC is plastic and can accommodate three different tags (His, HA and FLAG) without any noticeable effect on its function. EspC is also a potent T-cell antigen and, like the purified needle proteins, can self-polymerize *in vitro* to form filaments that are far longer than those associated with bacterial cells [15] (Fig.2.3d).

EspC is predicted to have a similar fold to the needle protein and displays functional similarities in its C-terminal domain [6]. Purified EspC oligomerizes *in vitro*, an event that is abolished by the C-terminal truncation, EspC<sup>CA6</sup>, implying that, in addition to the disulfide bond, the C-terminus mediates filament formation. Further proof was obtained from Ala-scanning experiments since the substitutions R95A and I98A resulted in less EspC in the culture filtrate, less EsxA secretion and

attenuation in *ex vivo* models (Fig.2.10 c-e, Table 2.1). R95 and I98 are predicted to be displayed on the same face of the alpha-helix.

Purified T3SS needle proteins self-polymerize to form a helical filament enclosing a central channel for passage of effector proteins [8,15,24]. The *in vitro* assembly of the T3SS needle involves two-steps, nucleation then elongation [15], similar to the time-dependent elongation of EspC filaments (Fig.2.3d). A molecular ruler, such as YscP of *Yersinia enterocolitica*, is utilized by the T3SS to halt needle elongation when it reaches mature length [10]. Therefore, a ruler protein is probably required to limit extension of EspC. The diameter of the EspC filament, estimated at  $\approx 10$ -15 nm, is sufficiently wide to allow the EsxA/EsxB heterodimer to pass since this is exported as a helical hairpin bundle [25,26].

Our localization studies also point towards a needle-like role as the EspC protein spans the capsule of *M. tb*, where EsxA is not detectable, and is only found in the culture filtrate when Tween-80 is present. Previous mass spectrometry analyses failed to identify EspC in the capsule [16], probably due to the paucity of trypsin cleavage sites. Using either immunogold-EM or immunofluorescence microscopy to observe intact cells, we demonstrated that EspC is exposed on the cell surface of *M. tb*. Furthermore, EspC filaments  $\sim 50$  nm in length were observed when the same immunogold-EM approach was used to examine cells from which the capsules had been removed, cryo-sectioned cells and Genapol X-080 extracts. From this combined analysis we conclude that EspC spans the capsule.

Our finding that C-terminus is essential for oligomerization of EspC also implies a new role for EccA1 (Rv3868), a cytosolic AAA+ ATPase. In contrast to the secreted EspC oligomer, cytoplasmic EspC is monomeric. Given its propensity for self-polymerization, a chaperone may be required to prevent premature assembly of EspC in the cytoplasm prior to secretion. One candidate is EspA that we found interacting with intracellular and membrane-associated EspC. Another potential chaperone is the EccA1 protein, which is known to interact with the C-terminus of EspC [4,27], the domain now shown to be essential for oligomerization. EccA1 is an

unusual AAA+ ATPase, with a tetratricopeptide repeat (TPR) within its N-terminal substrate binding domain, in addition to its C-terminal ATPase domain [28].

There is an intriguing parallel with the mechanism by which cytosolic class II chaperones of the T3SS prevent premature oligomerization of their needle complex subunits. YscG of *Yersinia pestis* for example utilizes a similar tetratricopeptide repeat to control polymerization of the T3SS needle protein YscF [29]. This is also the case for the needle protein PscF and the TPR-like protein PscG of *Pseudomonas aeruginosa* [30]. Based on our findings, and the published data for EspC-EccA1 interaction, we propose a new model for assembly of the supermolecular structure of the mycobacterial ESX-1 secretion system (Fig.2.14). In the mycobacterial cytosol, EspC forms a heterodimer with EspA and EccA1 binds to the C-terminal oligomerization domain of EspC thereby preventing premature filament assembly. Once this tripartite protein complex has reached the membrane-anchored translocation apparatus, EccA1 releases its cargo from the TPR motif, EspA and EspC dissociate, and EspC polymerizes *via* its C-terminus followed by export to the cell surface. On the basis of similarity in sequence and structure to the YxxxD/E region of EspB, Solomonson *et al.* have proposed that the C-terminus of EspC, and its paralogs, may serve as an “export arm” [14]. Residues R95 and I98 are part of this arm.

In the T3SS needles, the extreme C-terminal segment mediates polymer elongation by a process that involves part of the C-terminal alpha helix adopting a beta-sheet conformation [31]. We suspect that a similar process occurs in EspC and will now probe this using biochemical and structural approaches. Finally, based on its similarities to EspC, EspF may also form a filamentous structure that contributes to secretion but this is not necessary for ESX-1 function as *espF* mutants of *M. tb* secrete EsxA/B normally [32].

## 2.5 Materials and Methods

### Bacterial strains and culture conditions

*M. tb* and *M. smegmatis* were routinely grown in 7H9 broth supplemented with 0.2% glycerol, 10% ADC, 0.05% Tween-80 or on 7H11 agar supplemented with 0.5% glycerol and 10% OADC. The *M. smegmatis groEL1ΔC* strain used for EspC production was cultured in 7H9 broth containing 0.2% glycerol, 0.05% Tween-80, 0.2% glucose and 50 µg/ml hygromycin. *M. tb espC::Tn+espACD* and *espC::Tn+pMD31* were grown in medium containing 25 µg/ml kanamycin and 50 µg/ml hygromycin. *E. coli* TOP 10 (Invitrogen) used for cloning and propagation was grown on Luria-Bertani agar or broth.

### **Overexpression, purification and oligomeric state analysis**

*M. tb* EspC was PCR amplified and cloned into the vector pMyNT and used to generate EspC mutant constructs by site-directed mutagenesis with Pfu polymerase (Promega). These plasmids were transformed into *M. smegmatis groEL1ΔC* strain (EMBL, Hamburg) by electroporation. EspC overexpression was induced with acetamide when the bacteria were grown to OD<sub>600</sub> 0.6-0.8. After 30 h at 25°C, the cells were harvested and resuspended in lysis buffer containing 20 mM Tris pH8.0, 500 mM NaCl, 1 M urea, 0.5% Triton X-100, 5% glycerol, 10 mM imidazole and 2 mM BME with protease inhibitor cocktail and DNase I (Roche). Cells were lysed with an EmulsiFlex-C3 homogenizer followed by centrifugation to remove insoluble debris. N-terminally His-tagged EspC present in the supernatant was subjected to nickel affinity purification (Ni-NTA agarose, Invitrogen) and eluted with 20 mM Tris pH8.0, 500 mM NaCl, 300 mM imidazole, 2mM BME. Size exclusion chromatography (Hiload 16/60 Superdex200 column, GE healthcare) was used to further purify the recombinant EspC with elution buffer containing 20 mM Tris pH8.0, 500 mM NaCl and 2 mM BME. Fractions were analyzed by SDS-PAGE.

The same lysis buffer but containing 8 M urea was used to denature proteins in the cell lysate that were then loaded onto a nickel affinity column. After dialyzing the eluate to remove urea, size exclusion chromatography was performed on a Superdex200 (16/60) column to analyze the refolded proteins. To establish the oligomeric state of EspC and its mutants, the purified proteins were loaded onto a

Superdex200 (10/300GL) column (GE Healthcare) and eluted with buffer containing 20 mM Tris pH8.0, 500 mM NaCl and 2mM BME. Molecular weights of the proteins were estimated according to protein standards.

### **Circular dichroism (CD) measurement**

EspC was diluted to 0.375 mg/ml, transferred into a quartz cuvette of 1 mm path length and analyzed using a Jasco J-815 CD spectrometer. Due to strong UV absorbance of chloride ions at low wavelengths, the far-UV CD spectra were recorded between 200 nm and 250 nm. Spectra were acquired in triplicate and averaged after subtracting the buffer background.

### **Filament formation *in vitro* and transmission electron microscopy (TEM)**

Purified EspC (in 20 mM Tris pH8.0, 500 mM NaCl) was diluted to 1.8 mg/ml (20 mM Tris pH8.0, 50 mM NaCl) and analyzed after 3 days and 5 days at room temperature without shaking. After a short centrifugation at 10k rpm, the supernatant was applied to glow-discharged, carbon-coated 400 mesh grid (Canemco-Marivac) and stained with 2% uranyl acetate. Samples were viewed using TEM (Tecnai Spirit BioTWIN).

### **Macrophage cytotoxicity assay**

Macrophage viability was evaluated using potassium efflux measurement. Cell monolayers (mouse macrophage-like cell line RAW 264.7) were washed with PBS, and 1 ml of DMEM (buffered with HEPES pH7.4 and 1 µg/ml of trypsin/chymotrypsin inhibitor) was added to the wells. Cells were incubated with 100 µg/ml and 50 µg/ml of purified EspC for 2 h followed by washing once with choline buffer (129 mM cholineCl, 0.8 mM MgCl<sub>2</sub>, 1.5 mM CaCl<sub>2</sub>, 5 mM citric acid, 5.6 mM glucose, 10 mM NH<sub>4</sub>Cl and 5 mM H<sub>3</sub>PO<sub>4</sub>, pH7.4). EsxA (30 µg/ml) and EccA1 (1-280; 100 µg/ml) were used as positive and negative controls, respectively. After incubating in lysis buffer (choline buffer with 0.5% TritonX-100) for 30 min, the potassium content in the cell lysate was determined using a Sherwood M410 Flame photometer.

### **Genetic complementation of EspC transposon insertion mutant**

Plasmid pMD31-*espACD* contains the *espACD* operon preceded by 568 bp of DNA upstream of the *espA* start codon [33]. The Erdman *espC::Tn* (Hyg<sup>r</sup>) mutant was described previously [34]. The sequence encoding the HA epitope was inserted into the 5'-end of *espC* by Quick Change Mutagenesis (KAPA HiFi hotstar PCR Kits, KAPA Biosystems). This plasmid and the pMD31 empty vector were transformed into the *espC::Tn* mutant strain by electroporation. Transformants were selected on 7H11 agar plates containing 25 µg/ml kanamycin and 50 µg/ml hygromycin.

### **Preparation of culture filtrates, cell lysates and capsule extracts**

To analyze protein production and secretion, *M. tb espC::Tn+espAC<sub>HA</sub>D* and *espC::Tn+pMD31* strains were grown in Sauton's medium (plus 0.002% Tween-80) with a starting OD<sub>600</sub> 0.1. After 6 days growth at 37°C, culture filtrates and cell lysates, were prepared as described [33]. Cell membrane was separated from the crude lysate by ultracentrifugation at 125,000 x g for 1 h. Capsule layer proteins were extracted using 0.25% Genapol X-080 and enriched by TCA-precipitation [16]. Total protein concentration was determined using the BCA assay (Thermo Scientific).

### **Protein analysis by immunoblotting**

Culture filtrates, cell lysates and capsule extracts were analyzed by SDS-PAGE and immunoblotting as previously described [33]. For EspC, equivalent amounts of total proteins were boiled in SDS sample buffer with and without 5mM DTT before gel electrophoresis. HA-tagged EspC was detected with HRP-conjugated anti-HA mouse monoclonal antibody (Cell Signaling, #2999). Anti-EsxA (Abcam, ab26246) and anti-GroEL (Abcam, ab20045) mouse monoclonal antibodies, recognized by peroxidase (HRP) conjugated anti-mouse IgG antibodies (Sigma-Aldrich), were used respectively for EsxA and GroEL detection. Anti-Ag85 (Abcam, ab43019) and Anti-CFP10 (Abcam, ab45074) rabbit polyclonal antibodies, recognized by HRP conjugated anti-rabbit antibodies (Sigma-Aldrich).



### Macrophage infection assay

Phorbol myristate (50 nM) activated THP-1 cells ( $2 \times 10^6/\text{ml}$ ) were seeded in complete RPMI medium in a 96-well plate, infected with *M. tb* strains at a multiplicity of infection of 5 and incubated for 48 h at 37°C under 5% CO<sub>2</sub>. Cytotoxicity was evaluated by measuring cell viability using PrestoBlue Cell Viability Reagent (Invitrogen).

### Co-immunoprecipitation

Total cell lysate proteins (1 mg) of *M. tb* strains *espC::Tn+espAC<sub>HAD</sub>* and *espC::Tn+espACD* were added to 20 µl of agarose-conjugated anti-HA monoclonal antibody (Sigma-Aldrich) and incubated at 4°C for 4 h. Beads were washed 5 times with PBS, eluted with 80 µl SDS sample buffer and boiled for 3 min prior to electrophoresis. Eluted proteins were analyzed by silver staining (SilverQuest™ Silver Stain Kit, Invitrogen) or by LC-MS/MS and immunoblotting.

### LC-MS/MS analysis

Bands of interest were excised from SDS-PAGE gels and In-Gel digested using modified trypsin. Extracted peptides were then concentrated using a vacuum concentrator and analyzed by LC-MS/MS. Samples were separated by Reverse Phase on a Dionex RSLC Ultimate 3000nano UPLC connected in-line with an Orbitrap Elite high resolution Mass Spectrometer (Thermo Fisher Scientific). Chromatographic separation was performed over a 80 min gradient using a capillary column (Nikkoy Technos Co; C18; 3 µm-100 Å; 15 cm x 75 µm ID) at 250 nl/min. Data dependent acquisition mode was used with dynamic exclusion where the first 20 parent ions were fragmented and then excluded for the following 30 seconds. Database searching was performed with Proteome Discoverer 1.4 using Mascot 2.3 and Sequest HT as search engines against the TubercuList R27 FASTA Database. Met oxidation, Ser-Thr-Tyr phosphorylation and peptide N-acetylation were set as variable modifications while Cys carbamidomethylation was set as fixed modification. Final data inspection was carried out with Scaffold.



### **Immunogold-EM and immunofluorescence-microscopy**

For immuno-labeling of whole mount cells, *M. tb espC::Tn+espAC<sub>HA</sub>D* and *espC::Tn+pMD31* were cultured in Sauton's medium (without Tween) for 3 days to exponential growth phase when 5 ml of culture were mixed with equal volume of PBS buffer containing 4% paraformaldehyde and 0.4% glutaraldehyde and fixed for 90 min. Cells were pelleted and resuspended in 200 µl PBS containing 0.15 M glycine. Samples were incubated on formvar coated 200 mesh grids (Canemco-Marivac) for 10 min, then blocked with 1% BSA in PBS for 10 min prior to incubating with anti-HA mouse monoclonal antibody (Cell Signaling, #2367, 1/40 dilution) for 75 min. After washing twice with PBS and twice with 1% BSA-PBS, grids were incubated in PBS containing 1% BSA and anti-Mouse IgG (1/50 dilution) conjugated with 10 nm gold particles (Electron Microscopy Science, #25129) for 2 h. Grids were then washed four times with PBS and air dried before observation by TEM. For sectioning, cells were chemically fixed with a buffered mix of 2% paraformaldehyde and 0.1% glutaraldehyde, and embedded in 12% gelatin. Small cubes (1 mm width) were then infiltrated overnight in 20% sucrose before freezing in liquid nitrogen. These were then sectioned at -100°C to a thickness of 100 nm using an ultramicrotome (Leica UC7/FCS, Leica Microsystems, Vienna). Sections were collected on grids carrying a drop of methyl-cellulose at room temperature. These were then processed for immunogold labelling as above.

For immunofluorescent staining, fixed bacterial suspensions were loaded onto coverslips pretreated with 0.01% poly-L-lysine, blocked with 1% BSA-PBS for 30 min and incubated with anti-HA antibody (1/100 dilution) for 90 min. Subsequently, the cells were stained with Alexa Fluor-488 anti-mouse antibody (Life Technologies, 1/200 dilution) for 1 h and analyzed using a fluorescence microscope (ZeissAxio Imager Z1). The same exposure was used for *espC::Tn+espAC<sub>HA</sub>D* and *espC::Tn+pMD31* when imaging fluorescence.

## 2.6 Figures and Tables

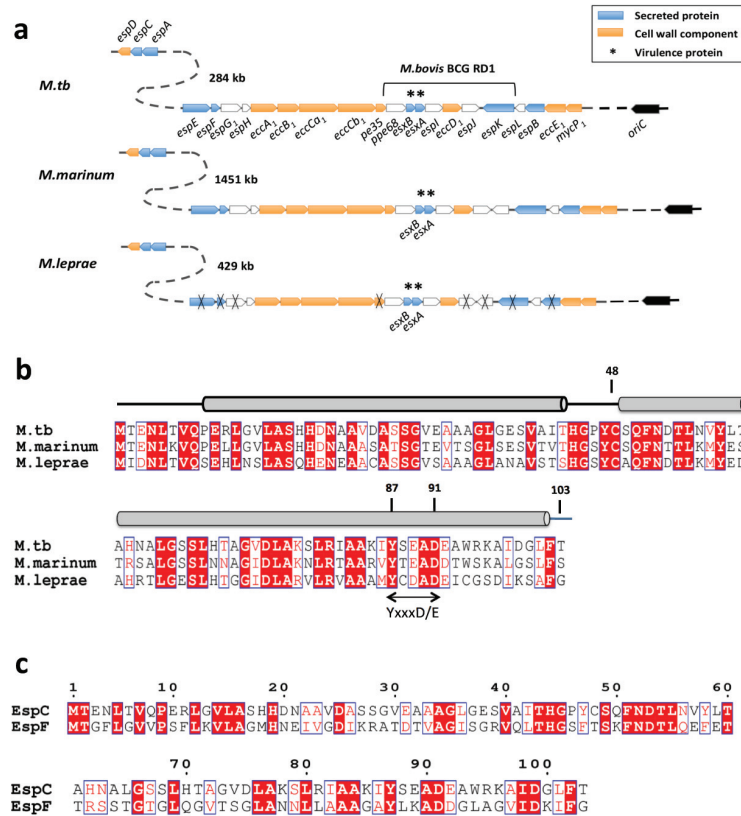


**Fig.2.1 Genetic organization of *espACD* and *esx-1* loci and EspC structural elements in three mycobacterial pathogens.**

**(a)** Comparison of genetic loci important for ESX-1 function in *M. tb*, *M. marinum* and *M. leprae*. Genes are color-coded according to the localization of their proteins – see key. White denotes no information available, crosses denote pseudogenes. Distances between loci are indicated in kb. **(b)** Primary and secondary structure alignments of EspC proteins derived from the same pathogens showing location of conserved Cys-48 and the YxxxD/E motif. Secondary structure analysis by PSI-PRED suggests that EspC is composed of two alpha helices (blue cylinders) connected by a loop. Identical and similar residues are shown in red and white boxes, respectively. **(c)** Primary structure alignment of EspC and EspF from *M. tb*.

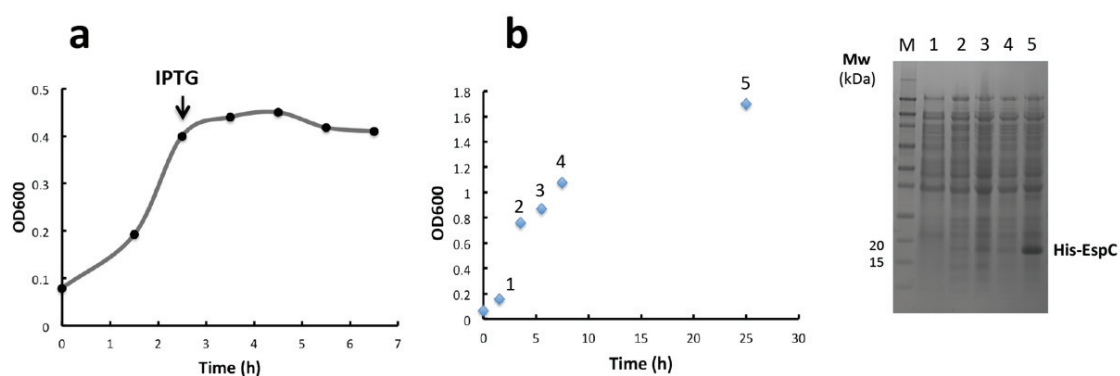


**Fig.2.2 Overexpression of recombinant EspC in *E. coli*.**

**(a)** *E. coli* BL21 (DE3) strain transformed with EspC-pET28 was grown in LB medium at 37°C and induced with IPTG for protein expression. Bacterial growth was inhibited after IPTG-induced EspC expression. **(b)** The bacteria were cultured at 30°C in autoinduction medium with lactose as mild inducer. EspC production at the indicated time points was monitored by SDS-PAGE and staining with Coomassie blue. Bacteria grew high cell density, and EspC was expressed in high yield.

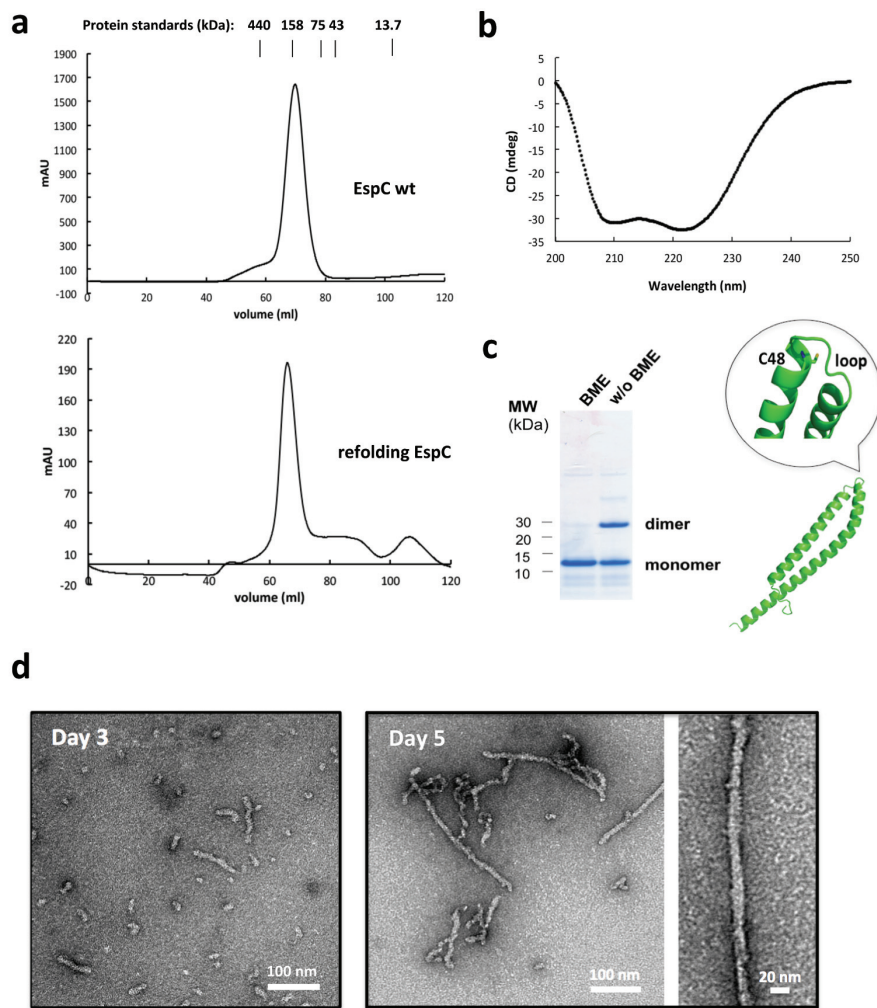


**Fig.2.3 Recombinant EspC overexpressed in *M. smegmatis* self-polymerizes into a filamentous structure.**

**(a)** Size exclusion chromatography profile of recombinant EspC on Superdex 200 (16/60) column indicates its polymeric nature - top. Urea-denatured EspC refolds into a polymer similar to the natural state - bottom. **(b)** CD spectrum reveals polymer to be mainly  $\alpha$ -helical. **(c)** Purified EspC was present as both dimer and monomer on an SDS-PAGE gel; the dimer became monomeric when treated with BME. In the tertiary structure predicted by I-TASSER (<http://zhanglab.ccmb.med.umich.edu/I-TASSER/>), Cys-48 localizes at the head of EspC. **(d)** Transmission electron micrographs of negatively stained filaments formed by recombinant EspC as a function of time. Filaments were variable in length and ~10-15 nm in diameter.

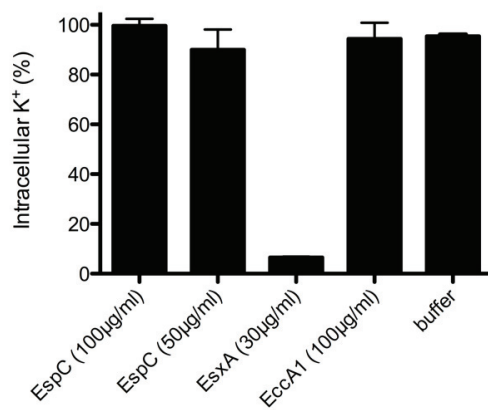


**Fig.2.4 EspC is not cytolytic.**

RAW 264.7 cells were incubated with 50 µg/ml and 100 µg/ml purified EspC for 2 hrs before measuring potassium efflux to evaluate cell viability. EsxA (30 µg/ml) and EccA1 (N-terminal domain 1-280; 100 µg/ml) were used as positive and negative controls. As a result, EspC did not show cytolytic activity while EsxA did. Mean + s.e.m of triplicate measurements of one representative results from two independent experiments is depicted.

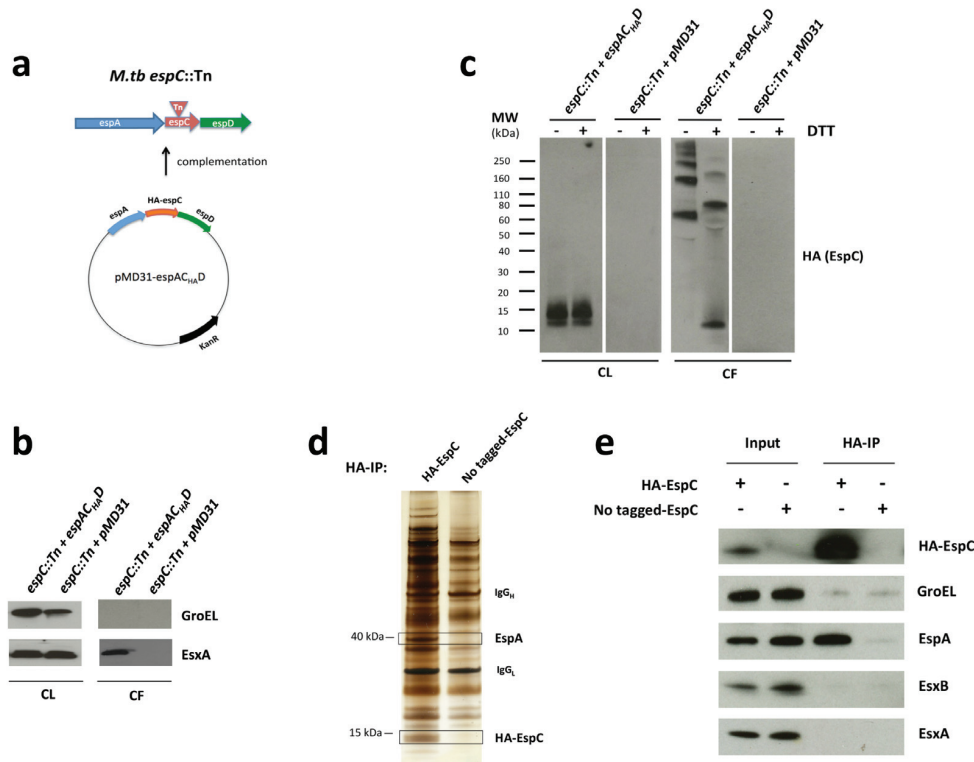


**Fig.2.5 EspC binds to EspA inside cells and polymerizes upon secretion from *M. tb*.**

**(a)** Scheme showing complementation of the *M. tb* *espC*::Tn mutant with pMD31-*espAC*<sub>HAD</sub>, encoding N-terminally HA-tagged EspC, or the empty vector. **(b)** EsxA secretion was restored by complementation. **(c)** Cell lysate (CL) proteins (5 µg) or culture filtrate (CF) proteins (15 µg) boiled in SDS buffer with or without DTT (5 mM), were electrophoresed on an SDS-PAGE gel. EspC was detected using an anti-HA antibody conjugated with HRP. In the CL, EspC was monomeric and unaffected by DTT. In the CF, EspC was an SDS-resistant polymer, which dissociated in the presence of DTT. This suggests that EspC polymerization occurs during translocation from the cytosol. **(d)** Pull-down experiment in which beads coated with monoclonal antibodies targeting the HA-tag were incubated with crude cell lysates containing either native EspC or HA-tagged EspC. Note the presence of a 40 kDa protein, identified by LC-MS/MS as EspA (Spectrum count: 18; Sequence coverage: 37%), only when HA-tagged EspC was used. **(e)** Immunoblot demonstrating interaction between EspA-EspC in cell lysates. Antibodies used are indicated at right.

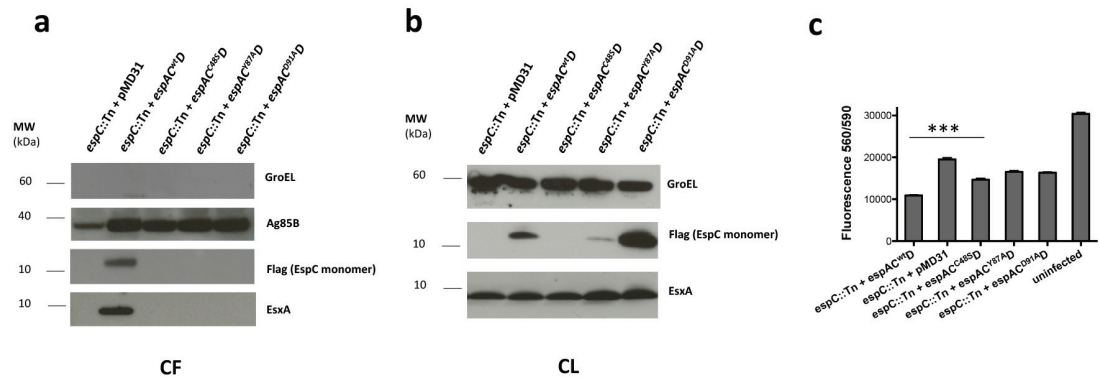


**Fig.2.6 ESX-1 protein secretion and expression in *M. tb* strains producing EspC<sup>C48S</sup>, EspC<sup>Y87A</sup> and EspC<sup>D91A</sup>.**

**(a)** EspC and EsxA were not detectable in the culture filtrates (CF) of the *espC::Tn+espAC<sup>C48S</sup>D*, *espC::Tn+espAC<sup>Y87A</sup>D* and *espC::Tn+espAC<sup>D91A</sup>D* strains. EspC was Flag-tagged and detected with anti-Flag antibody in this experiment. Ag85B and GroEL were used as loading control and autolysis control, respectively. **(b)** Immunoblot of cell lysates (CL) of the *espC::Tn+espAC<sup>C48S</sup>D* and *espC::Tn+espAC<sup>Y87A</sup>D* showed that the C48S and Y87A substitutions severely decreased stability of EspC in the cell. By contrast, the D91A variant of EspC accumulated in the cell lysate. GroEL was used as a loading control. **(c)** Fibroblast survival assay showing the respective cytotoxicity of EspC variants compared to wild-type *M. tb* Erdman control strains. Fluorescence levels indicate the metabolic activity of fibroblasts, which correlates with the infection state. Mean + s.e.m of quintuplicate measurements of one representative results from two independent experiments is depicted.

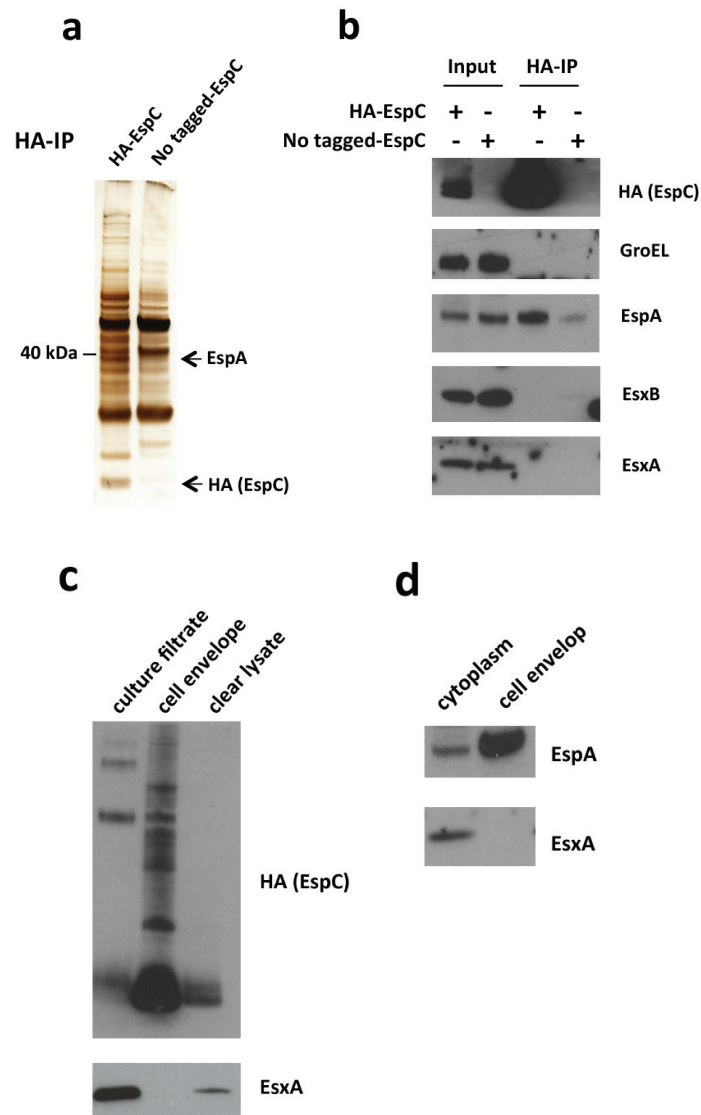


**Fig.2.7 EspC interacts with EspA in the cytoplasmic fraction. HA-tagged EspC was used in a pull-down assay to detect potential partner proteins.**

**(a)** SDS-PAGE analysis of silver-stained proteins present after pull-down of the cytoplasmic fraction of *M. tb* cells. **(b)** Pull-down and immunoblot analysis using the antibodies indicated at right. **(c)** Comparison of EspC in culture filtrate, cell membrane and cytoplasm fractions by immunoblot analysis. Note that EspC was more abundant in the cell membrane, whereas most of EsxA was secreted into the culture medium. **(d)** Immunoblot analysis of cytoplasm and cell membrane fractions. Note the presence of more EspA in the membrane fraction compared to the cytoplasm.



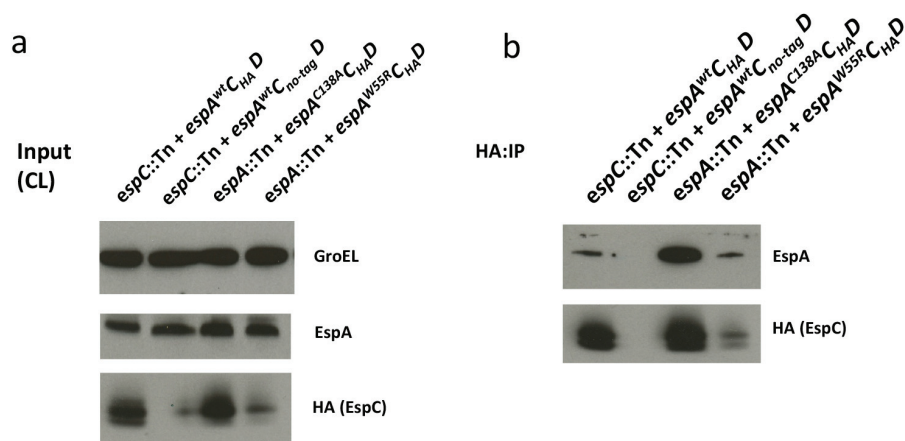


**Fig.2.8 Pull-down and immunoblot analysis of EspA/C interaction in the *M. tb* strains with EspA point mutation.**

HA-tagged EspC interacts with wildtype and mutant (C138A) EspA in cell lysates showing that Cys138 is not required for interaction with EspC. The blot **(a)** also shows that EspA<sup>W55R</sup> caused a reduced EspC level in the cell, indicating that the Trp-55 may mediate EspA/C association to stabilize intracellular EspC.

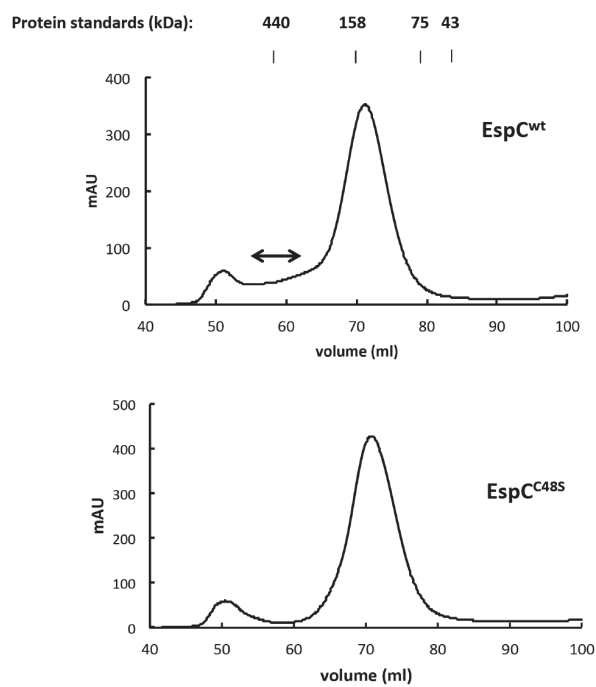


**Fig.2.9** Size exclusion chromatographic profiles of recombinant EspC<sup>wt</sup> and EspC<sup>C48S</sup>.

EspC<sup>C48S</sup> overexpressed by *M. smegmatis* was predominantly purified as a polymer of similar size to EspC<sup>wt</sup> suggesting that, in addition to disulfide bonding, another motif is required for EspC polymer formation. The arrow indicates a shoulder that was only seen with wild type EspC.

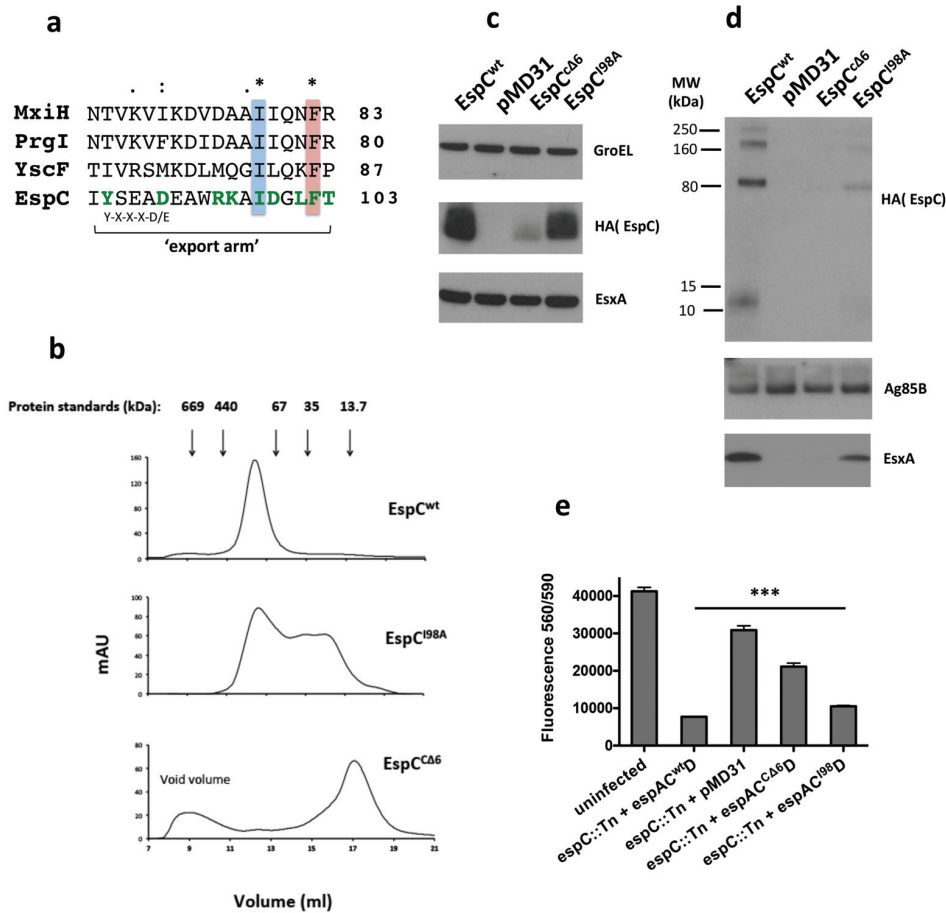


**Fig.2.10 C-terminus of EspC is critical for polymer assembly and ESX-1 function.**

**(a)** EspC shares a C-terminal motif with T3SS needle proteins (MxiH, PrgI, and YscF) located in the “export arm” affecting polymerization [14]. **(b)** Compared with EspC<sup>wt</sup> that was mainly polymeric on Superdex200 (10/300 GL) column chromatography, overexpressed EspC<sup>Δ6</sup> was mainly monomeric, while the 198A variant behaved as a mixture of monomer and polymer, implying that the C-terminal region is critical for polymer assembly. **(c)** Loss of last 6 amino acid residues destabilizes intracellular EspC. **(d)** The 198A mutation impacts EspC in the CF and polymerization. **(e)** The EspC<sup>Δ6</sup> and 198A mutations impact ESX-1 function as indicated by reduced EsxA secretion and lower cytotoxicity compared to *M. tb* expressing wild type EspC. Mean + s.e.m of triplicate measurements of one representative results from two independent experiments is depicted.

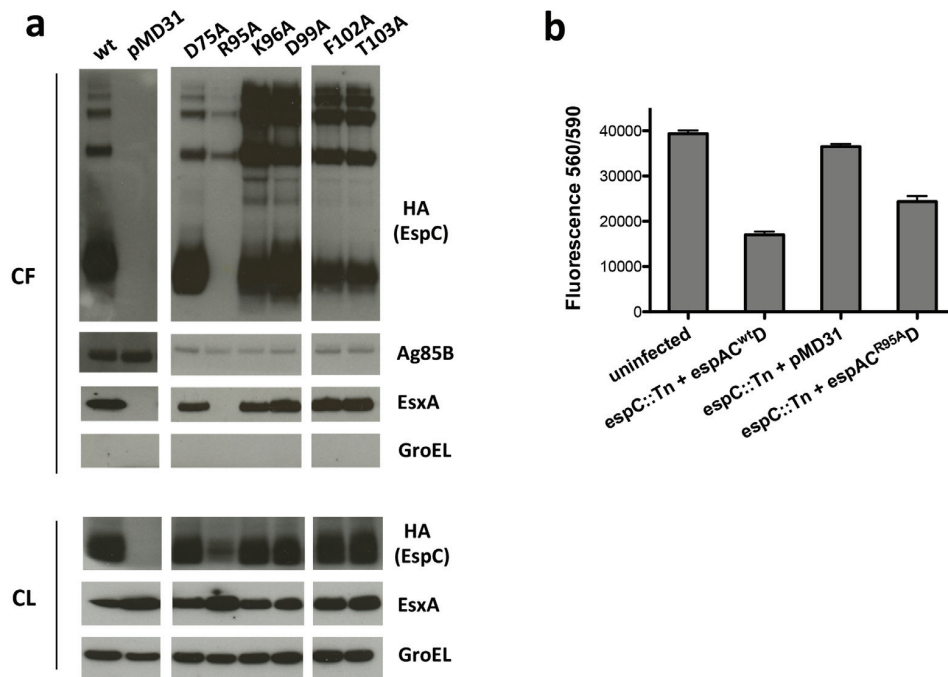


**Fig.2.11 Secretion, production and macrophage cytotoxicity of EspC variants.**

**(a)** EspC R95A was less abundant in CL, and not exported, and this mutation completely blocked EsxA secretion to the CF. **(b)** THP-1 cytotoxicity was diminished following infection with *M. tb* Erdman expressing EspC R95A. Other point mutants, discussed in the main text, and controls are shown. Mean + s.e.m of triplicate measurements of one representative results from two independent experiments is depicted.

Table 2.1 Summary of all EspC variants constructed in this study

	EspC alleles												
	wt	C48S	D75A	Y87A	D91A	R95A	K96A	I98A	D99A	L101A	F102A	T103A	CA6
Stability	+	+/-	+	-	+	+	+	+/-	+	+	+	+	-
Exported	+	-	+	-	-	-	+	+/-	+	+	+	+	-
Multimers	+	+	+	NT	NT	+	+	+	+	+	+	+	-
EsxA Secreted	+	-	+	-	-	-	+	+/-	+	+	+	+	-
Attenuated	-	+/-	NT	+	+	+	NT	+/-	NT	-	NT	NT	+

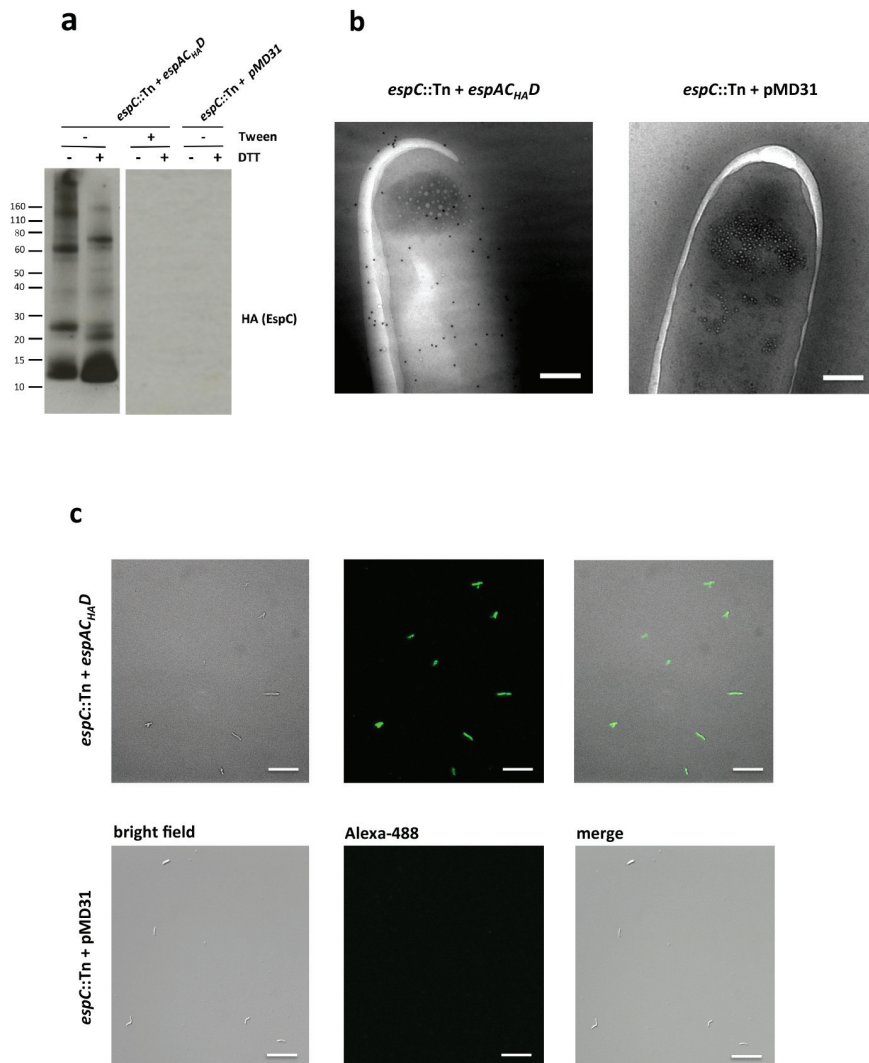


**Fig.2.12 EspC localizes on the cell surface.**

**(a)** *M. tb* strains were cultured in Sauton's medium with or without Tween-80 and extracted with Genapol X-080 to enrich capsular layer proteins. TCA-precipitated proteins (0.01  $\mu$ g) were treated with SDS buffer with or without DTT, separated by SDS-PAGE then immunoblotted. EspC was detectable in the capsular layer extract of strain *espC::Tn+espAC<sub>HA</sub>D*, the signal was equivalent to that of 15  $\mu$ g total CF protein using the same dilution of antibody. Immunogold-EM analysis of **(b)** whole *M. tb* cells (grown without Tween-80) demonstrates random distribution of EspC on cell surface; Strain *espC::Tn+pMD31* used as a negative control. **(c)** Immunofluorescence microscopy analysis

confirms surface localization of EspC. Fixed bacteria with an intact capsular layer were incubated with anti-HA antibody and subsequently stained with Alexa-488 labeled anti-mouse IgG. EspC was visualized on the surface of *espC::Tn+espAC<sub>HA</sub>D*. Strain *espC::Tn+pMD31* was used as a negative control with the same exposure time. Scale bar: 10  $\mu$ m.

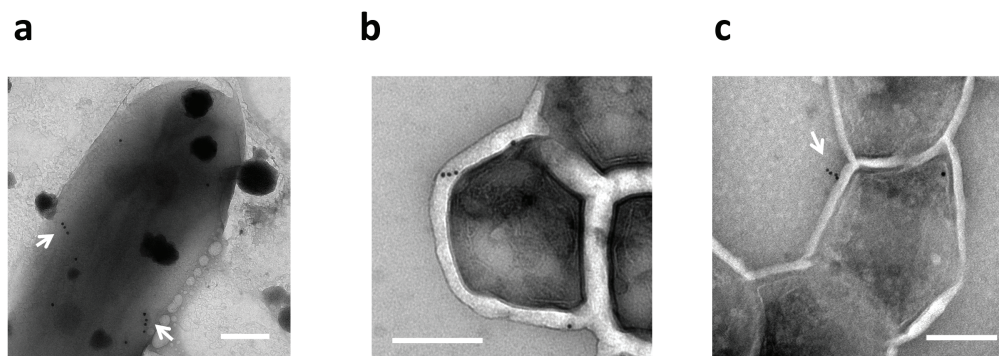


**Fig.2.13 EspC forms filament on the bacterial surface.**

**(a)** Whole cells grown without Tween-80 after extraction with 0.025% Genapol X-080;  
**(b)(c)** cryo-sections of whole cells grown without Tween-80; Bacteria or enriched proteins were stained with anti-HA antibody and 10 nm gold-conjugated anti-mouse IgG. Scale bar: 200 nm. Arrows indicate EspC filaments.

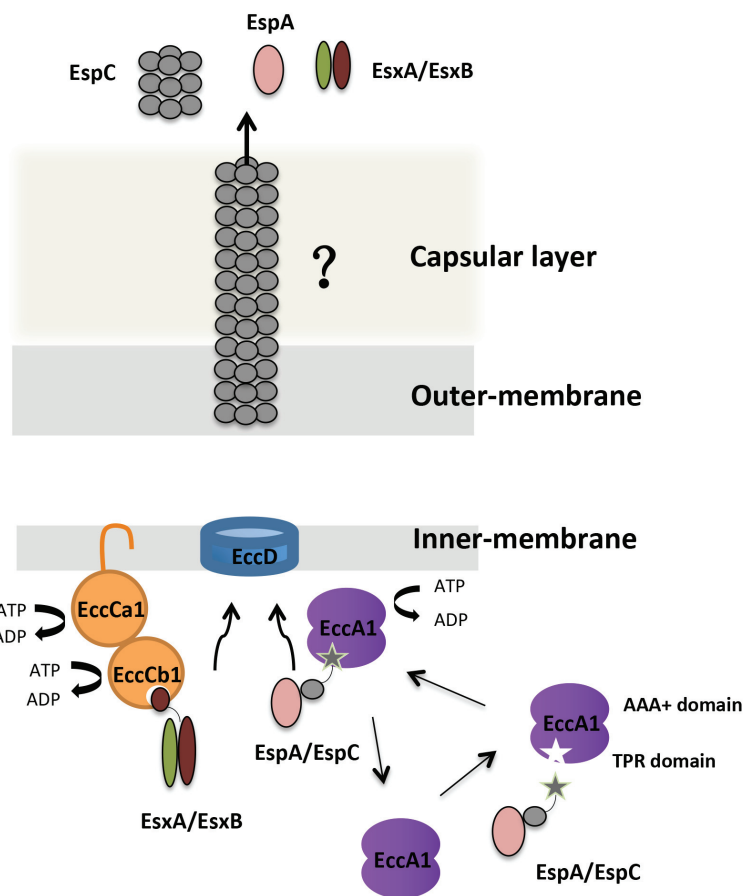


**Fig.2.14 Working model of ESX-1 secretion apparatus and EspC export.**

Simplified ESX-1 model showing how EspA and EspC form a heterodimer in the *M. tb* cytosol; the TPR domain of the AAA+ ATPase EccA1 binds to the C-terminus of EspC. Once the tripartite complex reaches the membrane-anchored translocation apparatus, EccA1 releases its cargo, EspA and EspC dissociate and EspC polymerizes *via* its C-terminus during export and forms a filamentous structure. By contrast, the membrane-associated ATPase EccCa1-EccCb1 binds the EsxA/EsxB heterodimer *via* the C-terminal signal sequence of EsxB and then facilitates its translocation through a channel potentially comprising EccD and EspC, and probably other proteins not shown.



## References

1. Millington KA, Fortune SM, Low J, Garces A, Hingley-Wilson SM, et al. (2011) Rv3615c is a highly immunodominant RD1 (Region of Difference 1)-dependent secreted antigen specific for *Mycobacterium tuberculosis* infection. *Proceedings of the National Academy of Sciences of the United States of America* 108: 5730-5735.
2. Uplekar S, Rougemont J, Cole ST, Sala C (2013) High-resolution transcriptome and genome-wide dynamics of RNA polymerase and NusA in *Mycobacterium tuberculosis*. *Nucleic Acids Res* 41: 961-977.
3. Das C, Ghosh TS, Mande SS (2011) Computational Analysis of the ESX-1 Region of *Mycobacterium tuberculosis*: Insights into the Mechanism of Type VII Secretion System. *Plos One* 6.
4. Champion PAD, Champion MM, Manzanillo P, Cox JS (2009) ESX-1 secreted virulence factors are recognized by multiple cytosolic AAA ATPases in pathogenic mycobacteria. *Molecular Microbiology* 73: 950-962.
5. Blocker AJ, Deane JE, Veenendaal AKJ, Roversi P, Hodgkinson JL, et al. (2008) What's the point of the type III secretion system needle? *Proceedings of the National Academy of Sciences of the United States of America* 105: 6507-6513.
6. Deane JE, Roversi P, Cordes FS, Johnson S, Kenjale R, et al. (2006) Molecular model of a type III secretion system needle: Implications for host-cell sensing. *Proceedings of the National Academy of Sciences of the United States of America* 103: 12529-12533.
7. Kenjale R, Wilson J, Zenk SF, Saurya S, Picking WL, et al. (2005) The needle component of the type III secretion of *Shigella* regulates the activity of the secretion apparatus. *Journal of Biological Chemistry* 280: 42929-42937.
8. Loquet A, Sgourakis NG, Gupta R, Giller K, Riedel D, et al. (2012) Atomic model of the type III secretion system needle (vol 486, pg 276, 2012). *Nature* 488.
9. Noens EE, Williams C, Anandhakrishnan M, Poulsen C, Ehebauer MT, et al. (2011) Improved mycobacterial protein production using a *Mycobacterium smegmatis* groEL1 Delta C expression strain. *Bmc Biotechnology* 11.
10. Dangelat S, Kowall J, Mattow J, Bumann D, Winter R, et al. (2003) The RD1 proteins of *Mycobacterium tuberculosis*: expression in *Mycobacterium smegmatis* and biochemical characterization. *Microbes and Infection* 5: 1082-1095.
11. de Jonge MI, Pehau-Arnaudet G, Fretz MM, Romain F, Bottai D, et al. (2007) ESAT-6 from *Mycobacterium tuberculosis* dissociates from its putative chaperone CFP-10 under acidic conditions and exhibits membrane-lysing activity. *Journal of Bacteriology* 189: 6028-6034.
12. De Leon J, Jiang GZ, Ma Y, Rubin E, Fortune S, et al. (2012) *Mycobacterium tuberculosis* ESAT-6 Exhibits a Unique Membrane-interacting Activity That

- Is Not Found in Its Ortholog from Non-pathogenic *Mycobacterium smegmatis*. *Journal of Biological Chemistry* 287: 44184-44191.
13. Simeone R, Bottai D, Brosch R (2009) ESX/type VII secretion systems and their role in host-pathogen interaction. *Current Opinion in Microbiology* 12: 4-10.
  14. Solomonson M, Setiাপutra D, Makepeace KA, Lameignere E, Petrotchenko EV, et al. (2015) Structure of EspB from the ESX-1 type VII secretion system and insights into its export mechanism. *Structure* 23: 571-583.
  15. Poyraz O, Schmidt H, Seidel K, Delissen F, Ader C, et al. (2010) Protein refolding is required for assembly of the type three secretion needle. *Nature Structural & Molecular Biology* 17: 788-U726.
  16. Sani M, Houben ENG, Geurtsen J, Pierson J, de Punder K, et al. (2010) Direct Visualization by Cryo-EM of the Mycobacterial Capsular Layer: A Labile Structure Containing ESX-1-Secreted Proteins. *Plos Pathogens* 6.
  17. Fortune SM, Jaeger A, Sarracino DA, Chase MR, Sasseti CM, et al. (2005) Mutually dependent secretion of proteins required for mycobacterial virulence. *Proc Natl Acad Sci U S A* 102: 10676-10681.
  18. Rosenberg OS, Dovala D, Li X, Connolly L, Bendebury A, et al. (2015) Substrates Control Multimerization and Activation of the Multi-Domain ATPase Motor of Type VII Secretion. *Cell* 161: 501-512.
  19. Korotkova N, Piton J, Wagner JM, Boy-Rottger S, Japaridze A, et al. (2015) Structure of EspB, a secreted substrate of the ESX-1 secretion system of *Mycobacterium tuberculosis*. *J Struct Biol*.
  20. Chen JM, Zhang M, Rybniker J, Basterra L, Dhar N, et al. (2013) Phenotypic profiling of *Mycobacterium tuberculosis* EspA point mutants reveals that blockage of ESAT-6 and CFP-10 secretion in vitro does not always correlate with attenuation of virulence. *J Bacteriol* 195: 5421-5430.
  21. Garces A, Atmakuri K, Chase MR, Woodworth JS, Krastins B, et al. (2010) EspA acts as a critical mediator of ESX1-dependent virulence in *Mycobacterium tuberculosis* by affecting bacterial cell wall integrity. *PLoS Pathog* 6: e1000957.
  22. Barrett BS, Markham AP, Esfandiary R, Picking WL, Picking WD, et al. (2010) Formulation and Immunogenicity Studies of Type III Secretion System Needle Antigens as Vaccine Candidates. *Journal of Pharmaceutical Sciences* 99: 4488-4496.
  23. Betts HJ, Twigg LE, Sal AS, Wyrick PB, Fields KA (2008) Bioinformatic and biochemical evidence for the identification of the type III secretion system needle protein of *Chlamydia trachomatis*. *Journal of Bacteriology* 190: 1680-1690.
  24. Demers JP, Sgourakis NG, Gupta R, Loquet A, Giller K, et al. (2013) The Common Structural Architecture of *Shigella flexneri* and *Salmonella typhimurium* Type Three Secretion Needles. *Plos Pathogens* 9.
  25. Renshaw PS, Panagiotidou P, Whelan A, Gordon SV, Hewinson RG, et al. (2002) Conclusive evidence that the major T-cell antigens of the *Mycobacterium tuberculosis* complex ESAT-6 and CFP-10 form a tight, 1 : 1 complex and

- characterization of the structural properties of ESAT-6, CFP-10, and the ESAT-6-CFP-10 complex - Implications for pathogenesis and virulence. *Journal of Biological Chemistry* 277: 21598-21603.
26. Brodin P, de Jonge MI, Majlessi L, Leclerc C, Nilges M, et al. (2005) Functional analysis of early secreted antigenic target-6, the dominant T-cell antigen of *Mycobacterium tuberculosis*, reveals key residues involved in secretion, complex formation, virulence, and immunogenicity. *Journal of Biological Chemistry* 280: 33953-33959.
  27. Luthra A, Mahmood A, Arora A, Ramachandran R (2008) Characterization of Rv3868, an Essential Hypothetical Protein of the ESX-1 Secretion System in *Mycobacterium tuberculosis*. *Journal of Biological Chemistry* 283: 36532-36541.
  28. Wagner JM, Evans TJ, Korotkov KV (2014) Crystal structure of the N-terminal domain of EccA(1) ATPase from the ESX-1 secretion system of *Mycobacterium tuberculosis*. *Proteins-Structure Function and Bioinformatics* 82: 159-163.
  29. Sun P, Tropea JE, Austin BP, Cherry S, Waugh DS (2008) Structural characterization of the *Yersinia pestis* type III secretion system needle protein YscF in complex with its heterodimeric chaperone YscE/YscG. *Faseb Journal* 22.
  30. Quinaud M, Ple S, Job V, Contreras-Martel C, Simorre JP, et al. (2007) Structure of the heterotrimeric complex that regulates type III secretion needle formation. *Proc Natl Acad Sci U S A* 104: 7803-7808.
  31. Poyraz O, Schmidt H, Seidel K, Delissen F, Ader C, et al. (2010) Protein refolding is required for assembly of the type three secretion needle. *Nat Struct Mol Biol* 17: 788-792.
  32. Bottai D, Majlessi L, Simeone R, Frigui W, Laurent C, et al. (2011) ESAT-6 Secretion-Independent Impact of ESX-1 Genes *espF* and *espG(1)* on Virulence of *Mycobacterium tuberculosis*. *Journal of Infectious Diseases* 203: 1155-1164.
  33. Chen JM, Boy-Rottger S, Dhar N, Sweeney N, Buxton RS, et al. (2012) *EspD* Is Critical for the Virulence-Mediating ESX-1 Secretion System in *Mycobacterium tuberculosis*. *Journal of Bacteriology* 194: 884-893.
  34. Dhar N, McKinney JD (2010) *Mycobacterium tuberculosis* persistence mutants identified by screening in isoniazid-treated mice. *Proceedings of the National Academy of Sciences of the United States of America* 107: 12275-12280.
  35. Zumla A, George A, Sharma V, Herbert RH, Baroness Masham of I, et al. (2015) The WHO 2014 global tuberculosis report--further to go. *Lancet Glob Health* 3: e10-12.

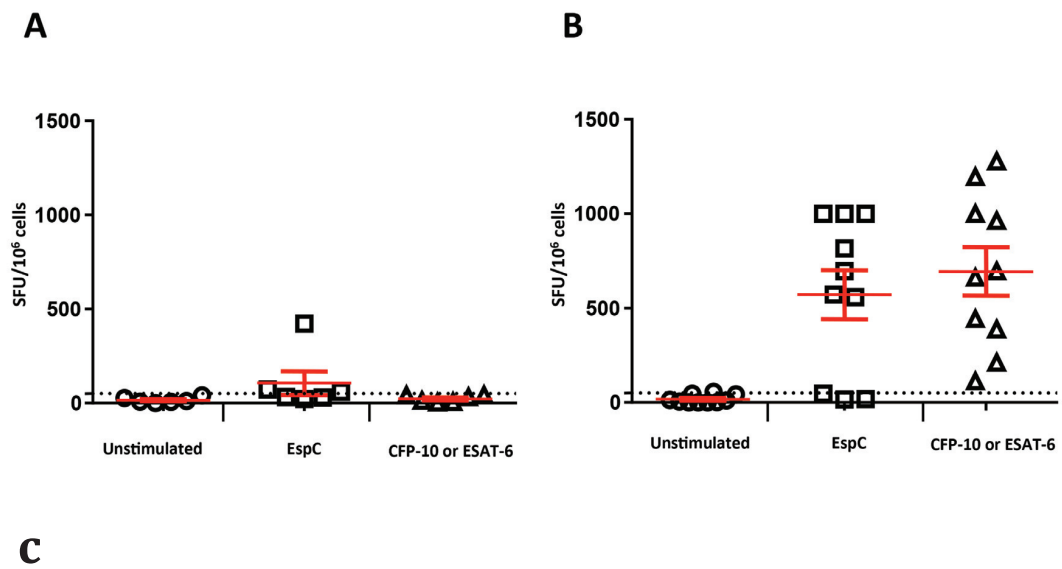
## Supplementary

### Full-length EspC is a highly immunodominant antigen

EspC was identified as an immunodominant antigen, which induced T-cell response as specific as the responses to ESAT-6 and CFP-10 (EsxA and EsxB) [1]. The experiment was performed using synthesized peptides from EspC, since the protein has not been purified previously. In this project (collaboration with Centre Hospitalier Universitaire Vaudois), we evaluated full-length EspC-specific T-cell responses in ten LTBI patients by IFN- $\gamma$  release assay (ELISpot). ESAT-6 or CFP-10 was used as a positive control. To evaluate the potential false-positive response raised from the EspC co-purified endotoxin, such as lipopolysaccharide, the IFN- $\gamma$  productions in six healthy individuals were also tested.

As a result, weak false-positive responses to EspC were observed in two of the six uninfected persons ( $> 50$  SFU/ $10^6$  cells is defined as positive) (Fig.S2.1). Given that it is also occasionally observed with ESAT-6 and CFP-10 [1], and the other three individuals showed negative results, we tended to exclude the interference from the endotoxin present in the EspC sample.

As expected, all of the ten LTBI patients tested had ESAT-6 or CFP-10 specific T-cell frequencies  $>50$  SFU/ $10^6$  cells. Seven of them demonstrated EspC-specific T-cell responses, moreover, the frequencies were as high as those induced by ESAT-6 or CFP-10 (Fig.S2.1). This is consistent with the previous observations using EspC peptides, again suggesting that EspC is a promising TB vaccine candidate or diagnostic antigen.



Sample ID	Clinic	CFP-10 or ESTAT-6	EspC	BCG vaccination state
396	LTBI	695	47	-
313	LTBI	> 1000	> 1000	-
363	LTBI	433	558	-
101	LTBI	113	18	No
450	LTBI	388	817	-
853	LTBI	662	572	-
922	LTBI	> 1000	> 1000	-
254	LTBI	963	> 1000	No
410	LTBI	> 1000	15	-
625	LTBI	212	695	-
695	healthy	3	30	Yes
209	healthy	7	32	Yes
442	healthy	13	22	Yes
196	healthy	32	60	No
664	healthy	42	422	Yes
223	healthy	43	72	-

**Fig.S2.1 Interferon-Gamma Release assays showed the T-cell responses induced by full-length EspC and ESAT-6/CFP-10 in the healthy persons (A) and the LTBI patients (B).**

## Plasmids, primers and bacterial strains

**Table S2.1 Plasmids and primers**

Plasmids	Description	Reference
pMyNT	AmiS promoter, N-terminal in frame 6x His Tag, Hyg <sup>R</sup> , <i>oriE</i> , <i>oriM</i>	[9]
pMD31	Episomal, multicopy, Kan <sup>R</sup> , <i>oriE</i> , <i>oriM</i>	[33]
pMDespACD	<i>espA</i> promoter, <i>espACD</i> operon, Kan <sup>R</sup> , <i>oriE</i> , <i>oriM</i>	[33]
Primers	Sequence (5'-3')	Reference
EspC Forward	GCGCCATGGACACGGAAAACTTGACCGTC	This study
EspC Reverse	CCCAAGCTTTCAGGTAAACAACCCGTC	This study
EspC <sup>Δ6</sup> Forward (pMyNT)	GCGCCATGGACACGGAAAACTTGACCGTC	This study
EspC <sup>Δ6</sup> Reverse (pMyNT)	CCCAAGCTTTCAGGTAAACAACCCGTC	This study
HA-EspC (sense)	GCGCAATGCTAAACGGAAGGGACACGATCAATGTACCC ATACGATGTTCCAGATTACGCTGGAATGACGGAAAACT TGACCGTCCAGCCCGAG	This study
C48S (sense)	CACTCACGGTCCGTACTCCTCACAGTTCAACGACAC	This study
D75A (sense)	CATACGGCCGGTGTCTGCTCTCGCCAAAAGTCTTC	This study
Y87A (sense)	GAATTGCGGCGAAGATAGCTAGCGAGGCCGACG	This study
D91A (sense)	TATATAGCGAGGCCGCCGAAGCGTGGCGCAAG	This study
R95A (sense)	GCCGACGAAGCGTGGGCCAAGGCTATCGACGGG	This study
K96A (sense)	GACGAAGCGTGGCGCGCGGCTATCGACGGGTTG	This study
I98A (sense)	CGTGGCGCAAGGCTGCCGACGGGTTGTTTAC	This study
D99A (sense)	GGCGCAAGGCTATCGCCGGGTTGTTTACCTG	This study
L101A (sense)	CAAGGCTATCGACGGGGCGTTTACCTGACCACG	This study
F102A (sense)	CTATCGACGGGTTGGCTACCTGAAAGCTTATC	This study
T103A (sense)	CGACGGGTTGTTTGCCTGACCACGTTTGCTG	This study
I98A / F102A (sense)	1: CGTGGCGCAAGGCTGCCGACGGGTTGTTTAC 2: CTGCCGACGGGTTGGCTACCTGAAAGCTTATC	This study
EspC <sup>Δ6</sup> (pMDespAC <sub>HAD</sub> , sense)	1: GCGTGGCGCAAGGCTTGAGACGGGTTGTTTACC 2: GACGGGTTGTTTACCGGACCACGTTTGCTGC	This study

**Table S2.2 Bacterial strains**

Strains	Description	Reference
<i>M. smeg groEL1ΔC</i>	<i>M. smegmatis</i> strain modified with deletion of histidine-rich C-terminus of GroEL1, which is used to overexpress EspC and the mutants.	[9]
<i>M. tb</i> Erdman	Wild type	[3]
<i>M. tb</i> Erdman <i>espC</i> ::Tn	Transposon insertion mutant in <i>espC</i>	[33]
<i>espC</i> ::Tn+ <i>espAC</i> <sup>wt</sup> <i>D</i>	<i>M.tb</i> Erdman <i>espC</i> ::Tn fully complemented	[33]
<i>espC</i> ::Tn+pMD31	<i>M.tb</i> Erdman <i>espC</i> ::Tn complemented with empty vector	[33]
<i>espC</i> ::Tn+ <i>espAC</i> <sub>HAD</sub>	<i>M.tb</i> Erdman expressing HA-tagged EspC	This study
<i>espC</i> ::Tn+ <i>espAC</i> <sup>CΔ6</sup> <i>D</i>	<i>M.tb</i> Erdman expressing HA-tagged EspC <sup>CΔ6</sup>	This study
<i>espA</i> ::Tn+ <i>espAC</i> <sup>C138A</sup> <i>C</i> <sub>HAD</sub>	<i>M.tb</i> Erdman expressing HA-tagged EspC and EspA <sup>C138A</sup>	This study
<i>espC</i> ::Tn+ <i>espAC</i> <sub>D75A</sub> <i>D</i>	<i>M.tb</i> Erdman expressing HA-tagged EspC	This study
<i>espC</i> ::Tn+ <i>espAC</i> <sup>R95A</sup> <i>D</i>	<i>M.tb</i> Erdman expressing HA-tagged EspC <sup>R95A</sup>	This study
<i>espC</i> ::Tn+ <i>espAC</i> <sup>K96A</sup> <i>D</i>	<i>M.tb</i> Erdman expressing HA-tagged EspC <sup>K96A</sup>	This study
<i>espC</i> ::Tn+ <i>espAC</i> <sup>D99A</sup> <i>D</i>	<i>M.tb</i> Erdman expressing HA-tagged EspC <sup>D99A</sup>	This study
<i>espC</i> ::Tn+ <i>espAC</i> <sup>L101A</sup> <i>D</i>	<i>M.tb</i> Erdman expressing HA-tagged EspC <sup>L101A</sup>	This study
<i>espC</i> ::Tn+ <i>espAC</i> <sup>F102A</sup> <i>D</i>	<i>M.tb</i> Erdman expressing HA-tagged EspC <sup>F102A</sup>	This study
<i>espC</i> ::Tn+ <i>espAC</i> <sup>T103A</sup> <i>D</i>	<i>M.tb</i> Erdman expressing HA-tagged EspC <sup>T103A</sup>	This study
<i>espC</i> ::Tn+ <i>espAC</i> <sub>Flag</sub> <i>D</i>	<i>M.tb</i> Erdman expressing Flag-tagged EspC	[33]
<i>espC</i> ::Tn+ <i>espAC</i> <sup>C48S</sup> <i>D</i>	<i>M.tb</i> Erdman expressing Flag-tagged EspC <sup>C48S</sup>	This study
<i>espC</i> ::Tn+ <i>espAC</i> <sup>Y87A</sup> <i>D</i>	<i>M.tb</i> Erdman expressing Flag-tagged EspC <sup>Y87A</sup>	This study
<i>espC</i> ::Tn+ <i>espAC</i> <sup>D91A</sup> <i>D</i>	<i>M.tb</i> Erdman expressing Flag-tagged EspC <sup>D91A</sup>	This study





## **Chapter 3**

### **Characterization of EccCb1 as an ATPase**



### 3.1 Abstract

EccCa1 and EccCb1, encoded by *rv3870* and *rv3871*, are two conserved hypothetical proteins of the ESX-1 secretion system. They possess sequence homology with FtsK/SpoIIIE protein family of the AAA+ ATPases, involved in DNA translocation and chromosomal segregation. Therefore, EccCa1 and EccCb1 are predicted to function as molecular motors for protein export. In this study, we overexpressed EccCb1 fused with a NusA tag in *Escherichia coli*, and purified the fusion protein using affinity chromatography. We found that EccCb1 hydrolyzed ATP, rather than GTP, in the presence of the cofactor magnesium. Furthermore, the ATPase activity was significantly reduced when mutations were introduced to the conserved lysine residues in the two Walker A motifs in the catalytic sites of EccCb1. The gel filtration profiles showed that NusA-EccCb1 was predominantly in a hexameric form, in agreement with the previous prediction that EccCb1 belongs to FtsK/SpoIIIE family. Altogether, we provided direct evidence to prove that EccCb1 of *Mycobacterium tuberculosis* (*M. tb*) is an ATPase of the ESX-1 secretion system, which likely functions as a molecular motor for the secretion.

## 3.2 Introduction

A bacterial secretion system comprises different types of proteins that assemble into a nanomachine at the cell envelope, whereby the substrates are exported from the cytosol to the extracellular space. Each individual component contributes to the secretion pathway through its distinct function. ATPase is generally required as an energy supplier for secretory apparatus assembly and substrate translocation- two processes that consume energy. Thus, it is critical for protein transport.

In the ESX-1 secretion system, several proteins with ATPase domains have been identified and characterized using biochemical or structure-based approaches, including EspI, EccA1, EccB1 and EccC1 [1-9]. EccA1 and EccC1 are of particular interest since they are directly involved in substrate recognition and interaction [8,10]. It was indicated by yeast two-hybrid studies that the known ESX-1 substrates, EsxA/EsxB and EspC, are differentially targeted for secretion via the interaction with different ATPases. Although the C-terminal region of these substrates share the general type VII signal sequence YxxxD/E, they are not equivalent with respect to ATPase recognition [8,11]. While EspC was shown to interact with EccA1, EsxA/EsxB are targeted to EccC1. Therefore, it is important to investigate the structure of the individual ATPases and to study their interaction with the respective substrates.

EccA1 (Rv3868) was first characterized as an ATPase in 2008 [3], and the N-terminal structure was solved by X-ray crystallography in 2013 [12]. As predicted by bioinformatics, EccA1 is a cytosolic AAA+ ATPase. The N-terminal TPR fold of EccA1 interacts with the exported cargo, and the C-terminal motif that possesses ATPase activity, is predicted to be involved in oligomerization. According to the molecular model, EccA1 is organized in a hexameric ring with a central pore, which can open or close to allow the passage of the substrates. This process is driven by ATP hydrolysis.

*M. tb* EccC1, consisting of two proteins- EccCa1 (747 amino acid) and EccCb1 (591 amino acid), is encoded by the genes *rv3870* and *rv3871* in the *esx-1* locus. The architecture of EccC1 in the ESX-1 of *M. tb* is unique, as the EccC paralogues in other T7S systems consist of a single protein with multi-ATPase domains [7,13,14]. Based on the result of a yeast two-hybrid assay showing the protein interaction *in vitro*, EccCa1 and EccCb1 are speculated to act as a single functional unit [6]. Sequence analyses of the two proteins reveal that they harbor FtsK-SpoIIIE AAA+ ATPase domains (Fig.3.1A,B). This ATPase family is conserved throughout bacteria and plays an important role in translocation of DNA and proteins through the membrane-spanning pore it forms [15,16]. Typically, proteins of the FtsK-SpoIIIE family contain an ATP-binding motif and an ATP-hydrolysis motif, termed Walker A and Walker B respectively. The two motifs interact with the phosphate groups of the bound ATP, as well as the cofactor magnesium. As shown in Fig.3.1, the conserved Walker A sequence A/GxxxxGKT/S and Walker B sequence hhhhDE (h denotes a hydrophobic amino acid) are present in both EccCa1 and EccCb1. This suggests that EccCa1 and EccCb1 may play an essential role in supplying energy for the ESX-1 secretion pathway, which is consistent with the fact that mutations in either *rv3870* or *rv3871* blocked EsxA/EsxB secretion [6,17]. Recently, structural and functional characterization of EccC in *T. curvata* was published [7]. *TcEccC* contains three ATPase domains. The authors reported that the N-terminal ATPase 1 of *TcEccC*, equivalent to EccCa1 in the ESX-1 of *M. tb*, may serve as the active motor domain. In contrast, ATPase 2 and ATPase 3, the two ATPase domains present in EccCb1 of ESX-1, were catalytically inactive but function to modulate EccC enzymatic activity through interaction with ATPase 1. In agreement with this, another group studying the ESX ATPase YukBA in YUK secretion system of *Bacillus subtilis*, showed that only the N-terminal ATPase domain was required for protein translocation, whereas the other two ATPase domains were thought to be involved in oligomerization and apparatus assembly [13]. In contrast, the ATPase domains separated into EccCa1 and EccCb1, which together comprising the EccC in *M. tb*, were both required for ESX-1 secretion [13].

In this chapter, we sought to determine the ATPase activity and oligomeric state of the *M. tb* EccCb1 *in vitro*. EccCb1, in the form of a fusion protein with NusA, was overexpressed and purified. As a result, the hexameric EccCb1 was verified to possess ATPase activity as previously predicted by the bioinformatics analyses.

### 3.3 Results

#### Overexpression of EccCa1 and EccCb1 in *E.coli*

To characterize the ATPase activity, we cloned and expressed the recombinant protein in *E. coli*. EccCa1 was expressed as a truncated protein (248-747) corresponding to the ATPase domain lacking the N-terminal transmembrane region (Fig.3.1A). In contrast, the cytosolic protein EccCb1 was expressed as a full-length protein. In both cases, a histidine tag was added to allow affinity purification. Both proteins were highly expressed in *E. coli* after IPTG induction, however, they were mainly detected in the insoluble fraction, suggesting that the proteins were improperly folded and accumulated as inclusion bodies (Fig.3.2). Given the more difficulties in purification of the membrane protein EccCa1, we first worked on EccCb1.

In order to improve the expression level and solubility of EccCb1, a variety of *E. coli* expression strains were tested, including BL21 (DE3) CodonPlus PR, Arctic Express (DE3) PR and BL21 (DE3) pLysS. The EccCb1 gene was inserted into pDEST15 and pET44 vectors prior to transformation into *E. coli*, resulting in production of GST- and NusA-EccCb1 fusion proteins. The results are summarized in Table 3.1. Since the NusA-EccCb1 fusion protein expressed by the BL21 (DE3) CodonPlus PR strain was partially soluble, it was chosen for the further purification and characterization.

#### Purification of EccCb1

In order to increase the yield of soluble protein thereby facilitating downstream purification, it is important to optimize the buffer conditions to improve protein

solubility and stability. We noticed that in buffers containing low NaCl concentrations, protein aggregation occurred soon after being released from the *E. coli* (data not shown). Thus, 500 mM NaCl and 2 mM MgCl<sub>2</sub> were added to the buffer system to stabilize the putative AAA+ ATPase. However, the protein amount in the soluble fraction was insufficient for future purification, as the majority of the expressed recombinant NusA-EccCb1 was detected in the cell debris. We also observed constant co-purification with the molecular chaperone GroEL (Fig.3.3B left). As such, different additives were screened to define a buffer system for the purification of NusA-EccCb1. We found that addition of 0.5% CHAPS, a zwitterionic detergent, largely increased the solubility of EccCb1-NusA (Fig.3.3A) and disrupted the interaction with GroEL. With CHAPS in the buffer, the GroEL was subsequently excluded after Ni-purification (Fig.3.3B right), and pure NusA-EccCb1 was obtained. Unfortunately, cleavage of NusA tag from the fusion protein caused aggregation. Therefore, the following characterization was performed using NusA-EccCb1 fusion protein.

#### **Recombinant EccCb1 is hexameric**

Due to the presence of two predicted AAA+ domains, EccCb1 is a putative ATPase in the ESX-1 secretion system. Since AAA+ ATPases form hexamer, we first analyzed the oligomeric state of EccCb1. The purified NusA-EccCb1 was loaded onto a Sephacryl S-400 HR column for size exclusion chromatography. According to the molecular weights determined from the calibration curve, the size of the eluted protein at the main peak was estimated at around 780 kDa. This is around 6 times that of NusA-EccCb1, revealing that the fusion protein was predominantly in the form of a hexamer (Fig.3.4). The peak derived from the monomeric NusA-EccCb1 was at ~130 kDa in the chromatograph. Since NusA alone does not oligomerize [18], we conclude that the EccCb1 component was responsible for the hexamerization of the NusA-EccCb1 fusion protein. To further visualize the structure of the hexamer, the protein was negatively stained with 2% uranyl acetate and observed by transmission electron microscope. The preliminary EM image demonstrates that the NusA-EccCb1 hexamer appeared to form homogeneous and structured particles (Fig.3.5). The resolution of the

image needs to be improved to further analyze whether the hexamer assembles into a ring-like structure.

### **EccCb1 is an essential energizing component of ESX-1 secretion system**

ATPase activity of the proteins was measured by the PiPer assay. To establish the experiment, we first determined the optimal amount of enzyme required to catalyze ATP hydrolysis. Since the enzyme activity measured by the PiPer assay is continuously monitored in real time, data can be selected from the ideal region of the progress curve. In our test assay, Pi release was proportional to the increasing amount of protein in the range between 0 to 2.25  $\mu\text{g}$  (Fig.3.6A). Thus, 2  $\mu\text{g}$  of protein was used in the following assays. For the measurement of the kinetic parameters  $K_m$  and  $V_{max}$ , ATP concentrations ranging from 10  $\mu\text{M}$  to 1 mM were used. The activity increased in a concentration-dependent manner until it reached the maximum value at around 500  $\mu\text{M}$  ATP. A  $K_m$  of 63.15  $\mu\text{M}$  and  $V_{max}$  of 6.53 nmol/min/mg were obtained (Fig.3.6B). Given that NusA does not bind and hydrolyze NTPs, the overall ATPase activity of the fusion protein can be attributed to EccCb1 [19].

Previous studies have shown that the lysine in the Walker A motif of the AAA+ domain is essential for ATP binding and hydrolysis. In order to further exclude the impact of GroEL and NusA on the ATPase activity determination, thereby confirming our observation, we generated a NusA-EccCb1 double-mutant protein with substitution of the two Walker A lysines by alanines (NusA-EccCb1 K90A/K382A). As expected, the activity of the mutant decreased by  $\sim 7$ -fold from 6.26 nmol/min/mg to 0.84 nmol/min/mg (Fig.3.6C), thereby validating that the overall ATPase activity of the fusion protein is indeed attributable to EccCb1. To investigate if EccCb1 utilizes NTP substrates other than ATP, 1mM of GTP was tested. NusA-EccCb1 displayed  $\sim 5\%$  hydrolysis activity with GTP relative to that of ATP (Fig.3.6D), suggesting that EccCb1 is an ATP-specific ATPase.



### 3.4 Discussion

In this study, we characterized the function of the EccCb1 components as ATPases in the ESX-1 secretion system. Although EccCa1 and EccCb1, the two putative molecular motors, are essential for protein transport, neither of them has been purified and used for *in vitro* biochemical characterization. One reason can be the poor solubility of the mycobacterial proteins expressed in *E. coli*. Statistical analyses show that more than half of the *M. tb* proteins were overexpressed as inclusion bodies [18]. Although EccCb1 is a cytoplasmic protein and predicted to be soluble, most of the EccCb1 was detected in the cell debris. Moreover, co-purification of GroEL with the recombinant EccCb1 is problematic, since GroEL is highly expressed in *E. coli* and tends to interact with the protein of interest [18]. GroEL shares several features with EccCb1, such as similar size, ability to form higher order oligomers and ATPase activity. Even a low contamination from GroEL would cause false positive results. Thus, expression and purification of EccCb1 were the most challenging part of this project. To solve these problems, we fused EccCb1 to a highly soluble protein NusA, expressed the fusion protein in *E. coli* CodonPlus PR strain, and added CHAPS detergent into the buffer system to further improve the protein solubility. As a consequence, the solubility was largely increased, and the NusA-EccCb1 interaction with GroEL was disrupted, allowing subsequent enzymatic activity profiling.

EccC in the ESX-1 secretion system of *M. tb* has a unique architecture composed of EccCa1 and EccCb1. EccC in *T. curvata*, YukBA in *B. subtilis* and EssC in *S. aureus*, all of which harbor ATPase domains with only the N-terminal one active in ATP hydrolysis [7,13,19]. In contrast, EccCa1 and EccCb1 in *M. tb* are both required for ESX-1 secretion [13]. This is in agreement with our data indicating that EccCb1, which contains two C-terminal ATPase domains, is enzymatically active in the absence of EccCa1. Furthermore, EccCb1 is able to oligomerize to form a homohexameric complex without EccCa1. However, given the weak activity, instability and tendency to bind GroEL, we speculate that EccCb1 on its own might not function as a solo ATPase for ESX-1 substrate translocation.

Instead, EccCa1 and EccCb1 may associate to form a stable complex that is anchored to the cell membrane via the N-terminal transmembrane domain of EccCa1. This complex would have three ATPase units, which together act as a single functional translocase.

## **3.5 Materials and Methods**

### **Bioinformatics**

EccCa1 and EccCb1 sequences of *M. tb* were downloaded from TubercuList at EPFL (<http://tuberculist.epfl.ch>). Protein domains were predicted using NCBI Conserved Domain Search. Prediction of the protein structure was made using I-TASSER server (<http://zhanglab.ccmb.med.umich.edu/I-TASSER/>). The protein structures were displayed using Pymol.

### **Cloning, protein expression, purification and mutagenesis**

Truncated EccCa1 (248-747) and full-length EccCb1 were cloned in pHis9 (Gateway-adapted vector), pDEST15 (Gateway-adapted vector) and pET44 (Novagen). The *E. coli* strains BL21 (DE3), BL21 (DE3) CodonPlus RP, Arctic Express (DE3) RP and BL21 (DE3) pLysS were used for protein overexpression, and TOP 10 cell was used for propagation. Protein expression was induced by 0.5 mM IPTG at 16°C for 16 hrs in LB medium, except for ArcticExpress (DE3) RP where the expression was induced at 4°C. Cells were pelleted and lysed by sonication in lysis buffer containing 50 mM Tris pH7.5, 500 mM NaCl, 2 mM MgCl<sub>2</sub>, 0.5% CHAPS, 5% glycerol, 0.5% Triton X-100, 10 mM imidazole and 2 mM BME. After removal of cell debris by centrifugation at 1,800 rpm, the supernatant was loaded onto Ni-NTA that binds the His-tagged recombinant protein. The protein was eluted using buffer containing 300 mM imidazole, and analyzed with SDS-PAGE. Further purification and size analysis were performed in Sephacryl S-400 HR column using FPLC. Proteins were eluted using buffer with 50 mM Tris pH7.5 and 500 mM NaCl.

The double mutant NusA-EccCb1 K90A/K382A was constructed by site-directed mutagenesis using pET44-*eccCb1* as a template. The primers were shown as below:

(K90A: 5'- CGCACCTCAAACCGGGGCGTCGACGCTACTGCAGAC -3';

K382A: 5'- GCGGCCAAATCGGGCGCGACGACCATTTGCCAC -3')

### **Negative Stain EM**

NusA-EccCb1 hexamer was diluted to 0.01 mg/ml, stained with 2% uranyl acetate, and visualized using a Tecnai Spirit transmission electron microscope (FEI).

### **ATPase activity measurements**

The PiPer assay (Life Technologies) was used to detect the inorganic phosphate (Pi) released from the ATP hydrolysis by the enzyme. The reaction was performed according to the manufacturer's instructions. ATPase activity was quantified based on the amount of free Pi, which was determined from a standard curve of a serial dilution of potassium phosphate. To ensure that Pi liberation is proportional to the enzyme, 2.25 µg, 1.125 µg, 0.56 µg and 0.27 µg of fresh NusA-EccCb1 oligomer (determined by Bradford assay) were incubated with 1 mM ATP. For measurement of the kinetic parameters  $K_m$  and  $V_{max}$ , the ATP concentrations ranging from 10 µM to 1 mM were used as the substrates for 2 µg of NusA-EccCb1. Michaelis-Menten calculations were performed using Prism. To measure the ATPase and GTPase activities, 1mM of ATP or GTP was used as the substrate for 2 µg of NusA-EccCb1. The reaction buffer was composed of 100 mM Tris pH7.5 and 5 mM MgCl<sub>2</sub>.

### 3.6 Figures and Tables

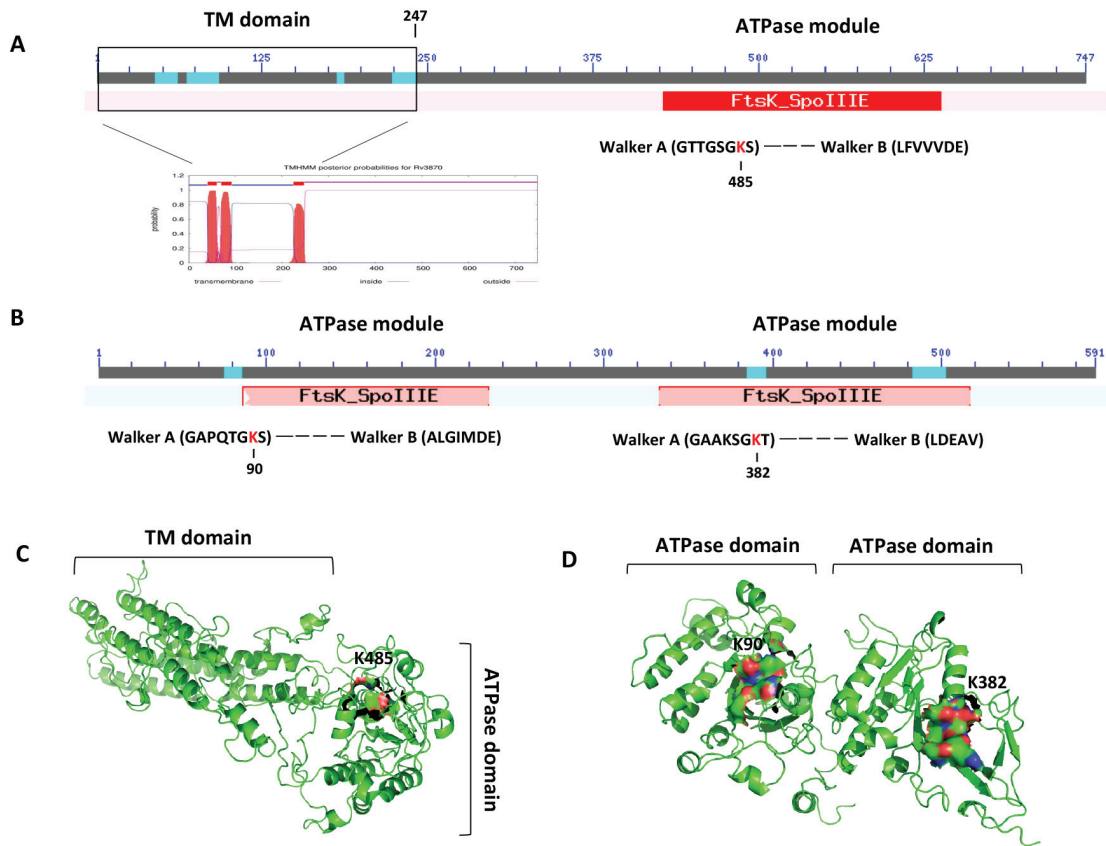


**Fig.3.1 Structural elements of EccCa1 and EccCb1.**

**(A)** EccCa1 contains a transmembrane domain (TM domain, 1-247) at the N-terminus and a FtsK-SpoIII ATPase domain at the C-terminus. **(B)** EccCb1 is a cytoplasmic protein with three FtsK-SpoIII ATPase domains. The Walker A and Walker B motifs at the catalytic sites are highlighted in red and blue. **(C),(D)** Structural models of EccCa1 and EccCb1 (predicted by I-TASSER server). The conserved lysines- EccCa1 K485 and EccCb1 K90/K382 at the Walker A motifs, are labeled.

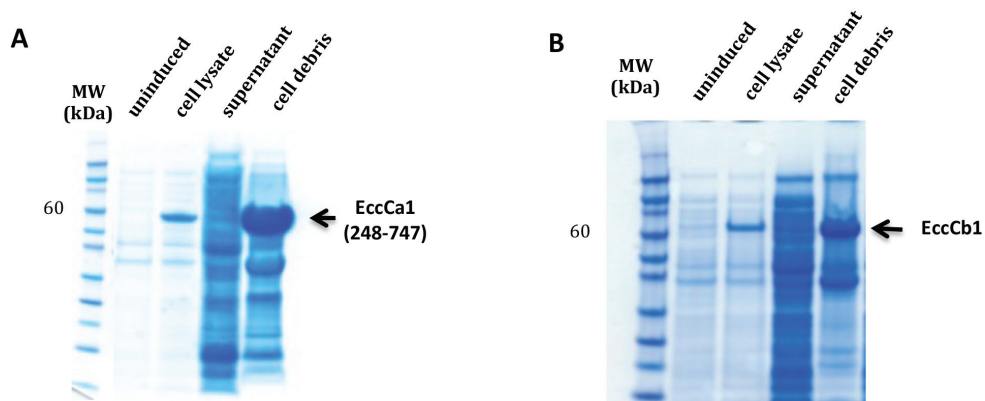


**Fig.3.2 SDS-PAGE gels of the overexpressed EccCa1 (248-747) (A) and EccCb1 (B) in *E. coli* BL21 (DE3).**

The proteins were overexpressed after IPTG induction. Most of EccCa1 (248-747) (54.6 kDa) and EccCb1 (64.5 kDa) were expressed as inclusion bodies that were detected in the cell debris.

**Table 3.1 Overexpression and solubility of recombinant EccCb1**

<b>Strain Vector</b>	<b>BL21 (DE3)</b>	<b>BL21 (DE3) Codon Plus RP</b>	<b>Arctic Express (DE3)</b>	<b>BL21 (DE3) pLysS</b>
<b>pHis9 (His tag)</b>	Expressed, Inclusion body	Expressed, Inclusion body	Expressed, Inclusion body	Expressed, Inclusion body
<b>pDEST15 (GST tag)</b>	No expression	No expression	-	-
<b>pET44 (NusA/S/His tag)</b>	No expression	Expressed, Partially soluble	-	No expression

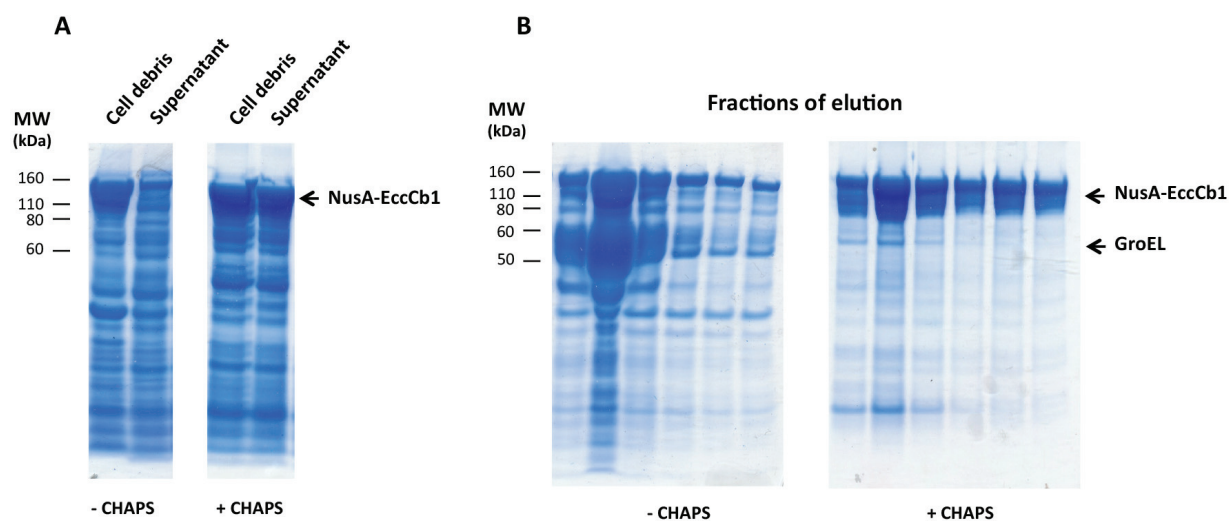


**Fig.3.3 Addition of CHAPS detergent into buffer system improves solubility and purity of NusA-EccCb1.**

**(A)** With 0.5% CHAPS in the buffer, more NusA-EccCb1 was detected in the supernatant after bacterial lysis, indicating an improved solubility by CHAPS. **(B)** When eluted from the Ni column, co-purification with GroEL, an endogenous *E.coli* chaperon protein, was observed (Left). With CHAPS in the buffer, GroEL was removed from NusA-EccCb1 because the interaction was disrupted (Right).

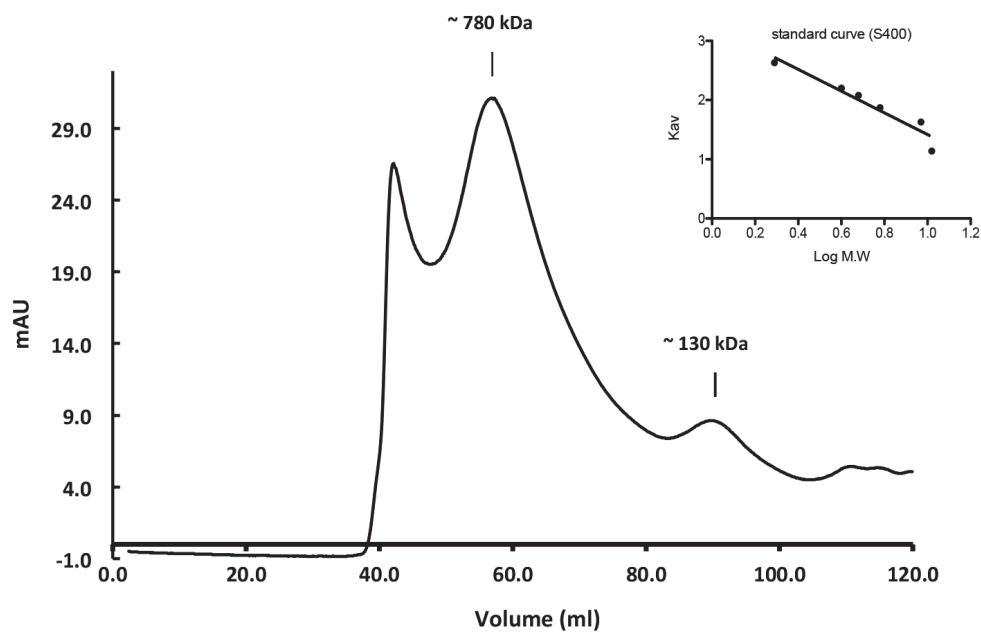


**Fig.3.4 NusA-EccCb1 forms a hexamer.**

Size exclusion chromatography profile of NusA-EccCb1 showed a main peak at ~780 kDa indicated as a hexamer, and a minor peak at ~130 kDa indicated as a monomer. The molecular weights were estimated on the basis of a standard curve.



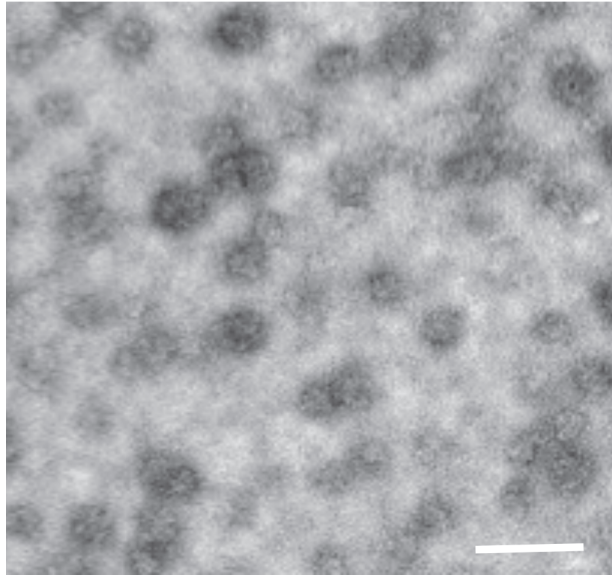


**Fig.3.5 NusA-EccCb1 hexamer forms homogenous and structured particles.**

The hexamer was negatively stained and observed using TEM. Scale bar: 100 nm.

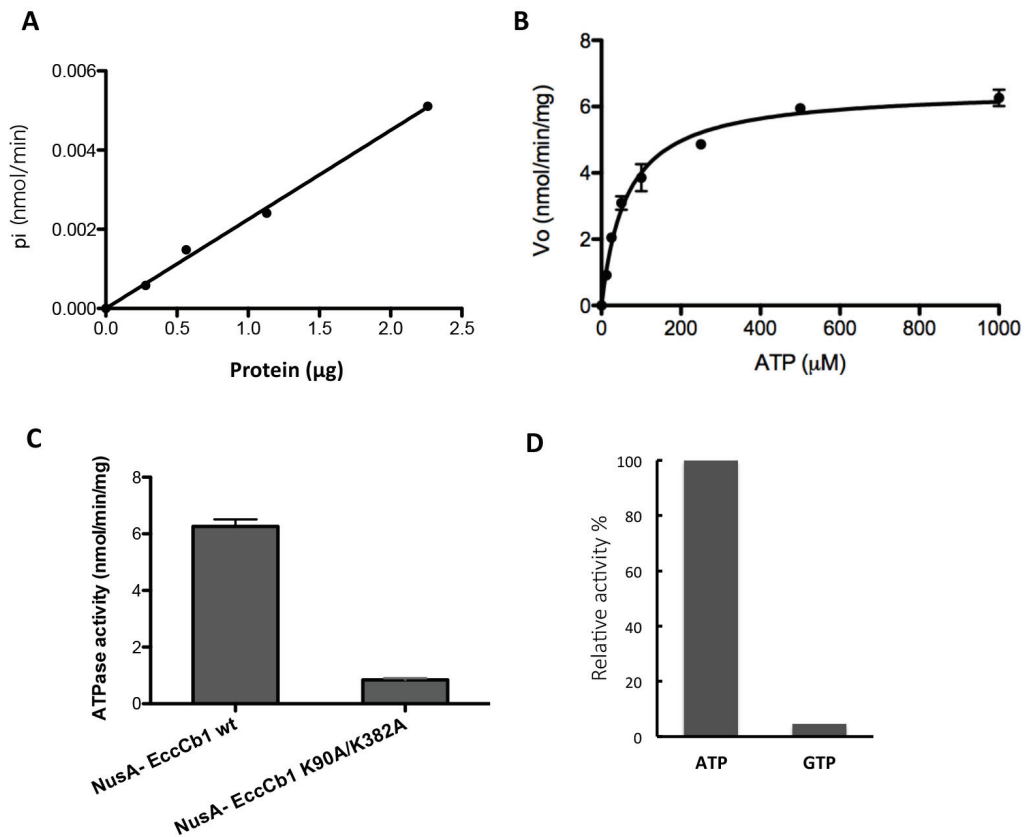


**Fig.3.6 NusA-EccCb1 is an ATPase.**

**(A)** The enzymatic activities were proportional to the indicated amount of Nus-EccCb1. **(B)** Michaelis–Menten plot demonstrated the kinetics of ATP hydrolysis by Nus-EccCb1. The measured  $K_m$  was 63.15  $\mu$ M and  $V_{max}$  was 6.53 nmol/min/mg. **(C)** Mutation of the essential lysines, K90 and K382 at the two Walker A motifs, significantly reduced the ATPase activity of NusA-EccCb1, which confirmed that EccCb1 is an FtsK-SpoIIIE AAA+ ATPase. **(D)** EccCb1 specifically hydrolyzed ATP, whereas only ~5% of GTPase activity was observed.

## References

1. Zhang M, Chen JM, Sala C, Rybníček J, Dhar N, et al. (2014) EspI regulates the ESX-1 secretion system in response to ATP levels in *Mycobacterium tuberculosis*. *Mol Microbiol* 93: 1057-1065.
2. Luthra A, Gaur A, Ramachandran R (2013) Rv3868 (EccA1), an essential component of the *Mycobacterium tuberculosis* ESX-1 secretion system, is thermostable. *Biochim Biophys Acta* 1834: 1181-1186.
3. Luthra A, Mahmood A, Arora A, Ramachandran R (2008) Characterization of Rv3868, an essential hypothetical protein of the ESX-1 secretion system in *Mycobacterium tuberculosis*. *J Biol Chem* 283: 36532-36541.
4. Zhang XL, Li DF, Fleming J, Wang LW, Zhou Y, et al. (2015) Core component EccB1 of the *Mycobacterium tuberculosis* type VII secretion system is a periplasmic ATPase. *FASEB Journal* 29: 4804-4814.
5. Xie XQ, Zhang XL, Qi C, Li DF, Fleming J, et al. (2016) Crystallographic observation of the movement of the membrane-distal domain of the T7SS core component EccB1 from *Mycobacterium tuberculosis*. *Acta Crystallographica Section F-Structural Biology Communications* 72: 139-144.
6. Stanley SA, Raghavan S, Hwang WW, Cox JS (2003) Acute infection and macrophage subversion by *Mycobacterium tuberculosis* require a specialized secretion system. *Proc Natl Acad Sci U S A* 100: 13001-13006.
7. Rosenberg OS, Dovala D, Li X, Connolly L, Bendebury A, et al. (2015) Substrates Control Multimerization and Activation of the Multi-Domain ATPase Motor of Type VII Secretion. *Cell* 161: 501-512.
8. Champion PA, Champion MM, Manzanillo P, Cox JS (2009) ESX-1 secreted virulence factors are recognized by multiple cytosolic AAA ATPases in pathogenic mycobacteria. *Mol Microbiol* 73: 950-962.
9. Pallen MJ (2002) The ESAT-6/WXG100 superfamily -- and a new Gram-positive secretion system? *Trends Microbiol* 10: 209-212.
10. Champion PA, Stanley SA, Champion MM, Brown EJ, Cox JS (2006) C-terminal signal sequence promotes virulence factor secretion in *Mycobacterium tuberculosis*. *Science* 313: 1632-1636.
11. Daleke MH, Ummels R, Bawono P, Heringa J, Vandenbroucke-Grauls CM, et al. (2012) General secretion signal for the mycobacterial type VII secretion pathway. *Proc Natl Acad Sci U S A* 109: 11342-11347.
12. Wagner JM, Evans TJ, Korotkov KV (2014) Crystal structure of the N-terminal domain of EccA(1) ATPase from the ESX-1 secretion system of *Mycobacterium tuberculosis*. *Proteins-Structure Function and Bioinformatics* 82: 159-163.
13. Ramsdell TL, Huppert LA, Sysoeva TA, Fortune SM, Burton BM (2015) Linked domain architectures allow for specialization of function in the

- FtsK/SpoIIIE ATPases of ESX secretion systems. *J Mol Biol* 427: 1119-1132.
14. Gey Van Pittius NC, Gamielien J, Hide W, Brown GD, Siezen RJ, et al. (2001) The ESAT-6 gene cluster of *Mycobacterium tuberculosis* and other high G+C Gram-positive bacteria. *Genome Biol* 2: RESEARCH0044.
  15. Iyer LM, Makarova KS, Koonin EV, Aravind L (2004) Comparative genomics of the FtsK-HerA superfamily of pumping ATPases: implications for the origins of chromosome segregation, cell division and viral capsid packaging. *Nucleic Acids Res* 32: 5260-5279.
  16. Thomsen ND, Berger JM (2008) Structural frameworks for considering microbial protein- and nucleic acid-dependent motor ATPases. *Molecular Microbiology* 69: 1071-1090.
  17. Pym AS, Brodin P, Majlessi L, Brosch R, Demangel C, et al. (2003) Recombinant BCG exporting ESAT-6 confers enhanced protection against tuberculosis. *Nat Med* 9: 533-539.
  18. De Marco V, Stier G, Blandin S, de Marco A (2004) The solubility and stability of recombinant proteins are increased by their fusion to NusA. *Biochemical and Biophysical Research Communications* 322: 766-771.
  19. Ryu GH, Tanaka H, Kim DH, Kim JH, Bae SH, et al. (2004) Genetic and biochemical analyses of Pfh1 DNA helicase function in fission yeast. *Nucleic Acids Res* 32: 4205-4216.
  20. Noens EE, Williams C, Anandhakrishnan M, Poulsen C, Ehebauer MT, et al. (2011) Improved mycobacterial protein production using a *Mycobacterium smegmatis* groEL1 Delta C expression strain. *Bmc Biotechnology* 11.
  21. Burts ML, Williams WA, DeBord K, Missiakas DM (2005) EsxA and EsxB are secreted by an ESAT-6-like system that is required for the pathogenesis of *Staphylococcus aureus* infections. *Proc Natl Acad Sci U S A* 102: 1169-1174.

## **Chapter 4**

### **Calcium deprivation promotes ESX-1 secretion and persistence of *M. tb***



## 4.1 Introduction

In Chapter 2, we demonstrated that EspC in the mycobacterial ESX-1 secretion system shares many properties with the needle proteins of T3SS. To study the parallels between the two systems, we further examined their similarities.

As a facultative intracellular pathogen, *M. tb* needs to differentiate between an extracellular and intracellular environments. When internalized, the bacterium encounters environmental stresses such as nutrient limitation, acidic pH, low-oxygen tension, change of ion level and other stimuli, which stimulate a survival response. In order to adapt to these stresses, *M. tb* is equipped with 11 two-component signal transduction systems (TCSS), 5 orphaned response regulators (RR) and several sensor kinases (SK) [1,2], which allow the bacteria to mount a response when it is exposed to specific stimuli within the host.

Divalent cations such as  $Mg^{2+}$  and  $Ca^{2+}$  can act as signals to regulate virulence gene expression and/or protein secretion. The intracellular calcium concentration is in the range of 50 to 150 nM, while extracellular compartments, such as the mucosa and the blood, have calcium concentrations in the millimolar range [3,4]. Studies of *Yersinia* species and *Pseudomonas aeruginosa* have revealed that pathogens equipped with a T3SS respond to a low calcium signal (so called “low calcium response”) for secreting effector proteins [5-7]. It was speculated that the bacterial needle inserted into the host cell, senses the reduced calcium level in the host cell’s cytoplasm and triggers the secretion cascade. Similarly, magnesium also plays an important role in bacterial virulence through regulation of T3SS [8,9]. For instance, the facultative intracellular pathogen *Salmonella typhimurium* senses the environmental magnesium level during its entry and inversely regulates the two independent T3SSs: SPI-1 and SPI-2. SPI-1 is critical for the initial invasion from outside of the cell [10], whereas SPI-2 is important for survival in host cell vacuoles [11,12]. Likewise, under laboratory culture conditions, SPI-2 gene expression in *S. typhimurium*

was induced when the bacteria were grown in culture medium containing lower concentration of magnesium [13].

A “low calcium response” is also observed in *M. tb*. Here we show that excess calcium impairs *M. tb* virulence in two important aspects. Firstly, ESX-1 secretion is blocked by the addition of  $\text{CaCl}_2$  to the culture medium. Secondly, bacterial persistence, but not growth rate, is reduced, a likely consequence of the down-regulation of hypoxia response genes. In other words, calcium deprivation could promote ESX-1-dependent secretory function and *M. tb* persistence.

## 4.2 Results

### Calcium stress blocks ESX-1 secretion

Calcium availability affects the virulence of certain pathogenic Gram-negative bacteria utilizing the T3SS. Since EspC of the ESX-1 secretion system is thought to be functionally orthologous to the needle proteins of T3SS, we tested if calcium deprivation affects ESX-1 secretion. The bacteria were cultured with different calcium concentrations mimicking those encountered in the phagosome and extracellular environment. When grown in media with elevated levels of  $\text{CaCl}_2$ , *M. tb* secreted less EsxA and EspC, which were completely blocked at 500  $\mu\text{M}$   $\text{CaCl}_2$ . The intracellular level of EsxA did not change, whereas EspC was slightly reduced with elevation of calcium concentration (Fig.4.1). Furthermore, the bacteria grown with 750  $\mu\text{M}$   $\text{CaCl}_2$  plus 2 mM EGTA showed a similar phenotype in secretion with those grown in the calcium free medium (data not shown), verifying that calcium caused their defect in secretion. Collectively, low calcium promotes mycobacterial ESX-1 secretion system.

### Effect of calcium stress on *M. tb* growth

In addition to secretion, the effects of calcium on bacterial growth in Sauton's medium were also investigated. In all test conditions, the doubling times did not



vary in the early exponential phase. However, after ~5 days, the growth rate began to decrease in media containing >500  $\mu\text{M}$  calcium (Fig.4.2). We also observed a significant reduction in the cell density of bacteria cultured for 8 days. In contrast, bacteria in the calcium-free media grew normally to stationary phase, revealing that bacterial viability was affected by high calcium concentrations.

### **Calcium stress repressed DevR regulon**

The lower viability, as well as the slight EspC reduction in the cytosol when the bacteria were grown in the culture medium with a higher concentration of calcium, prompted us to perform RNA-seq experiments to investigate the impact of high calcium on global changes in gene expression. The top up-regulated and top down-regulated genes are listed in Table 4.1 and Table 4.2 respectively. Surprisingly, exposure to 750  $\mu\text{M}$   $\text{CaCl}_2$  led to a strong repression of the hypoxia response genes. All of these genes are in the DevR regulon, which are under the control of the two-component response regulator DevRS. The hypoxia response genes allow the bacteria to enter a “dormant” non-replicative state that ensures long-term intracellular survival and latency. Thus, the down-regulation of these genes by high calcium levels would reduce the persistence of *M. tb*. Consistent with this view, we observed a significant decrease in bacterial viability at the stationary phase in response to high calcium stress (Fig.4.2). Among the differentially expressed genes, only ~20 genes were induced in response to high concentrations of calcium, 12 of which encode PE/PPE proteins. Although EspC was slightly decreased in the cytoplasm of *M. tb* cultured in the presence of 750  $\mu\text{M}$   $\text{CaCl}_2$ , the mRNA level of EspC, as well as those of EspA and EspD from the same operon, were not significantly altered. Therefore, high calcium-mediated reduction in the ESX-1 secretion may not be a consequence of transcription repression.

### 4.3 Discussion

The divalent cations calcium and magnesium are required for regulation of T3SS. In this study, we asked if divalent cations function similarly in the ESX-1 secretion system of *M. tb*. Since a high level of magnesium is essential for mycobacterial growth [14], we did not deplete it from the defined Sauton's culture medium containing ~2 mM MgSO<sub>4</sub> (Table S4.1). As such, this chapter focuses only on the effects of calcium.

The link between calcium signaling and mycobacterial infection has been intensively studied previously. Infection of *M. tb* alters cell signaling in immune cells by increasing intracellular calcium levels [15-17]. As a consequence, phagosomal maturation is promoted, resulting in the killing of intracellular *M. tb*. Thus, reduced survival was reported when *M. tb* infected macrophages were exposed to ionophore A23187, a compound used to elevate intracellular calcium [16]. In addition to what was described, our work examines *M. tb* virulence and susceptibility from a different angle. Since EsxA secretion is necessary for cytolysis and phagosomal escape of *M. tb*, it is plausible that the reduced bacterial survival could be partially attributed to the inhibition of EsxA secretion by higher cytosolic calcium concentrations. Thus, a low cytosolic calcium level (~100 nM) enables EsxA export via the ESX-1 secretion system which damages the phagosomal membrane and promotes *M. tb* survival.

Based on our RNA-seq data, several PE/PPE proteins were up-regulated by the calcium. These PE/PPE family members are quite abundant in the pathogenic mycobacteria, which comprise around 10% of the coding potential of genome in *M. tb* [29]. Multiple of PE/PPE proteins were found exported to the bacterial surface via the ESX secretion systems, tightly associated with the cell wall, and function to modulate innate immune responses [30]. It is likely that due to the relatively higher amount of extracellular calcium (in a millimolar level), the up-regulation of a certain PE/PPE proteins might promote bacterial entry into macrophages at the early stage of infection.

It was shown that higher calcium in the culture medium caused significant down-regulation of hypoxia response genes, most of which are in the DevR regulon [19]. DevRS is one of the TCSs in *M. tb* associated with mycobacterial dormancy. Survival of *M. tb* relates to expression of hypoxia response genes, as dormancy or latency appear to be linked to hypoxic conditions in the host that allow the bacterium to escape from immune recognition [18,19]. Thus, a blunt hypoxia response may underlie the increased susceptibility in the macrophage with elevated intracellular calcium level [16]. Besides, repression of hypoxia response genes had a negative effect on the bacterial growth. *M. tb* stopped growing after 5 days and died rapidly (Fig.4.2). The similar *in vitro* growth arrest by hypoxia was also observed previously [20]. Taken together, low calcium environment not only promotes ESX-1 secretion to arrest phagolysosomal fusion, but should also improve *M. tb* intracellular persistence.

Conversely, the cation zinc was found to dose-dependently enhance secretion of EsxA [21]. Like calcium, zinc is not involved in the transcriptional regulation of ESX-1-related genes (unpublished data). Surprisingly, none of the genes in the PhoPR and MprAB regulon were significantly altered by calcium/zinc, although PhoPR and MprAB two-component systems are known to mediate the regulation of ESX-1 secretion and mycobacterial virulence via regulating *espR* and *espACD* [22-24]. It appears that calcium and zinc regulate the ESX-1 pathway at a post-translational level rather than at the transcriptional level. The mechanism is under investigation.

## 4.4 Materials and Methods

### Bacterial strains and growth conditions

*M. tb espC::Tn+espAC<sub>HAD</sub>* strain used in the experiments was genetically modified to express the HA-tagged EspC as described previously. Cells were routinely grown at 37°C in Middlebrook 7H9 broth (supplemented with 0.2% glycerol, 10% ADC, and 0.05% Tween-80) or in Sauton's medium (Table S4.1) containing

0.005% Tween-80 in the case of culture filtrate analysis. Hygromycin and kanamycin were added to the media at a final concentration of 50 µg/ml and 25 µg/ml. To study the effects of calcium, 250 µM, 500 µM and 750 µM of CaCl<sub>2</sub> were supplemented to the media respectively.

### **Detection of ESX-1 secretion using immunoblot**

Culture filtrates and cell lysates were prepared as described previously. Briefly, they were obtained from the 5-days bacterial cultures in Sauton's medium containing 0.005% Tween-80 and the indicated concentrations of CaCl<sub>2</sub>. Then, the EsxA and EspC secreted into the culture medium are sufficient to be detected by immunoblot. After centrifugation, the supernatants were filtered through 0.22 µm filters and concentrated 100-fold using a Vivaspinn column with 5-kDa MW cut-off membranes. The pellets were resuspended in 1 ml PBS, homogenized by bead beater and subjected to centrifugation and filtering before analysis. ESX-1 associated proteins EsxA and EspC were detected by SDS-PAGE and immunoblot using anti-EsxA and anti-HA antibodies, respectively.

### **RNA extraction, library preparation for RNA-seq analysis and Illumina high-throughput sequencing**

*M. tb* Erdman were cultured in Sauton's medium with various calcium concentrations for 4 days when it reached exponential phase. Total RNA was extracted with TRIzol (Invitrogen) and treated with DNase I (Roche) twice before library preparation or generation of the cDNA template. The cDNA was synthesized with random hexamer primers using the RevertAid First Strand cDNA Synthesis Kit (Fermentas).

100 ng of total RNA were used for the library preparation according to the instructions provided in the TruSeq Stranded mRNA LT kit (Illumina). An aliquot of the libraries was quantified on Qubit (Life Technologies) and Agilent Fragment Analyzer (Advanced Analytical) prior to sequencing on Illumina HiSeq

2500 using the TruSeq SR Cluster Generation Kit v3 and TruSeq SBS Kit v3. Data were processed with the Illumina Pipeline Software v1.82.

### **Differential gene expression analysis**

Illumina reads were trimmed to remove adapters and low quality bases (average quality below 15 over 5 bases) using Trimmomatic [25] and aligned onto the *M. tb* Erdman genome sequence (a.n. NC\_020559) using Bowtie2 v.2.2.5 [26]. Counting reads over genes was done using featureCounts from the Subread package v1.4.6 [27]. DESeq2 [28] was used to infer differentially expressed genes.

# 4.5 Figures and Tables

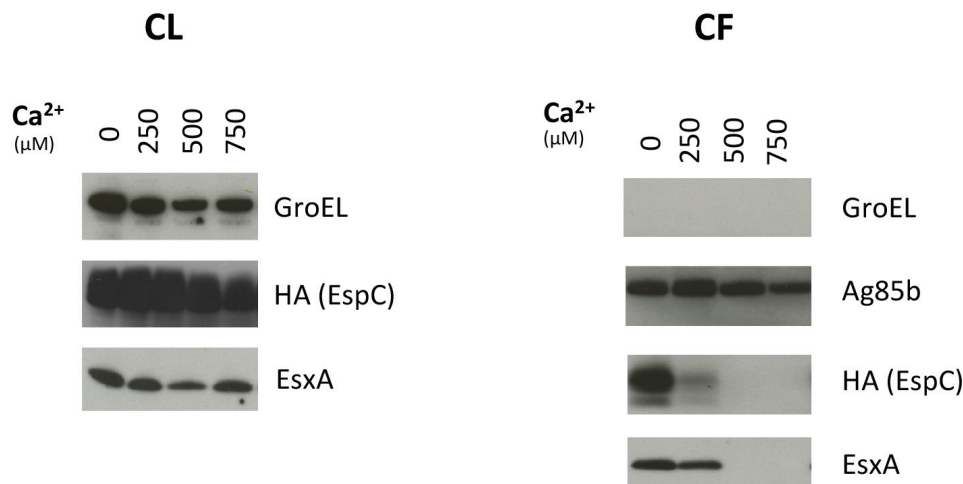


**Fig.4.1 Elevation of calcium inhibited ESX-1 secretion.**

Intracellular EspC was slightly reduced with increased calcium level, while EsxA remained the same. However, compared to the culture without calcium, less EsxA and EspC were secreted when the concentration of calcium reached 250  $\mu\text{M}$ . Furthermore, when calcium was above 500  $\mu\text{M}$ , EsxA and EspC were undetectable. It indicates that the ESX-1 secretion system is inactivated when the bacteria are exposed to high concentration of calcium in the culture medium. Results are representative of those from five independent experiments.

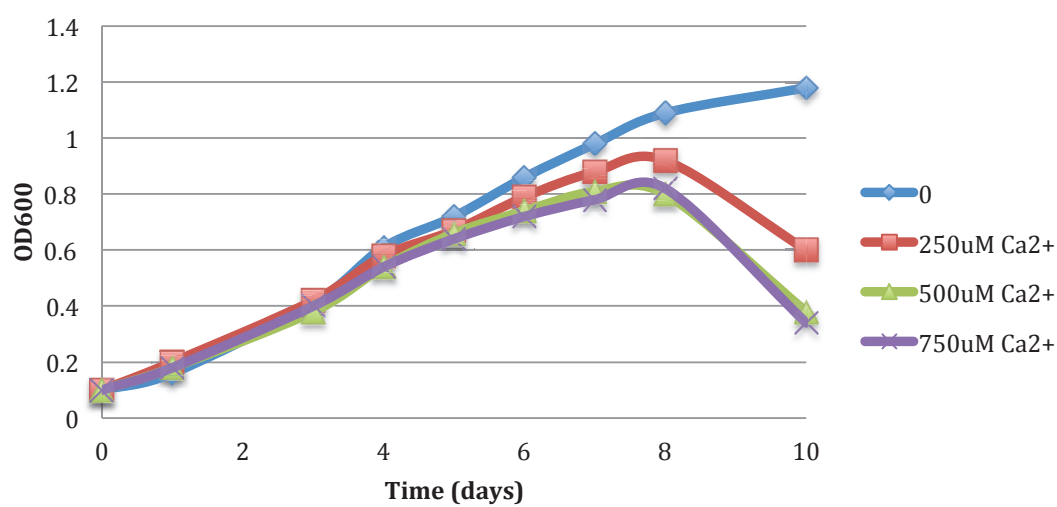


**Fig.4.2 Growth curve of *M. tb* grown in various concentrations of CaCl $_2$ .**

Bacteria were grown in Sauton's medium with 0, 250  $\mu\text{M}$ , 500  $\mu\text{M}$  and 750  $\mu\text{M}$  of CaCl $_2$ . The OD $_{600}$  were determined at the indicated time points. The result is a representative of two independent experiments.

**Table 4.1 Genes up-regulated by 750  $\mu$ M CaCl<sub>2</sub>**

<b>Pvalue</b>	<b>Fold Change</b>	<b>Rv</b>	<b>Rv gene name</b>	<b>Rv product</b>
1.51E-45	7.15	Rv1517	Rv1517	Conserved hypothetical transmembrane protein
2.66E-34	4.77	Rv1039c	PPE15	PPE family protein PPE15
8.50E-27	3.98	Rv1040c	PE8	PE family protein PE8
7.06E-22	3.26	Rv1518	Rv1518	Conserved hypothetical protein
2.15E-38	3.06	Rv0442c	PPE10	PPE family protein PPE10
1.58E-15	2.95	Rv0160c	PE4	PE family protein PE4
2.31E-26	2.76	Rv1004c	Rv1004c	Probable membrane protein
2.14E-30	2.71	Rv3558	PPE64	PPE family protein PPE64
1.62E-11	2.48	Rv0520	Rv0520	Possible methyltransferase/methylase (fragment)
3.42E-20	2.30	Rv3159c	PPE53	PPE family protein PPE53
2.88E-19	2.26	Rv0151c	PE1	PE family protein PE1
2.72E-10	2.21	Rv3621c	PPE65	PPE family protein PPE65
6.39E-09	2.18	Rv0320	Rv0320	Possible conserved exported protein
2.08E-14	2.18	Rv0159c	PE3	PE family protein PE3
7.71E-07	2.14	Rv0521	Rv0521	Possible methyltransferase/methylase (fragment)
9.55E-17	2.08	Rv1527c	pks5	Probable polyketide synthase Pks5
1.16E-14	2.05	Rv2990c	Rv2990c	Hypothetical protein
7.15E-09	2.03	Rv0280	PPE3	PPE family protein PPE3
4.57E-05	2.03	Rv3622c	PE32	PE family protein PE32
1.06E-13	2.00	Rv0341	iniB	Isoniazid inducible gene protein IniB
7.58E-11	1.99	Rv1135c	PPE16	PPE family protein PPE16
7.62E-16	1.99	Rv0835	lpqQ	Possible lipoprotein LpqQ

\* This is the result of RNA-seq analysis.



**Table 4.2 Genes down-regulated by 750  $\mu$ M CaCl<sub>2</sub>**

Pvalue	Fold Change	Rv	Rv gene name	Rv product
2.73E-50	-10.71	Rv1735c	Rv1735c	Hypothetical membrane protein
8.52E-71	-11.13	Rv3132c	devS	Two component sensor histidine kinase DevS
5.03E-125	-12.25	Rv3487c	lipF	Probable esterase/lipase LipF
1.50E-48	-12.38	Rv1736c	narX	Probable nitrate reductase NarX
9.84E-102	-12.52	Rv0570	nrdZ	Probable ribonucleoside-diphosphate reductase (large subunit) NrdZ (ribonucleotide reductase)
2.75E-99	-12.69	Rv2630	Rv2630	Hypothetical protein
1.27E-96	-13.84	Rv2004c	Rv2004c	Conserved protein
5.20E-53	-14.41	Rv2031c	hspX	Heat shock protein HspX (alpha-crystallin homolog) (14 kDa antigen) (HSP16.3)
3.85E-120	-17.00	Rv2629	Rv2629	Conserved protein
4.15E-106	-18.61	Rv3133c	devR	Two component transcriptional regulatory protein DevR (probably LuxR/UhpA-family)
1.39E-137	-29.00	Rv2028c	Rv2028c	Universal stress protein family protein
0	-30.17	Rv1996	Rv1996	Universal stress protein family protein
4.08E-146	-33.26	Rv2628	Rv2628	Hypothetical protein
0	-33.44	Rv0079	Rv0079	Unknown protein
1.42E-238	-36.24	Rv1997	ctpF	Probable metal cation transporter P-type ATPase A CtpF
0	-37.33	Rv0080	Rv0080	Conserved hypothetical protein
1.44E-240	-38.42	Rv1813c	Rv1813c	Conserved hypothetical protein
1.98E-228	-47.50	Rv3134c	Rv3134c	Universal stress protein family protein
8.11E-195	-48.78	Rv2029c	pfkB	6-phosphofructokinase PfkB (phosphohexokinase) (phosphofructokinase)
5.87E-190	-54.07	Rv2624c	Rv2624c	Universal stress protein family protein
1.53E-224	-54.40	Rv1737c	narK2	Possible nitrate/nitrite transporter NarK2
3.29E-247	-63.34	Rv3127	Rv3127	Conserved protein
7.23E-205	-70.15	Rv2007c	fdxA	Ferredoxin FdxA
1.53E-255	-74.59	Rv1733c	Rv1733c	Probable conserved transmembrane protein
1.39E-225	-74.94	Rv2625c	Rv2625c	Probable conserved transmembrane alanine and leucine rich protein
2.63E-289	-92.38	Rv3131	Rv3131	Conserved protein
1.27E-265	-99.85	Rv2623	TB31.7	Universal stress protein family protein TB31.7
0	-108.13	Rv2627c	Rv2627c	Conserved protein
3.09E-269	-114.71	Rv2626c	hrp1	Hypoxic response protein 1 Hrp1
0	-123.60	Rv2032	acg	Conserved protein Acg
0	-135.89	Rv1738	Rv1738	Conserved protein
0	-141.05	Rv3130c	tgs1	Triacylglycerol synthase (diacylglycerol acyltransferase) Tgs1

\* This is the result of RNA-seq analysis.

## References

1. Cole ST, Brosch R, Parkhill J, Garnier T, Churcher C, et al. (1998) Deciphering the biology of *Mycobacterium tuberculosis* from the complete genome sequence. *Nature* 393: 537-544.
2. Bretl DJ, Demetriadou C, Zahrt TC (2011) Adaptation to Environmental Stimuli within the Host: Two-Component Signal Transduction Systems of *Mycobacterium tuberculosis*. *Microbiology and Molecular Biology Reviews* 75: 566-582.
3. Christensen KA, Myers JT, Swanson JA (2002) pH-dependent regulation of lysosomal calcium in macrophages. *J Cell Sci* 115: 599-607.
4. Robinson NP, Kyle H, Webber SE, Widdicombe JG (1989) Electrolyte and Other Chemical Concentrations in Tracheal Airway Surface Liquid and Mucus. *Journal of Applied Physiology* 66: 2129-2135.
5. Cheng LW, Kay O, Schneewind O (2001) Regulated secretion of YopN by the type III machinery of *Yersinia enterocolitica*. *J Bacteriol* 183: 5293-5301.
6. Houppert AS, Kwiatkowski E, Glass EM, DeBord KL, Merritt PM, et al. (2012) Identification of chromosomal genes in *Yersinia pestis* that influence type III secretion and delivery of Yops into target cells. *PLoS One* 7: e34039.
7. Rimpilainen M, Forsberg A, Wolf-Watz H (1992) A novel protein, LcrQ, involved in the low-calcium response of *Yersinia pseudotuberculosis* shows extensive homology to YopH. *J Bacteriol* 174: 3355-3363.
8. Vescovi EG, Soncini FC, Groisman EA (1996) Mg<sup>2+</sup> as an extracellular signal: Environmental regulation of *Salmonella* virulence. *Cell* 84: 165-174.
9. Kuhle V, Hensel M (2004) Cellular microbiology of intracellular *Salmonella enterica*: functions of the type III secretion system encoded by *Salmonella* pathogenicity island 2. *Cell Mol Life Sci* 61: 2812-2826.
10. Lostroh CP, Lee CA (2001) The *Salmonella* pathogenicity island-1 type III secretion system. *Microbes Infect* 3: 1281-1291.
11. Kaur J, Jain SK (2012) Role of antigens and virulence factors of *Salmonella enterica* serovar Typhi in its pathogenesis. *Microbiol Res* 167: 199-210.
12. Lee AK, Detweiler CS, Falkow S (2000) OmpR regulates the two-component system SsrA-ssrB in *Salmonella* pathogenicity island 2. *J Bacteriol* 182: 771-781.
13. Deiwick J, Nikolaus T, Erdogan S, Hensel M (1999) Environmental regulation of *Salmonella* pathogenicity island 2 gene expression. *Mol Microbiol* 31: 1759-1773.
14. Piddington DL, Kashkouli A, Buchmeier NA (2000) Growth of *Mycobacterium tuberculosis* in a defined medium is very restricted by acid pH and Mg(2+) levels. *Infect Immun* 68: 4518-4522.

15. Vergne I, Chua J, Deretic V (2003) Tuberculosis toxin blocking phagosome maturation inhibits a novel Ca<sup>2+</sup>/calmodulin-PI3K hVPS34 cascade. *J Exp Med* 198: 653-659.
16. Malik ZA, Denning GM, Kusner DJ (2000) Inhibition of Ca<sup>2+</sup> signaling by *Mycobacterium tuberculosis* is associated with reduced phagosome-lysosome fusion and increased survival within human macrophages. *Journal of Experimental Medicine* 191: 287-302.
17. Majeed M, Perskvist N, Ernst JD, Orselius K, Stendahl O (1998) Roles of calcium and annexins in phagocytosis and elimination of an attenuated strain of *Mycobacterium tuberculosis* in human neutrophils. *Microb Pathog* 24: 309-320.
18. Wayne LG, Sohaskey CD (2001) Nonreplicating persistence of *mycobacterium tuberculosis*. *Annu Rev Microbiol* 55: 139-163.
19. Park HD, Guinn KM, Harrell MI, Liao R, Voskuil MI, et al. (2003) Rv3133c/dosR is a transcription factor that mediates the hypoxic response of *Mycobacterium tuberculosis*. *Molecular Microbiology* 48: 833-843.
20. Wayne LG, Hayes LG (1996) An in vitro model for sequential study of shutdown of *Mycobacterium tuberculosis* through two stages of nonreplicating persistence. *Infection and Immunity* 64: 2062-2069.
21. Rybniker J, Chen JM, Sala C, Hartkoorn RC, Vocat A, et al. (2014) Anticytolytic Screen Identifies Inhibitors of *Mycobacterial* Virulence Protein Secretion. *Cell Host & Microbe* 16: 538-548.
22. Gonzalo-Asensio J, Mostowy S, Harders-Westerveen J, Huygen K, Hernandez-Pando R, et al. (2008) PhoP: a missing piece in the intricate puzzle of *Mycobacterium tuberculosis* virulence. *PLoS One* 3: e3496.
23. Li AH, Waddell SJ, Hinds J, Malloff CA, Bains M, et al. (2010) Contrasting transcriptional responses of a virulent and an attenuated strain of *Mycobacterium tuberculosis* infecting macrophages. *PLoS One* 5: e11066.
24. Pang X, Samten B, Cao G, Wang X, Tvinnereim AR, et al. (2013) MprAB regulates the espA operon in *Mycobacterium tuberculosis* and modulates ESX-1 function and host cytokine response. *J Bacteriol* 195: 66-75.
25. Bolger AM, Lohse M, Usadel B (2014) Trimmomatic: a flexible trimmer for Illumina sequence data. *Bioinformatics* 30: 2114-2120.
26. Langmead B, Salzberg SL (2012) Fast gapped-read alignment with Bowtie 2. *Nat Methods* 9: 357-359.
27. Liao Y, Smyth GK, Shi W (2014) featureCounts: an efficient general purpose program for assigning sequence reads to genomic features. *Bioinformatics* 30: 923-930.
28. Love MI, Huber W, Anders S (2014) Moderated estimation of fold change and dispersion for RNA-seq data with DESeq2. *Genome Biol* 15: 550.

29. Cole ST, Brosch R, Parkhill J, Garnier T, Churcher C, et al. (1998) Deciphering the biology of *Mycobacterium tuberculosis* from the complete genome sequence. *Nature* 393: 537-544.
30. Abdallah AM, Verboom T, Weerdenburg EM, Gey van Pittius NC, Mahasha PW, et al. (2009) PPE and PE\_PGRS proteins of *Mycobacterium marinum* are transported via the type VII secretion system ESX-5. *Mol Microbiol* 73: 329-340.

**Table S4.1 Sauton's liquid medium**

<b>KH<sub>2</sub>PO<sub>4</sub></b>	0.5 g
<b>MgSO<sub>4</sub>·7H<sub>2</sub>O</b>	0.5 g
<b>L-Asparagine</b>	4.0 g
<b>Ferric ammonium citrate</b>	0.05 g
<b>Citric acid</b>	2.0 g
<b>1% ZnSO<sub>4</sub></b>	0.1 ml
<b>Glycerol</b>	60 ml
<b>H<sub>2</sub>O</b>	900 ml
<b>pH</b>	7.4



## **Chapter 5**

# **Discussion and Perspective**





Since the discovery of the type VII/ESX secretion system more than a decade ago, numerous efforts have been made to characterize the components of this secretion system. As demonstrated in Table 1.3 and Fig.1.6 of Chapter 1, when the role of each individual protein is uncovered, a global comprehension of this system becomes much clearer.

Although the type VII/ESX secretion system is widely expected to harbor a channel in the outer membrane, the identity of this protein remains unclear. This has been a missing piece of the ESX-1 apparatus for a long time. In this thesis, I identified the EspC as the putative pore forming protein localized in the mycobacterial outer membrane. We raised this hypothesis initially based on a comparison of EspC with the needle proteins of T3SS. In the early experiments, I found that they share considerable features, such as size, structure of the monomer, ability for self-polymerization in *in vitro* and *ex vivo* systems, and immunogenicity. Moreover, the C-terminal sequence of EspC which mediates its polymerization and stability, as well as the bacterial virulence, is similar to those described for T3SS needle proteins. These interesting findings let us further investigate if EspC plays a similar role in the ESX-1 pathway. Immunoblot analysis of the subcellular fractions indicated that EspC is enriched in the cell membrane and capsular layer. Consistent with this, immuno-EM images of the cryo-sectioned *M. tb* revealed that the EspC filaments span or extend out of the capsular layer. Altogether, these evidences indicate that EspC could serve as an outer membrane pore protein to facilitate the passage of EsxA/EsxB.

### **What is the function of EspF in mycobacteria?**

Given EspC's hypothesized role as a needle-like channel in the outer part of the cell envelope, we then asked if EspF, a paralogue of EspC (Fig.2.1 in Chapter 2), also functions as a needle-like pore protein similar to EspC. Previous results showed that EspF affected *M. tb* virulence in an EsxA-independent manner [1]. Therefore, although EspC and EspF share a high similarity in sequence, EspC is the preferred mediator of EsxA/EsxB export in *M. tb*. In the non-pathogenic

mycobacteria like *M. smegmatis*, where ESX-1 is present but the *espACD* locus is absent, this role may be played by another protein, conceivably EspF. In addition, we note that the EspF in *M. tb* and *M. smegmatis* share only 25 identical residues, whereas there are 83 identical ones between *M. tb* and *M. marinum* counterparts. Nevertheless, in spite of high similarity for the latter, EspF was only identified in the capsular layer of *M. marinum*, but was not detectable in that of *M. tb* [2]. It is likely that the components of ESX-1 in different mycobacterial species have diverged and co-evolved to recognize their own substrates. Therefore, the role of EspF as a pore forming protein cannot be ruled out in other mycobacterial species, and it remains to be investigated further.

### **How to visualize the ESX-1 apparatus?**

A complete understanding of the ESX-1 secretion system requires the visualization of the nanomachine in its natural setting. This will provide a broad view of the architecture and provide insights into the assembly process. It is generally accepted that ESX-1 secretion is a two-step process, whereby the substrates are exported into the periplasmic space prior to the translocation across the outer membrane (Fig.1.6 in Chapter 1). However, as we found EspC to be homologous to the needle proteins of T3SS, a central channel spanning the whole cell envelope may exist in the form of an association of Ecc(BCDE)1 complex with the EspC conduit, which could make the ESX-1 apparatus an intact structure with single-step translocation like it is observed in the T3SS (Fig.5.1) [3]. If this hypothesis is validated, it should be possible to isolate the embedded secretion apparatus from the mycobacterial cell wall for observation using cryo-EM.

Direct visualization of the ESX-1 apparatus *in situ* is a second approach, which can be achieved by combining vitreous sections and electron cryo-tomography. Cryo-tomography is an advanced technique that delivers 3D images of an intact cell in a near-native, life-like state, and is increasingly used to solve the structure of macromolecules. In recent years, the *in situ* architectures of T3SS and T6SS

have been successfully illustrated in high resolution by cryo-tomography and sub-tomogram averaging [4,5]. Similarly, this technique may be used to resolve the structure of T7SS/ESX-1 secretion system.

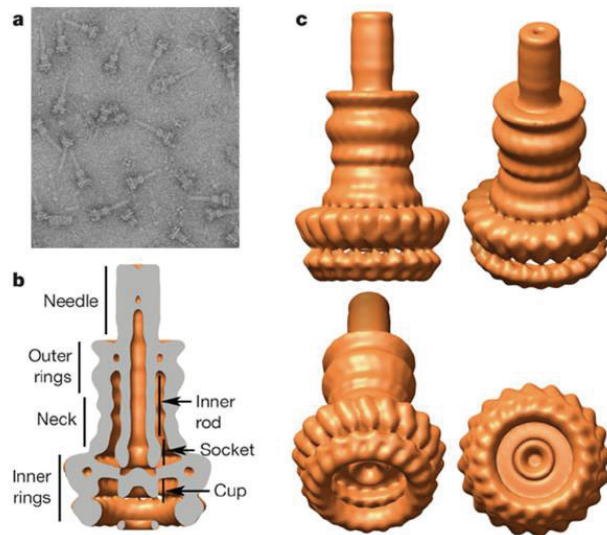


**Fig.5.1 Structure of needle complex in T3SS [3]**

### **How is the ESX-1 secretion system triggered and inactivated intracellularly?**

Many efforts have been made to understand the regulation of the ESX-1 secretion system. Indeed for a facultative intracellular pathogen like *M. tb*, growth and virulence are adapted to the environmental cues. Apart from the well-understood PhoPR two-component system which effectively regulates expression of EspR and WhiB6 thereby affecting ESX-1 secretion system [6-8], the findings described in Chapter 4 provide an insight about the mechanism of ESX-1 activation from a different angle, suggesting that calcium may affect ESX-1 secretion at a post-transcriptional level, which is still unknown.

Since EsxA and EsxB are detectable in the host-free culture medium where the bacteria are grown, it is thought that unlike T3SS, activation of the ESX-1 secretion system does not require physical contact with the host cell. However, the growth condition *in vitro* is artificial. For technical reasons, culture filtrates in most assays are prepared from bacteria grown in Sauton's medium. It was reported that while the secretion of EsxA/EsxB in *M. smegmatis* was normal in Sauton's medium, it was unexpectedly inhibited when the strain was grown in 7H9 medium. These observations suggest that the ESX-1 secretion system responds to a certain component of the culture medium [9]. In line with this, the calcium effect on ESX-1 shown in our experiments also highlights the importance of the growth conditions. Similarly, for the pathogens equipped with a T3SS, chelation of calcium from the culture medium was found to induce secretion of the effector proteins. Thus, reduction in calcium concentration probably mimics a physiological response to an unknown stimulus generated upon contact with the host cells [10]. Collectively, it is still an open question if ESX-1 secretion within host cell is constitutively active as is the case when *M. tb* is cultured in Sauton's medium. The requirement for intracellular activation and the fate of the ESX-1 apparatus after assembly warrant further investigation.

### **Potential application of EspC in TB vaccine and drug development**

Today, BCG is the only vaccine available for TB protection. Due to its inadequacy to protect adults from *M. tb* infection, vaccine development is an area of active research. The current BCG vaccine is derived from *M. bovis* lacking the RD1 locus. Thus, EsxA and EsxB, the two RD1 encoded antigens that elicit strong and specific T-cell responses, are absent in BCG, making them potential vaccine candidates. As a protein similar to EsxA/B in secondary structure, EspC (peptides) was reported as highly immunodominant as EsxA and EsxB in the patients with active TB and LTBI [11]. Preliminary data from IFN- $\gamma$  release assay using our purified full-length EspC validates the hypothesis that EspC strongly induces T-cell responses in LTBI infection (Supplementary section in Chapter 2). In the case of the BCG vaccine, secretion of EspC is blocked since ESX-1 is not functional, and therefore EspC is not surface-exposed. As such, EspC could be

exploited for vaccine development to enhance the protection from BCG. Compared to EsxA, EspC does not have the cytolytic activity that would potentially harm the host. Thus, it could be a preferred vaccine candidate.

Targeting bacterial secretion systems to attenuate virulence, rather than killing the bacteria itself, has been used as a strategy for drug discovery [12]. This strategy is particularly valuable for anti-TB drug development, given the emergence of MDR-TB and XDR-TB. A previous high-throughput screen (HTS) for compounds which inhibit ESX-1 secretion, resulted in the discovery of two novel molecules with antivirulence properties [13]. They effectively reduce the bacterial load in macrophages and prevent fibroblast cytolysis by *M. tb*. As an alternative to the whole-cell based HTS, targeting a particular ESX-1-associated protein, such as the ATPase EccC1, the protease MycP1 and the transcriptional regulator EspR, is a useful approach to identify ESX-1-specific inhibitors. The surface-exposed EspC polymer could also be a potential target of antivirulence drugs. In *Shigella*, a group of salicylidene acylhydrazides that inhibit effector protein secretion via T3SS were found to act on the needle assembly. When treated with these molecules, the bacteria failed to form the functional needle structure, and were subsequently cleared by the macrophage [14]. Likewise, potential inhibitory molecules affecting EspC assembly can be available from screening. The apparent advantage of targeting EspC is the non-necessity for the drug to be transported across the thick mycobacterial cell envelope which represents a barrier for drug delivery. Therefore, targeting EspC could provide a new therapeutic opportunity against TB.

## References

1. Bottai D, Majlessi L, Simeone R, Frigui W, Laurent C, et al. (2011) ESAT-6 secretion-independent impact of ESX-1 genes *espF* and *espG1* on virulence of *Mycobacterium tuberculosis*. *J Infect Dis* 203: 1155-1164.
2. Sani M, Houben ENG, Geurtsen J, Pierson J, de Punder K, et al. (2010) Direct Visualization by Cryo-EM of the Mycobacterial Capsular Layer: A Labile Structure Containing ESX-1-Secreted Proteins. *Plos Pathogens* 6.
3. Galan JE, Wolf-Watz H (2006) Protein delivery into eukaryotic cells by type III secretion machines. *Nature* 444: 567-573.
4. Nans A, Kudryashev M, Saibil HR, Hayward RD (2015) Structure of a bacterial type III secretion system in contact with a host membrane in situ. *Nat Commun* 6: 10114.
5. Basler M, Pilhofer M, Henderson GP, Jensen GJ, Mekalanos JJ (2012) Type VI secretion requires a dynamic contractile phage tail-like structure. *Nature* 483: 182-U178.
6. Solans L, Aguilo N, Samper S, Pawlik A, Frigui W, et al. (2014) A specific polymorphism in *Mycobacterium tuberculosis* H37Rv causes differential ESAT-6 expression and identifies *WhiB6* as a novel ESX-1 component. *Infect Immun* 82: 3446-3456.
7. Gonzalo-Asensio J, Mostowy S, Harders-Westervleen J, Huygen K, Hernandez-Pando R, et al. (2008) *PhoP*: a missing piece in the intricate puzzle of *Mycobacterium tuberculosis* virulence. *PLoS One* 3: e3496.
8. Blasco B, Chen JM, Hartkoorn R, Sala C, Uplekar S, et al. (2012) Virulence Regulator *EspR* of *Mycobacterium tuberculosis* Is a Nucleoid-Associated Protein. *Plos Pathogens* 8.
9. Converse SE, Cox JS (2005) A protein secretion pathway critical for *Mycobacterium tuberculosis* virulence is conserved and functional in *Mycobacterium smegmatis*. *Journal of Bacteriology* 187: 1238-1245.
10. Gode-Potratz CJ, Chodur DM, McCarter LL (2010) Calcium and iron regulate swarming and type III secretion in *Vibrio parahaemolyticus*. *J Bacteriol* 192: 6025-6038.
11. Millington KA, Fortune SM, Low J, Garces A, Hingley-Wilson SM, et al. (2011) *Rv3615c* is a highly immunodominant RD1 (Region of Difference 1)-dependent secreted antigen specific for *Mycobacterium tuberculosis* infection. *Proceedings of the National Academy of Sciences of the United States of America* 108: 5730-5735.
12. Feltcher ME, Sullivan JT, Braunstein M (2010) Protein export systems of *Mycobacterium tuberculosis*: novel targets for drug development? *Future Microbiol* 5: 1581-1597.

13. Rybníček J, Chen JM, Sala C, Hartkoorn RC, Vocat A, et al. (2014) Anticytolytic screen identifies inhibitors of mycobacterial virulence protein secretion. *Cell Host Microbe* 16: 538-548.
14. Veenendaal AKJ, Sundin C, Blocker AJ (2009) Small-Molecule Type III Secretion System Inhibitors Block Assembly of the Shigella Type III Secretion. *Journal of Bacteriology* 191: 563-570.





## Appendix

### Additional work

This section describes an additional piece of work in which I contributed to a collaboration between our research group and that of Prof. Andrea Ablasser. Results of this work show the role of ESX-1 in the activation of cGAS- and inflammasome-dependent intracellular immune responses.

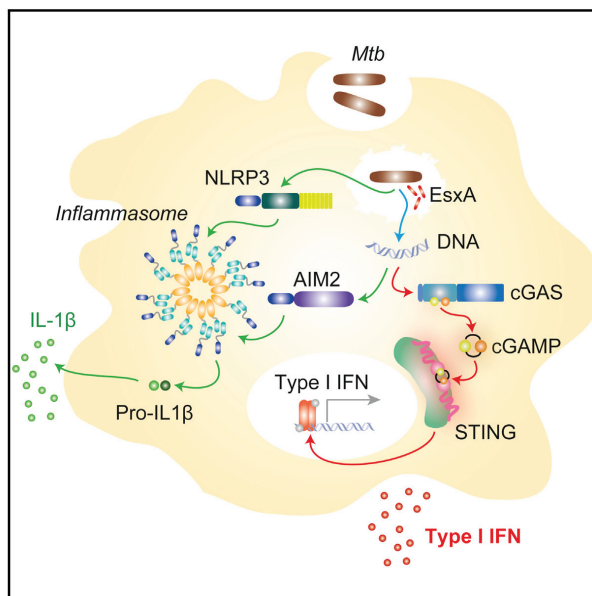
**Contributions:** making *M. tb* mutant strains, bacterial culture, macrophage infection, supernatant collection, RNA extraction.



# Cell Host & Microbe

## *Mycobacterium tuberculosis* Differentially Activates cGAS- and Inflammasome-Dependent Intracellular Immune Responses through ESX-1

### Graphical Abstract



### Authors

Ruth Wassermann,  
Muhammet F. Gulen, Claudia Sala, ...,  
Veit Hornung, Stewart T. Cole,  
Andrea Ablasser

### Correspondence

stewart.cole@epfl.ch (S.T.C.),  
andrea.ablasser@epfl.ch (A.A.)

### In Brief

The receptor(s) responsible for type I IFNs activation in response to *Mycobacterium tuberculosis* (*Mtb*) infection has remained elusive. Wassermann et al. find that intracellular *Mtb* DNA sensing by the cytosolic sensor cGAS drives type I IFN induction upon infection, and mutations in the *Mtb* ESX-1 secretion system abrogate this mechanism.

### Highlights

- The DNA sensor cGAS is essential for type I IFN induction in response to *Mtb* infection
- cGAS aggregates and colocalizes with DNA in the cytosol of *Mtb*-infected cells
- *Mtb* ESX-1 secretion system mutants abrogate cGAS-mediated type I IFN responses
- Modulation of the ESX-1 system uncouples IFN production from IL-1β responses to *Mtb*



Wassermann et al., 2015, Cell Host & Microbe 17, 799–810  
June 10, 2015 ©2015 Elsevier Inc.  
<http://dx.doi.org/10.1016/j.chom.2015.05.003>

CellPress

# *Mycobacterium tuberculosis* Differentially Activates cGAS- and Inflammasome-Dependent Intracellular Immune Responses through ESX-1

Ruth Wassermann,<sup>1,4</sup> Muhammet F. Gulen,<sup>1,4</sup> Claudia Sala,<sup>1,4</sup> Sonia Garcia Perin,<sup>1</sup> Ye Lou,<sup>1</sup> Jan Rybníček,<sup>1,3</sup> Jonathan L. Schmid-Burgk,<sup>2</sup> Tobias Schmidt,<sup>2</sup> Veit Hornung,<sup>2</sup> Stewart T. Cole,<sup>1,\*</sup> and Andrea Ablasser<sup>1,\*</sup>

<sup>1</sup>Global Health Institute, Ecole Polytechnique Fédérale de Lausanne (EPFL), 1015 Lausanne, Switzerland

<sup>2</sup>Institute for Molecular Medicine, University Hospital, University of Bonn, 53127 Bonn, Germany

<sup>3</sup>First Department of Internal Medicine, University of Cologne, 50937 Cologne, Germany

<sup>4</sup>Co-first author

\*Correspondence: [stewart.cole@epfl.ch](mailto:stewart.cole@epfl.ch) (S.T.C.), [andrea.ablasser@epfl.ch](mailto:andrea.ablasser@epfl.ch) (A.A.)

<http://dx.doi.org/10.1016/j.chom.2015.05.003>

## SUMMARY

Cytosolic detection of microbial products is essential for the initiation of an innate immune response against intracellular pathogens such as *Mycobacterium tuberculosis* (*Mtb*). During *Mtb* infection of macrophages, activation of cytosolic surveillance pathways is dependent on the mycobacterial ESX-1 secretion system and leads to type I interferon (IFN) and interleukin-1 $\beta$  (IL-1 $\beta$ ) production. Whereas the inflammasome regulates IL-1 $\beta$  secretion, the receptor(s) responsible for the activation of type I IFNs has remained elusive. We demonstrate that the cytosolic DNA sensor cyclic GMP-AMP synthase (cGAS) is essential for initiating an IFN response to *Mtb* infection. cGAS associates with *Mtb* DNA in the cytosol to stimulate cyclic GAMP (cGAMP) synthesis. Notably, activation of cGAS-dependent cytosolic host responses can be uncoupled from inflammasome activation by modulating the secretion of ESX-1 substrates. Our findings identify cGAS as an innate sensor of *Mtb* and provide insight into how ESX-1 controls the activation of specific intracellular recognition pathways.

## INTRODUCTION

Tuberculosis (TB) is a major cause of morbidity and mortality worldwide (Lechartier et al., 2014). Upon infection with *Mycobacterium tuberculosis* (*Mtb*), several factors contribute to the outcome of the disease, with the innate immune response representing one of the most critical determinants. To date several cytokines have been shown to participate in the innate host response against *Mtb*, where they can either function to confer host resistance or act as regulatory molecules that may exacerbate the infection (O'Garra et al., 2013). Studies have established the critical role of inflammatory cytokines, such as interleukin-1 $\beta$  (IL-1 $\beta$ ), in the containment of *Mtb* by

enhancing the antimicrobial function of macrophages (Fremond et al., 2007). On the contrary, animal models and studies in humans have revealed that type I interferons (IFNs) have probacterial activity and are associated with disease progression in TB (Berry et al., 2010; Manca et al., 2005; Stanley et al., 2007). The immunomodulatory effect of type I IFNs appears to be related to their anti-inflammatory properties, principally by antagonizing the production and activity of IL-1 $\beta$  (Mayer-Barber et al., 2011).

A key feature of pathogenic mycobacteria is the type VII secretion system ESX-1 that manipulates innate immune responses, presumably by translocating bacterial effector molecules into the host cytosol (Stoop et al., 2012). In macrophages intracellular detection of *Mtb*-associated molecular patterns is regulated via two major sensing systems that are linked to distinct signaling pathways. One pathway involves the multimeric inflammasome complex, which employs a sensor molecule, NLRP3 or AIM2, the adaptor ASC, and caspase-1 to regulate the secretion of IL-1 $\beta$  (Mishra et al., 2010; Saiga et al., 2012). Whereas AIM2 recognizes DNA, the NLRP3 inflammasome is stimulated by a mechanism involving K<sup>+</sup> efflux (Dorhoi et al., 2012). The second pathway, which is responsible for the expression of type I IFNs, relies on the cyclic dinucleotide (CDN) sensor STING (Manzanillo et al., 2012). Within this pathway, activation of STING by CDNs recruits the kinase TBK-1, which phosphorylates the transcription factor IRF-3 to promote transcription of IFN- $\beta$  and interferon-stimulated genes (ISGs). Notably, during intracellular bacterial infection activation of STING can be accomplished via two differential mechanisms. First, STING can directly recognize bacterial CDNs and thus function as a primary pattern recognition receptor (PRR) (Burdette et al., 2011). Alternatively, DNA sensing via cGAS triggers the synthesis of the second messenger cGAMP, which then engages STING as a secondary receptor (Sun et al., 2013). But despite these advances in understanding the downstream part of these signaling cascades, the molecular events that lead to ESX-1-dependent activation of intracellular host receptors and the nature of the stimulatory elements remain poorly defined.

Here we report that the DNA sensor cGAS is essential for mounting type I IFN responses upon *Mtb* infection. We show that ESX-1-proficient mycobacteria trigger cGAS to form intracellular complexes that colocalize with DNA and promote



intercellular signal transduction via the production of cGAMP. Remarkably, by comparing the cytokine profile induced by distinct ESX-1 mutants, we observed that intracellular inflammasome-dependent and cGAS-mediated responses can be disconnected. Together, these data reveal the importance of cGAS in controlling interferon production upon mycobacterial infection and uncover a unique function of ESX-1 in eliciting specific innate immune responses.

## RESULTS

### cGAS Is Critical for IFN Responses upon *Mtb* Infection

In order to investigate the individual role of cytosolic PRRs during infection with *Mtb* in human cells, we employed human THP-1 cells, in which STING was knocked out via the CRISPR/Cas9 technology (see Figure S1A online). Similar to what had previously been shown in murine macrophages, we found that *Mtb*-triggered production of IP-10, a surrogate cytokine for type I IFN expression, was completely compromised in human THP-1 cells lacking STING (Figure S1B). The same was observed when gene expression of IFN- $\beta$  was directly analyzed by qPCR (Figure S1C). We furthermore noted that transfection of *Mtb* genomic DNA regulated the induction of IP-10 via STING (Figure S1D). Recently, Rv3586 was identified as a mycobacterial diadenylate cyclase, DacA, which synthesizes cyclic di-AMP (Bai et al., 2012). Overexpression of DacA in conjunction with STING in HEK293T cells induced robust transactivation of an IFN- $\beta$  reporter gene (Figure S1E). This effect was abolished when endogenous cyclic di-AMP levels were reduced by the activity of the cyclic di-AMP-specific phosphodiesterase YybT (Figure S1F) (Rao et al., 2010). In line with this, DacA was unable to activate IFN- $\beta$  upregulation when coexpressed with a STING variant that cannot sense cyclic di-AMP (data not shown). Finally, purified cyclic di-AMP also triggered IP-10 production in THP-1 cells in a STING-dependent fashion (Figure S1G). Together, these data confirm STING-mediated DNA/CDN sensing in human macrophages, but they also illustrate that during *Mtb* infection both mycobacterial cyclic di-AMP and genomic DNA may serve as the molecular pattern that initiates type I IFN induction.

To definitively clarify the role of DNA- versus CDN-mediated IFN regulation in *Mtb*-infected cells, we employed THP-1 cells knocked out for cGAS (Figure 1A). Using these cell lines we examined the role of cGAS in the innate recognition of *Mtb*. As expected, cGAS knockout cells did not activate a type I IFN response upon transfection with dsDNA (Figure 1B). As controls, cGAS knockout cell lines were not compromised in their response toward the RIG-I ligand triphosphate RNA or the STING agonists cGAMP or cyclic di-AMP (Figures 1B, S1H, and S1J and data not shown). Importantly, when infected with *Mtb*, cGAS knockout cells failed to mount a detectable level of IP-10 and IFN- $\beta$  production (Figures 1C and S1K). Moreover, gene expression of IFN- $\beta$  or the ISG IFIT2 was also completely absent in cGAS mutant cells after *Mtb* challenge (Figure 1D). To explore the relevance of cGAS for the immune response in murine cells, we infected bone marrow-derived macrophages (BMDMs) from cGAS<sup>-/-</sup> mice and compared their type I IFN response with that of wild-type macrophages. Whereas comparable levels of IP-10 and IFN- $\beta$  were induced

after stimulation with triphosphate RNA or cGAMP, BMDMs derived from cGAS<sup>-/-</sup> animals were almost completely unresponsive in terms of IP-10 and type I IFN production upon *Mtb* infection (Figures 1E and S1I). To provide definitive proof of the involvement of cGAS in the innate response to *Mtb*, we reconstituted cGAS knockout cells with a human Flag-tagged cGAS construct via lentivirus-mediated transduction, whereas a Flag-tagged GFP construct served as a control. In cells transduced with the cGAS construct, cGAS protein expression was restored to a level comparable to that of wild-type cells (Figure 1F). Consistently, when transfected with dsDNA, reconstituted THP-1 cells produced comparable levels of IP-10 and displayed similar induction of IFN- $\beta$  or IFIT2 as wild-type cells (Figure 1G and data not shown). Importantly, expression of cGAS-Flag but not GFP-Flag restored the ability of cGAS-deficient cells to respond to *Mtb* infection (Figure 1G). To assess the biological role of the cGAS-STING-IFN- $\beta$  pathway on *Mtb* virulence, we compared the cytotoxicity caused by two different *Mtb* strains, H37Rv and HN878, on wild-type, cGAS-deficient, and STING-deficient cell lines. HN878 is a clinical isolate belonging to the East Asia (W-Beijing) family, while H37Rv is a member of the Euro-American lineage (Reed et al., 2007). Notably, HN878 has been described as capable of inducing higher levels of type I IFN in the murine model of infection (Manca et al., 2005). Testing these strains confirmed the increased production of IP-10 by wild-type cells after HN878 challenge, while deletion of cGAS or STING abolished this response (Figure S2A). We observed that cell survival was partially rescued by cGAS and STING knockout cells upon HN878 infection (Figure S2B). Together, these results demonstrate that cGAS is crucial for the innate type I IFN response in both human and murine macrophages infected with *Mtb*. In addition, these findings suggest that dsDNA but not CDNs functions as the mycobacteria-associated pattern required for IFN regulation.

### cGAS Associates with DNA in the Cytosol

To further characterize the molecular mechanism of *Mtb*-driven cGAS activation, we examined the localization of cGAS in THP-1 cells by immunofluorescence microscopy. In untreated cells cGAS was distributed diffusely throughout the cytoplasm (Figure 2A). After transfection with dsDNA we observed cGAS forming punctate structures that colocalized with DNA (Figure 2A). Interestingly, the formation of these structures was specifically induced upon stimulation with DNA, but not after transfection with the endogenous cGAS enzymatic product cGAMP or triphosphate RNA (Figure S3). Strikingly, upon infection with *Mtb* we observed significant formation of cGAS aggregates, which colocalized with DNA (Figure 2A). In contrast, cells infected with an attenuated *Mtb* strain, H37Rv $\Delta$ RD1, which lacks IFN-stimulatory capacity due to loss of ESX-1 (see below), failed to stimulate cGAS punctate structure formation (Figure 2A). In addition, we found that pretreatment of cells with chloroquine, an inhibitor of autophagy, interfered with both DNA- and *Mtb*-triggered cGAS redistribution, suggesting the involvement of the autophagy machinery for the execution of the cGAS relocation process (Figure 2B). In accordance with this notion and as previously described, the observed cGAS punctate structures colocalized with the autophagy-related protein Beclin-1, but not with the inflammasome complex (Figure 2C) (Liang et al.,

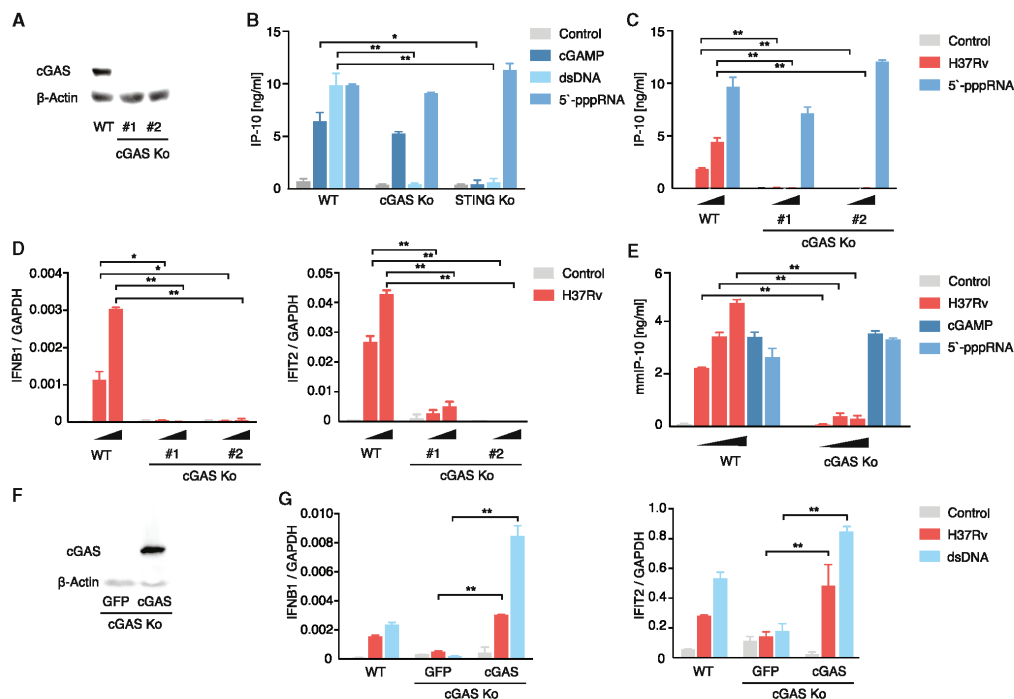


**Figure 1. cGAS Is Essential for Type I IFN Responses Triggered by *Mtb***

(A) Expression of cGAS was studied in wild-type (WT) THP-1 cells and two distinct cGAS knockout cell lines by immunoblot. (B) WT THP-1 cells, cGAS, and STING knockout cells were transfected with cGAMP, dsDNA, or 5'-triphosphate RNA (5'-pppRNA). IP-10 production was measured by ELISA 24 hr after stimulation. (C and D) WT THP-1 cells and cGAS knockout cells were infected with H37Rv (multiplicity of infection [moi] 5, 10) or stimulated with 5'-pppRNA as indicated. After 24 hr IP-10 levels were assessed by ELISA (C) or IFN-β and IFIT2 mRNA levels were quantified by qPCR (D). (E) ELISA measurement of IP-10 from the supernatants of BMDMs from WT mice and cGAS knockout mice after overnight culture left untreated, infected with H37Rv (moi 2.5, 5, and 10) or stimulated with cGAMP or 5'-pppRNA. (F) Immunoblot of reconstituted cGAS-deficient cell lines (cGAS). Transduction of GFP served as a control (GFP). (G) WT THP-1 cells and cells from (F) were left untreated, infected with H37Rv (moi 10) or transfected with dsDNA. After 24 hr mRNA levels of IFN-β and IFIT2 were measured by qPCR. Mean + SD of duplicate measurements from one representative experiments out of four (B), three (C), or two (D, E, and G) independent experiments are depicted, or representative results from two independent experiments are shown (A and F).  $p < 0.05$  (\*);  $p < 0.01$  (\*\*). See also Figures S1 and S2.

2014). Together, this shows that infection of macrophages with *Mtb* leads to cytosolic association of cGAS and DNA.

#### Dissemination of the *Mtb*-Triggered Host Response through cGAMP-Based Intercellular Communication

Next we assessed whether *Mtb* infection leads to the synthesis of cGAMP within human macrophages. Toward this goal we took advantage of the fact that cGAMP can activate bystander cells via its horizontal transfer through gap junctions (Ablasser et al., 2013b). We hypothesized that, even though individual cGAS or STING knockout cells are unable to upregulate type I IFNs in a cell-intrinsic fashion, the combination of both would restore this response upon DNA transfection or *Mtb* infection if cGAMP were produced (Figure 3A, left, and Figure 3C, left).

Indeed, when activated by transfection with dsDNA, monocultures of both cGAS- or STING-deficient cells failed to elicit type I IFN induction, yet the combination of both cell types resulted in marked upregulation of IFN-β or IFIT2 gene expression (Figure 3A, right, and data not shown). Consistent with a gap junction-dependent mode of transfer, this effect was abolished upon pretreating the mixed cocultures with the connexin inhibitor carbenoxolone (Figure 3B). We then tested whether cGAMP-dependent in *trans* signaling would also occur in the context of *Mtb* infection (Figure 3C, left). Similar to the results obtained above, coculturing of cGAS- or STING-deficient cells led to strong upregulation of IFN-β mRNA levels and of IFN-β secretion (Figure 3C, right, and Figure 3E). Again, this phenomenon was sensitive to carbenoxolone treatment

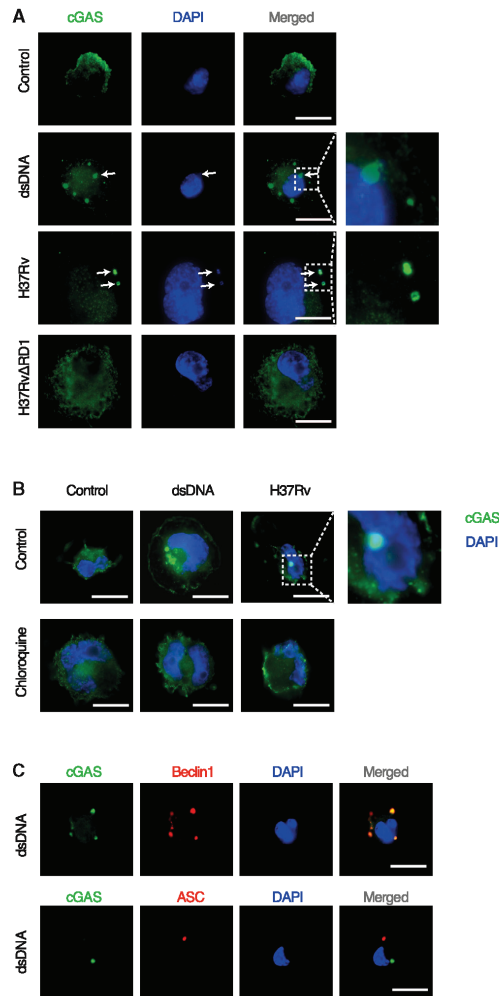


**Figure 2. Upon *Mtb* Infection cGAS Forms Aggregates and Colocalizes with DNA**

(A and B) THP-1 cells stably expressing cGAS-Flag were seeded on coverslips and treated as depicted. Sixteen hours after dsDNA transfection or 48 hr after *Mtb* infection in the absence (A) or presence of 50  $\mu$ M chloroquine (B), cells were stained for Flag-tagged cGAS (green) and nuclei/DNA (DAPI, blue). (C) Cells were stained for Flag-tagged cGAS (green), ASC or Beclin-1 (red), and nuclei/DNA (DAPI, blue). Scale bar, 5  $\mu$ m; right, magnification of area outlined. Arrows highlight spots of DNA and cGAS colocalization. Representative images out of three independent experiments are shown. See also Figure S3 and Table S1.

(Figure 3D). These results reveal that during *Mtb* infection macrophages produce cGAMP. Furthermore, this suggests that the detection of *Mtb* can be relayed from infected macro-

phages to noninfected neighboring cells via gap-junction-mediated communication.

### Comparison of ESX-1- and cGAS-Regulated Cytokine Responses

We next sought to better characterize the molecular events that lead to DNA-dependent activation of cGAS. To this end we analyzed a selection of cytokines, which are known as central mediators of the in vivo response toward *Mtb* infection, including TNF- $\alpha$ , IL-1 $\beta$ , and IL-10. Besides using the wild-type *Mtb* strain H37Rv, macrophages were also infected with the attenuated vaccine strain *Mycobacterium bovis* BCG, which lacks the ESX-1 protein secretion system, known to be required for type I IFN responses (Stanley et al., 2007). As expected, macrophages only produced type I IFN and the related cytokines IP-10 and IL-10 after infection with H37Rv, but not with BCG (Figures 4A and 4C). In addition, upon analyzing the levels of IP-10 and IL-10 from wild-type, cGAS-deficient, and STING-deficient cells, we observed that expression of IP-10 and IL-10 was equally affected in the knockout cell lines (Figure 4B), thereby confirming that ESX-1- and DNA/cGAS-dependent cytokines are coregulated. On the other hand, production of the proinflammatory cytokines TNF- $\alpha$  and IL-6 was similarly triggered by both strains (Figure 4A and data not shown) and not altered in the mutant cell lines as compared to the wild-type cells (Figure 4B). However, these congruent patterns differed when IL-1 $\beta$  production was assessed. Whereas BCG failed to promote IL-1 $\beta$  secretion, absence of cGAS or STING did not compromise IL-1 $\beta$  secretion following H37Rv infection (Figures 4A and 4B). These findings can be explained by the inflammasome-mediated regulation of IL-1 $\beta$ , which reportedly also involves an ESX-1-dependent mechanism of activation (Kurenuma et al., 2009). In this regard it is interesting to note that the stimulation of the inflammasome by *Mtb* also appears to involve a sensing mechanism relying on the detection of intracellular DNA via AIM2 (Saiga et al., 2012). However, studies also reported NLRP3 as the main mediator of inflammasome activation through a mechanism triggered via K<sup>+</sup> efflux (Dorhoi et al., 2012; Kurenuma et al., 2009; Mishra et al., 2010). To elucidate the individual roles of these factors, we targeted AIM2 and the shared inflammasome adaptor molecule ASC in THP-1 cells. We found that the absence of AIM2 reduced IL-1 $\beta$  levels to 50% in response to *Mtb* infection, while the absence of ASC completely abrogated the IL-1 $\beta$  signal (Figure S4A). Type I IFN responses in both AIM2- and ASC-mutated cells were comparable to those of wild-type cells (Figure S4A). Importantly, inhibition of NLRP3 via blocking K<sup>+</sup> efflux by glibenclamide entirely blocked the residual secretion of IL-1 $\beta$  in AIM2 knockout cells, indicating that *Mtb*-triggered activation of the inflammasome complex in human macrophages is mediated by the collective actions of AIM2 and NLRP3 (Figure S4B). So far, our data suggest that during infection with virulent tubercle bacilli two intracellular DNA sensing systems—cGAS and AIM2—become activated, each inducing a complementary cytokine response—type I IFNs and IL-1 $\beta$ , respectively. In addition, more than one ESX-1-controlled mechanism operates in *Mtb*-infected cells to trigger IL-1 $\beta$  release via an inflammasome-dependent mechanism.



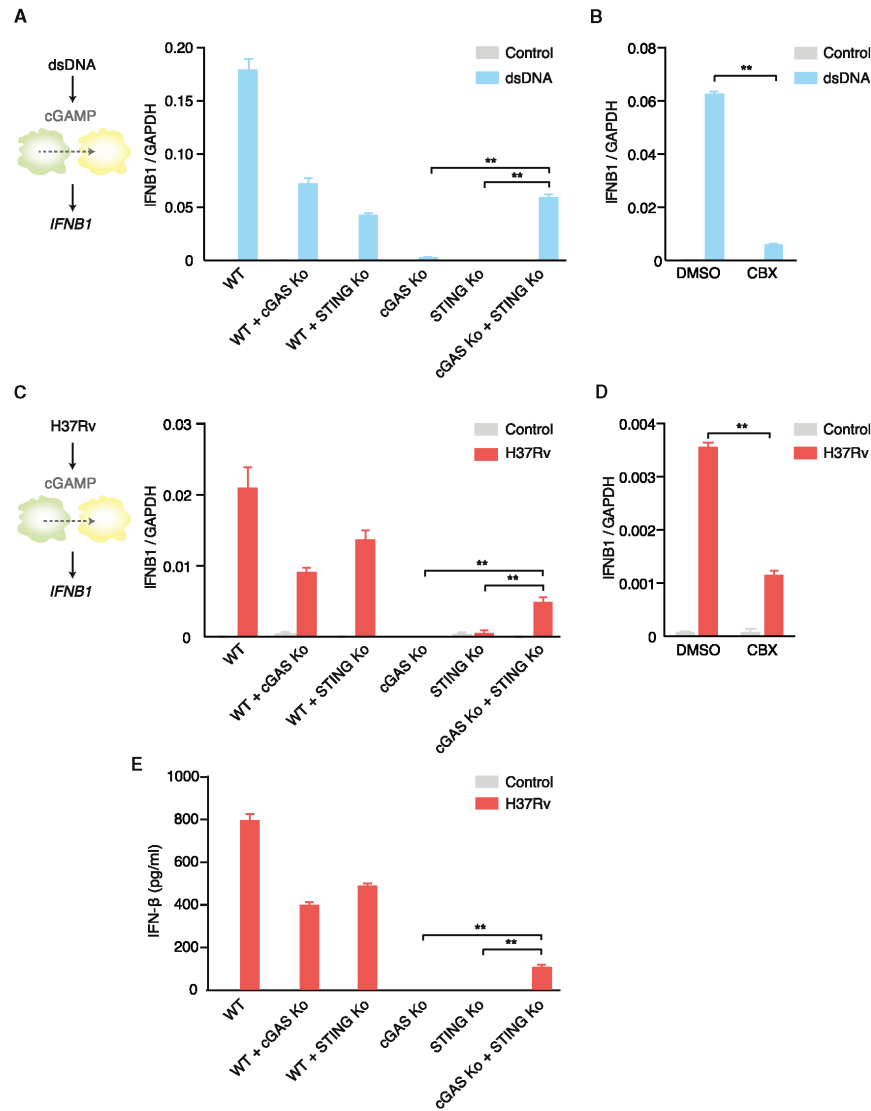


**Figure 3. cGAMP Shuttling through Gap Junctions Restores Type I IFN Responses upon *Mtb* Infection in Mixed Cocultures**

(A and C) (Left) Scheme depicting model of horizontal transfer of cGAMP upon DNA transfection (A) or H37Rv infection (C); (right) mono- and cocultures (as indicated) of WT THP-1 cells, cGAS-deficient cells, or STING-deficient cells, which were left untreated or stimulated via DNA transfection (A) or H37Rv infection (moi 10) (C). After 24 hr, mRNA levels of IFN-β were measured by qPCR.

(B and D) Cocultures of cGAS- and STING-deficient THP-1 cells were left untreated or transfected with DNA (B), or infected with H37Rv (moi 10) (D) in the presence or absence of carbenoxolone (CBX; 100 μM) as indicated. mRNA levels of IFN-β were assessed by qPCR after 24 hr.

(E) Type I IFN was measured 24 hr postinfection of mono- and cocultures of WT THP-1 cells, cGAS-deficient cells, and STING-deficient cells. Mean + SD of duplicate measurements of representative results from two independent experiments is depicted. \*\*p < 0.01.



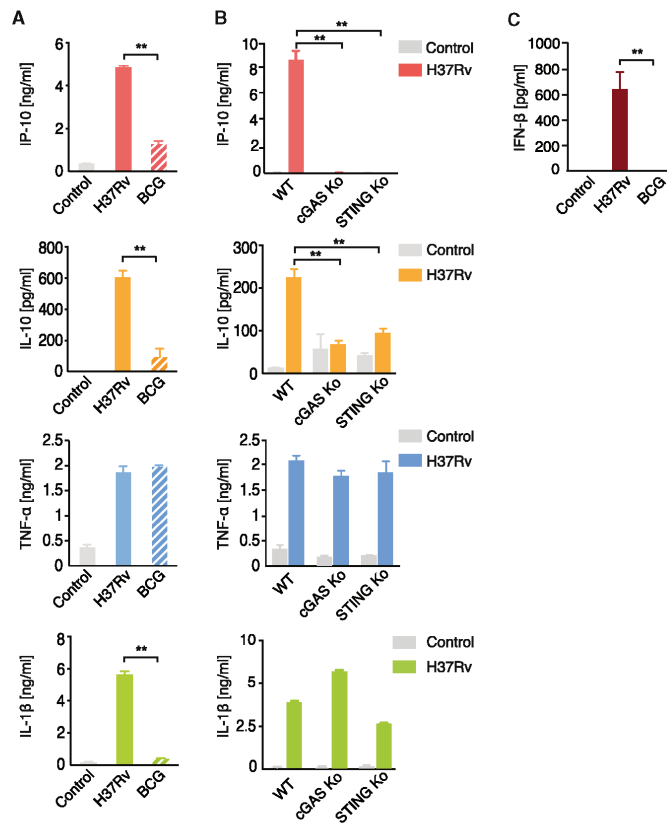


**Figure 4. Virulent and Attenuated Mycobacteria Differentially Activate Innate Cytokine Responses**

(A and C) THP-1 cells were infected with H37Rv and BCG (moi 10).

(B) WT THP-1 cells, cGAS-deficient cells, or STING-deficient THP-1 cells were infected with H37Rv (moi 10). After 24 hr supernatants were assessed by ELISA for production of IP-10, IL-10, TNF-α, IL-1β, or IFN-β.

Mean + SD of duplicate measurements of representative results from three independent experiments is depicted. \*\*p < 0.01. See also Figure S4 and Table S1.

Furthermore, we found that the residual IL-1β response upon H37Ra infection was profoundly reduced upon pretreatment with glibenclamide (Figure 5B). This suggests that H37Ra can still stimulate the cytosolic sensor NLRP3, despite its inability to trigger cytosolic DNA-sensing pathways based on AIM2 and cGAS. To confirm the physiological relevance of this finding, we infected primary human macrophages with H37Ra, which consistently resulted in the secretion of IL-1β, while at the same time IP-10 production was markedly reduced (Figure 5C). These results indicate that ESX-1-dependent activation of two central yet opposite host responses can be uncoupled.

#### Dissecting the Activation of Intracellular Host Sensors by Manipulating ESX-1

The above results indicate that secretion of EsxA or another ESX-1 substrate is an essential feature for activating intracellular DNA-sensing pathways in macrophages. In contrast to the strains BCG or H37RvΔRD1, in which the genes encoding EsxA are deleted, the undetectable secretion of EsxA in H37Ra is achieved by an indirect mechanism involving lack of PhoP-mediated expression of the *espACD* operon, a region distal to the RD1 locus but required for full ESX-1 function (Figure 6A, right) (Stoop et al., 2012). To directly assess the contribution of the EspA/C substrates, we used the respective *espA* and *espC* mutants, with and without complementation, to analyze the host cytokine response (Chen et al., 2012). Compared to the wild-type strain or the respective complemented strains, both mutants failed to trigger IP-10 production upon infection of macrophages (Figure 6A left). In contrast, we observed significant levels of IL-1β production (Figure 6B). Consistent with the involvement of NLRP3 for this cellular response, the IL-1β signal triggered by both EspA/C-deficient strains was inhibited by glibenclamide (Figure 6C). Thus, we conclude that EsxA secretion is essential for provoking intracellular DNA sensing pathways and that reducing the EsxA levels in the secreted fraction by genetic means does not abolish the cytosolic activation of the NLRP3 inflammasome. These findings

#### Mutations within ESX-1 Abrogate cGAS-Dependent IFN Responses

To further explore the role of ESX-1 for the stimulation of intracellular signaling pathways, we tested distinct mycobacterial strains for their capability to induce type I IFNs or IL-1β responses, which we speculated to be coregulated and used as an indirect means to monitor the functionality of the secretory system. First, we focused on the region of difference 1 (RD1) locus, given that its loss led to the attenuation of BCG (Pym et al., 2002). Next to strains harboring disruptions of the entire and extended RD1 locus, H37RvΔRD1 and H37RvΔΔRD1 (Bottai et al., 2011), respectively, we also tested the attenuated H37Ra strain of *Mtb*, which carries the S129L mutation in the transcriptional regulator *phoP* and is defective for secretion of EsxA, a major substrate of ESX-1 (Frigui et al., 2008). Analyzing cytokine levels of infected macrophages, we observed that none of the mutant strains were able to activate IP-10 production and, as expected from the experiments above, both H37RvΔRD1 and H37RvΔΔRD1 were impaired in inducing IL-1β secretion (Figure 5A). Surprisingly, infection with H37Ra still led to significant release of IL-1β, even though no IP-10 was produced (Figure 5A).

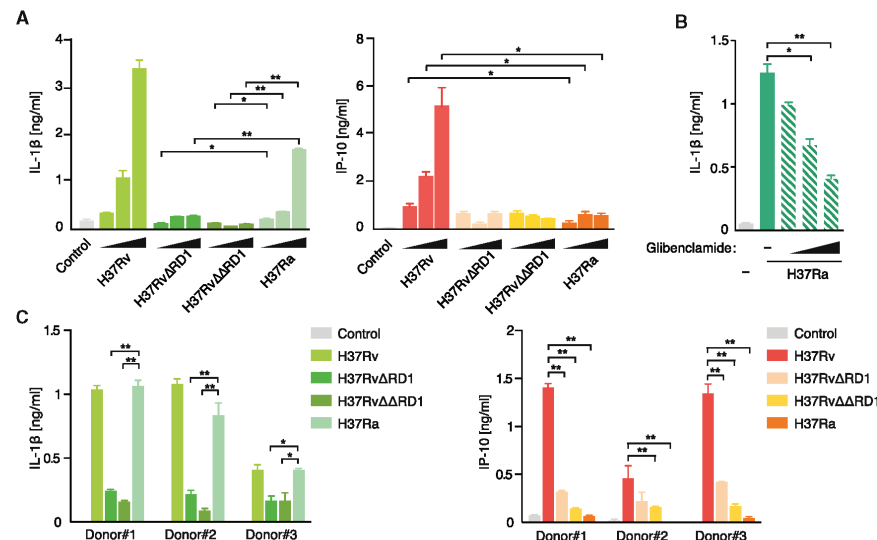


**Figure 5. Intracellular Recognition Pathways Are Differentially Activated by Virulent and Attenuated *M. tuberculosis***  
(A and C) THP-1 cells (A) or primary human macrophages (C) were infected with the following bacterial strains: H37Rv, H37RvΔRD1, H37RvΔΔRD1, or H37Ra (moi 2.5, 5, and 10). After 24 hr, IP-10 and IL-1β levels were assessed by ELISA.  
(B) ELISA measurement of IL-1β in the supernatant of THP-1 cells after 24 hr of infection with H37Ra (moi 10) in the presence of glibenclamide (0, 25, 50, and 100 μg/ml).  
Mean + SD of duplicate measurements of representative results from three independent experiments is depicted. \*p < 0.05; \*\*p < 0.01; p > 0.05 (n.s.). See also Table S1.

raised the possibility that a pharmacological intervention targeting ESX-1 function and hence EsxA release may be exploited to selectively inhibit cGAS-mediated type I IFN responses while leaving NLRP3-triggered IL-1β production intact. To prove this hypothesis, we tested two small compounds, the benzothio-phenyl inhibitor BTP15 and the benzyloxybenzylidene-hydrazine compound BBH7, which we have recently identified as potent inhibitors of EsxA secretion in *Mtb* (Figure S5A) (Rybníček et al., 2014). Treatment of *Mtb* with both BTP15 and BBH7 resulted in significantly lower amounts of IP-10 production from infected THP-1 cells (Figure 6D). In contrast, neither compound affected the release of IL-1β (Figure 6D). Of note, a similar pattern was observed in *Mtb*-infected primary human macrophages, where a decrease in IP-10 was measured, while IL-1β was unaltered (Figure 6E). In a control experiment, upon stimulation with DNA, IL-1β responses were not altered in the presence of BTP15 and BBH7, thereby confirming that both compounds inhibit *Mtb* and not host functions (Figure S5B). Thus, we conclude that pharmacological manipulation of the ESX-1 secretion system can sway the *Mtb*-triggered immune cytokine pattern in favor of host-protective IL-1β production by accentuating intracellular sensing via the inflammasome complex (Figure S6).

## DISCUSSION

Our study demonstrated that in *Mtb*-infected cells cGAS is the sole sensor driving the synthesis of type I IFNs and ISGs. We re-

vealed that infection of macrophages with virulent and attenuated *Mtb* can engage distinct cytosolic PRR systems, namely the cGAS-IFN-axis and the inflammasome-IL-1β-pathway, and that the decision as to which pathway is triggered is determined by the relative abundance of EsxA and/or by additional ESX-1/EsxA-dependent effectors. Our results disclose an as-yet-unnoticed interconnection between the mycobacterial virulence factors and the cytokine pattern of mammalian cells.

The host protein STING has been identified as a central signaling molecule in the innate immune response to various pathogens, including DNA viruses, retroviruses, and intracellular bacteria (Barber, 2014). During DNA virus or retrovirus infection STING seems to carry out this function by being part of the intracellular, cGAS-based DNA sensing pathway and by detecting host-derived cGAMP (Sun et al., 2013; Gao et al., 2013). However, when considered in the context of intracellular bacterial infection, such as with *Mtb*, the role of STING and cGAS/cGAMP is less consistent. Some authors have proposed that mycobacterial CDNs can be secreted into the cytosol and bind directly to STING (Bai et al., 2012; Woodward et al., 2010). Another report has proposed IFI204 as a putative DNA sensor for *Mtb* in murine BMDMs, where shRNA silencing of IFI204 resulted in reduced expression levels of IFIT1 and IFN-β upon *Mtb* infection (Manzanillo et al., 2012). Using both human and murine cGAS-deficient cells, we clearly demonstrated that cGAS is critical for the induction of IFN-β after infection with *Mtb*. We found that cGAS and intracellular DNA come together in the cytosol, supporting its

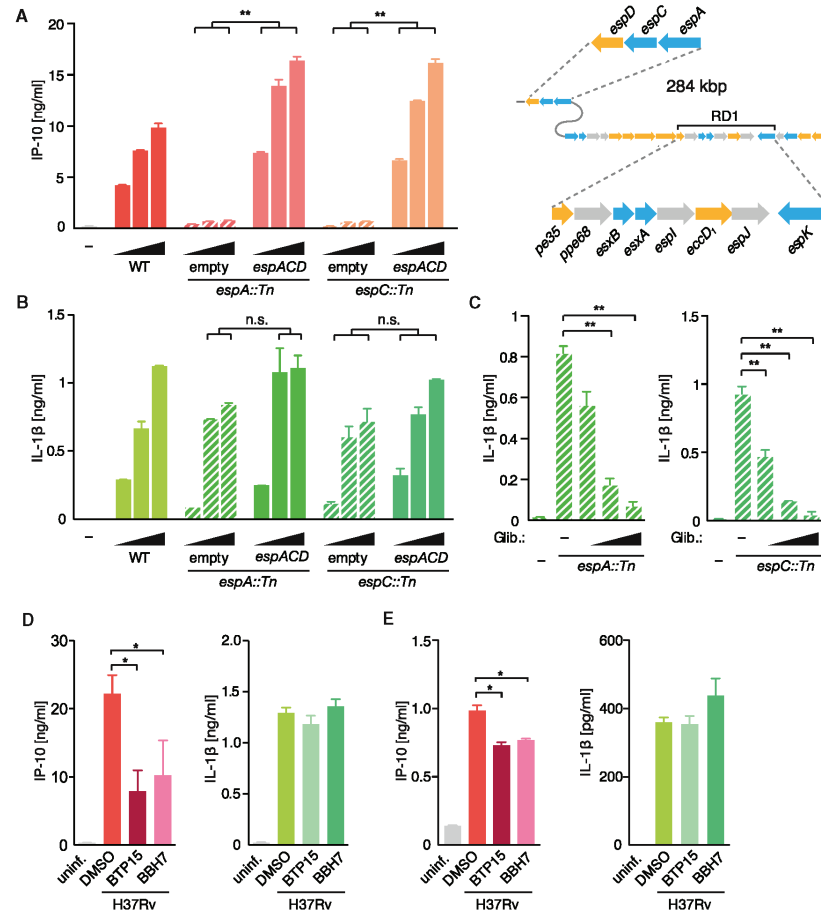


**Figure 6. Selective Disruption of the ESX-1 Secretion System Uncouples Intracellular Recognition Pathways of *Mtb***

(A and B) THP-1 cells were infected with the following bacterial strains: Erdman (WT), Erdman *espA::Tn*/pMD31 ("empty" in figure), Erdman *espA::Tn*/pMD*espACD*, Erdman *espC::Tn*/pMD31, and Erdman *espC::Tn*/pMD*espACD* (moi 2.5, 5, and 10). After 24 hr IP-10 (A) and IL-1β (B) levels of the supernatants were assessed by ELISA. (Upper right panel) Scheme of the *espACD* operon and the ESX-1 locus of the *Mtb* genome is depicted; RD1, region of difference 1. (C) ELISA measurement of IL-1β in the supernatant of THP-1 cells after 24 hr of infection with the strains Erdman *espA::Tn*/pMD31 and Erdman *espC::Tn*/pMD31 (moi 10) in the presence of glibenclamide (Glib., 0, 25, 50, and 100 μg/ml). (D) H37Rv was incubated with BTP15 (10 μM) or BBH7 (10 μM) for 24 hr. THP-1 cells were infected with the inhibitor-treated H37Rv (moi 10) as indicated or left untreated (uninf.). After 24 hr, IP-10 and IL-1β production was quantified by ELISA. (E) H37Rv was incubated with BTP15 (10 μM) or BBH7 (10 μM) for 24 hr. Primary human macrophages were infected with the inhibitor-treated H37Rv (moi 10) as indicated or left untreated (uninf.). After 24 hr, IP-10 and IL-1β production was quantified by ELISA. Representative results out of three (A–D) and two (E) independent experiments are depicted, whereas data are presented as mean + SD of duplicate measurements. \*p < 0.05; \*\*p < 0.01; p > 0.05 (n.s.). See also Figure S5 and Table S1.

role as a DNA receptor. As such, our study provides genetic proof that cGAS is necessary to confer responsiveness to an intracellular bacterial pathogen and indicates that at least in an

ex vivo setting mycobacterial-derived CDNs play a minor role, if any, in triggering IFN-β gene upregulation. Notably, in parallel to our own work, two independent studies by Chen, Shiloh,

and colleagues and Cox and colleagues, in this issue of *Cell Host & Microbe*, report the same finding, that cGAS is essential for the induction of type I IFN in *Mtb*-infected macrophages (Collins et al., 2015; Watson et al., 2015).

Interestingly, we observed that *Mtb* can trigger the expression of type I IFNs even in the absence of an intact, cell-intrinsic cGAS-cGAMP-STING signaling pathway. We explain this phenomenon by the existence of an intercellular second-messenger-based signaling network that exploits gap junctions to deliver cGAMP into neighboring cells and thus complements the cGAS or STING deficiency when mutant cell lines are cocultured (Ablasser et al., 2013b). Indeed, the sensitivity of this phenomenon to carbenoxolone treatment shown in the present work confirms the gap junction dependency. In the lungs of infected mice, macrophages have been reported to communicate immunomodulatory signals via  $\text{Ca}^{2+}$  waves using gap junctions as the conducting pathway (Westphalen et al., 2014). Future studies are needed to elucidate whether in vivo cGAMP-based intercommunication might also participate in modulating the immune response to *Mtb*.

It is interesting to note that cells infected by the HN878 strain, belonging to the W-Beijing lineage, but not by the H37Rv strain, benefited from the cGAS-STING knockout when analyzed for cell survival. This finding agrees with the literature, where a correlation between IFN- $\beta$  production and the virulence of W-Beijing strains has been established (Manca et al., 2001; 2005). Moreover, a recent investigation of the association between type I IFN production and bacterial virulence demonstrated a role for type I IFN in inducing the immunosuppressive cytokine IL-10 and in repressing the cytoprotective effect of IFN- $\gamma$  in *Mtb*-infected macrophages (McNab et al., 2014). These results are consistent with our data, which show both strongly suppressed production of IL-10 and enhanced macrophage survival in cGAS knockout and STING knockout cells.

*Mtb* also elicits inflammatory responses, an event that is not mediated by cGAS or STING but by the intracellular inflammasome complex. Interestingly, the inflammasome-mediated host response also relies on the presence of cytosolic DNA, which is sensed by AIM2 (Saiga et al., 2012; Hornung et al., 2009). We proved that deletion of AIM2 causes reduction of IL-1 $\beta$  production but that a significant inflammatory IL-1 $\beta$  signal is maintained via a functional NLRP3-dependent inflammasome system (Dorhoi et al., 2012).

When characterizing the cytokine signature of several mutated mycobacterial strains, we noticed that expression of type I IFNs correlated with the secretion of the ESX-1 substrate EsxA. Surprisingly, mutations compromising EsxA secretion (as in H37Ra) did not affect inflammasome activation in the same way, but instead shifted the *Mtb*-induced host response toward the selective production of IL-1 $\beta$ . It has been generally assumed that activation of the cGAS-STING-IFN-pathway and the inflammasome-IL-1 $\beta$ -pathway in response to virulent mycobacteria is coregulated and triggered by a common (unknown) mechanism mediated by ESX-1. Our work has now revealed that intracellular host recognition pathways can be stimulated differentially according to the level of EsxA secreted. Based on the results obtained, we propose the following molecular explanation. Strains H37Rv $\Delta$ RD1 and H37Rv $\Delta$ RD1 lack the genes for most of the ESX-1 secretion apparatus and its substrate EsxA, and therefore they generate no measurable intracellular

host response. EsxA is still produced by the *espA* and *espC* mutants and by H37Ra, but its secretion is not detectable (Chen et al., 2013; Fortune et al., 2005; Frigui et al., 2008). However, a small amount of EsxA may be released intracellularly by these bacteria, for instance by cell lysis, and this suffices to stimulate production of IL-1 $\beta$ . In other words, EsxA levels shift the host response either toward the detrimental cytokines (type I IFN and downstream effectors) or toward the beneficial IL-1 $\beta$ . In this sense, Solans et al. demonstrated that the reported degree of virulence of various *Mtb* strains in guinea pigs correlates with different levels of EsxA expression and secretion (Solans et al., 2014) (Palanisamy et al., 2008). In accordance with this explanation, W-Beijing strains, which secrete more EsxA (Solans et al., 2014), elicit higher levels of IP-10, as demonstrated in this work. This interpretation predicts that the specific expression of distinct cytokine classes can be achieved by manipulating the ESX-1 system. Indeed, we found that blocking EsxA secretion by pharmacological means significantly downregulates IFN expression yet still allows for robust production of IL-1 $\beta$ , as further discussed below.

Insight into the mechanism of ESX-1-regulated innate immune response is highly relevant for the development of vaccine adjuvants or immunotherapeutics. Effective live vaccines have to balance “harmlessness” with eliciting powerful and specific immune responses. In this respect it is interesting to note that the attenuated *Mtb*  $\Delta$ phoPR mutant, which serves as the candidate TB vaccine, MTBVAC (Arbues et al., 2013), displays greatly reduced secretion of EsxA (Frigui et al., 2008). One plausible reason for the advantageous efficacy of MTBVAC involves its ability to selectively trigger inflammatory cytokines and hence to bypass the pathological consequences of the type I IFN system. Alternatively, manipulating the IFN- $\beta$ -IL-1 regulatory cytokine network may represent a potential approach for the treatment of established *Mtb* infection (Mayer-Barber et al., 2014). Our finding that coregulation of the inflammasome-IL-1 $\beta$ -pathway and the cGAS-IFN- $\beta$ -pathway can be disconnected via manipulation of the mycobacterial ESX-1 secretory system could guide the development of a novel class of anti-TB drugs for use in conjunction with conventional chemotherapy. As proof of concept, our ex vivo data indicate that selective EsxA secretion inhibitors (BTP15 or BBH7) can shift the innate immune cytokine profile effectively toward the host-beneficial, antimicrobial IL-1 $\beta$  direction. The experimental design, which involved pre-treatment of the bacilli with BTP15 or BBH7 and thus preventive depletion of EsxA, did not allow any reduction of IL-1 $\beta$  to be observed, despite this being partly AIM2/DNA dependent. We reason that intracellular *Mtb* multiplication was associated with de novo secretion of EsxA. However, the levels of EsxA did not reach those of the DMSO-treated bacteria, and we therefore observed a decrease in IP-10 while IL-1 $\beta$  remained unaffected. This confirms that wild-type levels of EsxA stimulate both type I IFN and IL-1 $\beta$ , whereas a decrease in EsxA secretion mainly affects type I IFN production while leaving the host-protective IL-1 $\beta$  response virtually intact. This is corroborated by knocking down EsxA secretion by genetic means in the *espA* and *espC* mutants. In the latter cases, the amount of secreted EsxA is undetectable in vitro, and this is reflected in an even greater impact on IP-10 and IL-1 $\beta$  as compared to chemical inhibition. Importantly, the data obtained with BTP15 and BBH7 directly correlate

with their level of protection of *Mtb*-infected fibroblasts, as demonstrated recently (Rybníček et al., 2014). Future investigations will be required to see whether such a host-directed anti-TB treatment may also prove to be successful in an in vivo infection model.

## EXPERIMENTAL PROCEDURES

### Reagents and Plasmids

DNA oligonucleotides corresponding to the 90 bp long dsDNA (sense sequence, 5'-TACAGATCTACTAGTGATCTATGACTGATCTGTACATGATCTACATACAGATCTACTAGTGATCTATGACTGATCTGTACATGATCTACA-3') were obtained from Metabion and annealed in PBS. 5'-triphosphate RNA was prepared as previously described (Schlee et al., 2009). PMA (Phorbol 12-myristate 13-acetate), coelenterazine, chloroquine, carbenoxolone, and DAPI were obtained from Sigma-Aldrich. Cyclic di-AMP and cGAMP (2'-5') were obtained from Biolog. Expression plasmids for YybT and DacA (Rv3586) were kind gifts from Professor Zhao-Xun Liang (School of Biological Sciences, Nanyang Technological University) and Professor Guangchun Bai (Center for Immunology and Microbial Disease, Albany Medical College), respectively. An expression plasmid coding for human GFP-tagged cGAS was previously described (Ablasser et al., 2013b). Expression plasmids coding for murine STING and human STING are based on pEFBOS (Ablasser et al., 2013a).

### CRISPR/CAS9-Mediated Knockout Cell Line Generation

THP-1 cells were coelectroporated with a gRNA- and a mCherry-Cas9-expression plasmid as described (Schmid-Burgk et al., 2014). The gRNA target sequences used were GAACCTTCCCGCCTTAGGCAGGG (cGAS), TCCATCCATCCCGTGTCCAGGG (STING), GCTGGAGAACCTGACCGCCGAGG (ASC), and TTTGGCAAAACGCTCTCAGGAGG (AIM2). After FACS enrichment of mCherry-Cas9-positive cells, monoclones were grown out for 2 weeks and were genotyped using deep sequencing as described. For each target gene, two clones bearing all-allelic frameshift mutations were expanded for further study.

### Cell Line Generation by Lentiviral Transduction

The method for lentivirus-based expression of cGAS-Flag and GFP-Flag in cGAS mutated THP-1 cells was performed according to the standard protocol (Barde et al., 2010). Stable cGAS- or GFP-expressing cell lines were generated under puromycin selection.

### Cell Culture

HEK293T cells were cultured in DMEM and human macrophages (CD14<sup>+</sup> cells differentiated with GM-CSF [20 ng/ml]), and PMA-activated THP-1 cells were cultured in RPMI1640, both supplemented with 10% (v/v) FCS, sodium pyruvate (all Life Technologies), and Ciprofloxacin (Bayer Schering Pharma). BMDMs were generated using L929-cell-conditioned medium (LCCM) as a source of granulocyte/macrophage colony stimulating factor. cGAS<sup>-/-</sup> mice were generated in the laboratory of Charles M. Rice (Schoggins et al., 2014). For the generation of human macrophages, PBMCs were obtained by Ficoll-Hypaque density gradient centrifugation, and CD14<sup>+</sup> cells were isolated by MACS using the CD14<sup>+</sup> cell isolation kit (Miltenyi Biotech) according to the manufacturer's instructions. Buffy coats were obtained from the blood transfusion center (Centre de Transfusion Interrégionale, Croix Rouge Suisse), and the experiments were approved by the Office Ethical Committee (Commission Cantonale D'éthique de la Recherche) with the authorization number 107/15.

### Cell Stimulation and Transient Transfection

Murine BMDMs (1 × 10<sup>6</sup>/ml), THP-1 cells (1 × 10<sup>6</sup>/ml), and human macrophages (1 × 10<sup>6</sup>/ml) were transfected using Lipofectamine 2000 (Invitrogen) according to the manufacturer's instructions. HEK293T cells (2 × 10<sup>5</sup>/ml) were transfected using GeneJuice (Novagen) according to the manufacturer's instructions. DsDNA and 5'-triphosphate RNA were transfected at a final concentration of 1.33 μg/ml. CDNs were transfected at a final concentration of 2 μg/ml.

### Bacterial Strains and Culture Conditions

*Mtb* strains (described in Table S1) were grown at 37°C in 7H9 medium (Difco) supplemented with 0.2% glycerol, 0.05% Tween 80, and 10% albumin-dextrose-catalase (ADC, Middlebrook) or on 7H10 plates supplemented with 0.5% glycerol and 10% oleic acid-albumin-dextrose-catalase (OADC, Middlebrook). Kanamycin (20 μg/ml) and hygromycin (50 μg/ml) were used when necessary.

### Preparation of *Mycobacterium tuberculosis* Cultures for Cell Infection

Bacteria were grown to exponential phase (optical density at 600 nm, OD<sub>600</sub>, between 0.4 and 0.8), washed once in 7H9 medium, resuspended in 7H9 to an OD<sub>600</sub> of 1, equivalent to 3 × 10<sup>8</sup> bacteria/ml. The required volume of *Mtb* bacterial suspension was then added to RPMI1640 or DMEM for infection of human THP-1 cells or mouse BMDM, respectively, at the multiplicity of infection (moi) reported in the text. Plates were sealed with gas-permeable sealing film and incubated at 37°C under 5% CO<sub>2</sub>.

### Cell Viability Assay

CellTiter-Blue Assay (Promega) was performed according to the manufacturer's instructions.

### Immunofluorescence Microscopy

THP-1 cells were activated with 100 ng/ml PMA and seeded on coverslips in 24-well plates. Cells were then either transfected with the indicated nucleic acids, CDNs, or infected with *Mtb* for indicated time periods. After incubation cells were fixed with 4% formaldehyde in PBS for 20 min at 25°C. Cells were then blocked and permeabilized in blocking buffer (2% BSA, 0.2% Triton X-100 in PBS) for 30 min. Cells were stained with anti-Flag (Sigma), anti-Beclin-1 (Cell Signaling), anti-ASC (Santa Cruz), Texas Red anti-rabbit, and Alexa Fluor 488 anti-mouse antibodies (Life Technologies) for 1 hr at 25°C. Imaging was performed using the Zeiss Axioplan fluorescence microscope.

### Immunoblotting

Cells were lysed in 1× Laemmli buffer and denatured at 95°C for 5 min. Cell lysates were separated by 10% SDS-PAGE and transferred onto nitrocellulose membranes. Blots were incubated with anti-STING (Cell Signaling), anti-MB21D1 (anti-cGAS, Sigma-Aldrich), anti-β-actin-HRP, and anti-rabbit-IgG-HRP (both Santa Cruz Biotechnology).

### Luciferase Reporter Assays

HEK293T cells (2 × 10<sup>4</sup> cells in each well of a 96-well plate) were transiently transfected with 25 ng IFN-β promoter reporter plasmid (pIFN-β-Gluc) in conjunction with expression vectors as indicated using GeneJuice (Novagen). cGAS was used to induce cGAMP production, and DacA was used to induce cyclic di-AMP production within HEK293T cells upon transient overexpression. Luciferase activity was assessed in the supernatants 14–20 hr posttransfection with coelenterazine (2.2 μM) as substrate.

### ELISA

Cell culture supernatants were removed from infected or transfected cells after 24 hr. In the case of infection, supernatants were filtered through NANOSEP centrifugal devices (Life Sciences) and assayed for mouse IP-10 (R&D Systems), human IP-10, IL-1β, TNF-α, IL-10 (BD Biosciences), and IFN-β (PBL Interferon Source) according to the manufacturer's instructions.

### Analysis of Murine Type I IFN Production via Bioassay

Mouse type I IFN levels were determined by incubating LL171 cells with supernatants from infected BMDMs for 4 hr. Luciferase activity was measured, and type I IFN levels were calculated using a dilution series of the standard.

### qPCR

RNA from cells was reverse transcribed using the RevertAid First Strand cDNA Synthesis kit (Fermentas), and quantitative PCR analysis was performed on an ABI 7900HT. All gene expression data are presented as relative expression to GAPDH. The sequences were as follows: GAPDH forward, 5'-GAGTCAACG GATTGGTCGT-3'; GAPDH reverse, 5'-GACAAGCTTCCGCTTCTCAG-3'.



IFNB1 forward, 5'-CAGCATCTGCTGGTTGAAGA-3'; IFNB1 reverse, 5'-CAT TACCTGAAGGCCAAGGA-3'; IFIT2 forward, 5'-GCGTGAAGAAGGTGAAG AGG-3'; and IFIT2 reverse, 5'-GCAGGTAGGCATTGTTGGT-3'.

#### SUPPLEMENTAL INFORMATION

Supplemental Information includes six figures and one table and can be found with this article at <http://dx.doi.org/10.1016/j.chom.2015.05.003>.

#### AUTHOR CONTRIBUTIONS

R.W., M.F.G., C.S., S.G.P., Y.L., J.R., and A.A. performed experiments. R.W., M.F.G., C.S., Y.L., J.R., A.A., and S.T.C. designed experiments and analyzed the data. J.L.S.-B., T.S., and V.H. developed the CRISPR/Cas9 targeting strategy. R.W., M.F.G., C.S., S.T.C., and A.A. wrote the manuscript with input and approval from all authors. S.T.C. and A.A. supervised the project.

#### ACKNOWLEDGMENTS

We thank J. Chen, D. Bottai, and R. Brosch for providing strains and A. Roers and J. Schoggins for knockout mice. This work was supported by the Swiss National Science Foundation (grant numbers 31003A\_159836 [A.A.] and 31003A\_140778 [S.T.C.]) and by the Else Kröner-Fresenius-Stiftung (grant number 2014\_A250 [A.A.]). J.R. and S.T.C. are named inventors on a patent pertaining to this work.

Received: December 2, 2014

Revised: March 2, 2015

Accepted: April 15, 2015

Published: June 2, 2015

#### REFERENCES

- Ablasser, A., Goldeck, M., Cavar, T., Deimling, T., Witte, G., Röhl, I., Hopfner, K.P., Ludwig, J., and Hornung, V. (2013a). cGAS produces a 2'-5'-linked cyclic dinucleotide second messenger that activates STING. *Nature* **498**, 380–384.
- Ablasser, A., Schmid-Burgk, J.L., Hemmerling, I., Horvath, G.L., Schmidt, T., Latz, E., and Hornung, V. (2013b). Cell intrinsic immunity spreads to bystander cells via the intercellular transfer of cGAMP. *Nature* **503**, 530–534.
- Arbues, A., Aguiló, J.I., Gonzalo-Asensio, J., Marinova, D., Uranga, S., Puentes, E., Fernandez, C., Parra, A., Cardona, P.J., Vilaplana, C., et al. (2013). Construction, characterization and preclinical evaluation of MTBVAC, the first live-attenuated *M. tuberculosis*-based vaccine to enter clinical trials. *Vaccine* **31**, 4867–4873.
- Bai, Y., Yang, J., Zhou, X., Ding, X., Eisele, L.E., and Bai, G. (2012). *Mycobacterium tuberculosis* Rv3586 (DacA) is a diadenylate cyclase that converts ATP or ADP into c-di-AMP. *PLoS ONE* **7**, e35206.
- Barber, G.N. (2014). STING-dependent cytosolic DNA sensing pathways. *Trends Immunol.* **35**, 88–93.
- Barde, I., Salmon, P., and Trono, D. (2010). Production and titration of lentiviral vectors. *Curr. Protoc. Neurosci. Chapter 4*, Unit 4, 21.
- Berry, M.P., Graham, C.M., McNab, F.W., Xu, Z., Bloch, S.A., Oni, T., Wilkinson, K.A., Banchereau, R., Skinner, J., Wilkinson, R.J., et al. (2010). An interferon-inducible neutrophil-driven blood transcriptional signature in human tuberculosis. *Nature* **466**, 973–977.
- Bottai, D., Majlessi, L., Simeone, R., Frigui, W., Laurent, C., Lenormand, P., Chen, J., Rosenkrands, I., Huerre, M., Leclerc, C., et al. (2011). ESAT-6 secretion-independent impact of ESX-1 genes *espF* and *espG1* on virulence of *Mycobacterium tuberculosis*. *J. Infect. Dis.* **203**, 1155–1164.
- Burdette, D.L., Monroe, K.M., Sotelo-Troha, K., Iwig, J.S., Eckert, B., Hyodo, M., Hayakawa, Y., and Vance, R.E. (2011). STING is a direct innate immune sensor of cyclic di-GMP. *Nature* **478**, 515–518.
- Chen, J.M., Boy-Röttger, S., Dhar, N., Sweeney, N., Buxton, R.S., Pojer, F., Rosenkrands, I., and Cole, S.T. (2012). *EspD* is critical for the virulence-mediating ESX-1 secretion system in *Mycobacterium tuberculosis*. *J. Bacteriol.* **194**, 884–893.
- Chen, J.M., Zhang, M., Rybníček, J., Boy-Röttger, S., Dhar, N., Pojer, F., and Cole, S.T. (2013). *Mycobacterium tuberculosis* *EspB* binds phospholipids and mediates *EsxA*-independent virulence. *Mol. Microbiol.* **89**, 1154–1166.
- Collins, A., Cai, H., Li, T., Franco, L., Li, X.-D., Nair, V., Scham, C., Stamm, C., Levine, B., Chen, Z., et al. (2015). Cyclic GMP-AMP synthase is an innate immune sensor of *Mycobacterium tuberculosis* DNA. *Cell Host Microbe* **17**, this issue, 820–828.
- Dorhoi, A., Nouailles, G., Jörg, S., Hagens, K., Heinemann, E., Pradl, L., Oberbeck-Müller, D., Duque-Correa, M.A., Reece, S.T., Ruland, J., et al. (2012). Activation of the NLRP3 inflammasome by *Mycobacterium tuberculosis* is uncoupled from susceptibility to active tuberculosis. *Eur. J. Immunol.* **42**, 374–384.
- Fortune, S.M., Jaeger, A., Sarracino, D.A., Chase, M.R., Sasseti, C.M., Sherman, D.R., Bloom, B.R., and Rubin, E.J. (2005). Mutually dependent secretion of proteins required for mycobacterial virulence. *Proc. Natl. Acad. Sci. USA* **102**, 10676–10681.
- Fremond, C.M., Togbe, D., Doz, E., Rose, S., Vasseur, V., Maillet, I., Jacobs, M., Ryffel, B., and Quesniaux, V.F. (2007). IL-1 receptor-mediated signal is an essential component of MyD88-dependent innate response to *Mycobacterium tuberculosis* infection. *J. Immunol.* **179**, 1178–1189.
- Frigui, W., Bottai, D., Majlessi, L., Monot, M., Josselin, E., Brodin, P., Garnier, T., Gicquel, B., Martin, C., Leclerc, C., et al. (2008). Control of *M. tuberculosis* ESAT-6 secretion and specific T cell recognition by PhoP. *PLoS Pathog.* **4**, e33.
- Gao, D., Wu, J., Wu, Y.T., Du, F., Aroh, C., Yan, N., Sun, L., and Chen, Z.J. (2013). Cyclic GMP-AMP synthase is an innate immune sensor of HIV and other retroviruses. *Science* **341**, 903–906.
- Hornung, V., Ablasser, A., Charrel-Dennis, M., Bauernfeind, F., Horvath, G., Caffrey, D.R., Latz, E., and Fitzgerald, K.A. (2009). AIM2 recognizes cytosolic dsDNA and forms a caspase-1-activating inflammasome with ASC. *Nature* **458**, 514–518.
- Kurenuma, T., Kawamura, I., Hara, H., Uchiyama, R., Daim, S., Dewamitta, S.R., Sakai, S., Tsuchiya, K., Nomura, T., and Mitsuyama, M. (2009). The RD1 locus in the *Mycobacterium tuberculosis* genome contributes to activation of caspase-1 via induction of potassium ion efflux in infected macrophages. *Infect. Immun.* **77**, 3992–4001.
- Lechartier, B., Rybníček, J., Zumla, A., and Cole, S.T. (2014). Tuberculosis drug discovery in the post-post-genomic era. *EMBO Mol. Med.* **6**, 158–168.
- Liang, Q., Seo, G.J., Choi, Y.J., Kwak, M.J., Ge, J., Rodgers, M.A., Shi, M., Leslie, B.J., Hopfner, K.P., Ha, T., et al. (2014). Crosstalk between the cGAS DNA sensor and Beclin-1 autophagy protein shapes innate antimicrobial immune responses. *Cell Host Microbe* **15**, 228–238.
- Manca, C., Tsenova, L., Bergtold, A., Freeman, S., Tovey, M., Musser, J.M., Barry, C.E., 3rd, Freedman, V.H., and Kaplan, G. (2001). Virulence of a *Mycobacterium tuberculosis* clinical isolate in mice is determined by failure to induce Th1 type immunity and is associated with induction of IFN- $\alpha$ /beta. *Proc. Natl. Acad. Sci. USA* **98**, 5752–5757.
- Manca, C., Tsenova, L., Freeman, S., Barczak, A.K., Tovey, M., Murray, P.J., Barry, C., and Kaplan, G. (2005). Hypervirulent *M. tuberculosis* W/Beijing strains upregulate type I IFNs and increase expression of negative regulators of the Jak-Stat pathway. *J. Interferon Cytokine Res.* **25**, 694–701.
- Manzanillo, P.S., Shiloh, M.U., Portnoy, D.A., and Cox, J.S. (2012). *Mycobacterium tuberculosis* activates the DNA-dependent cytosolic surveillance pathway within macrophages. *Cell Host Microbe* **11**, 469–480.
- Mayer-Barber, K.D., Andrade, B.B., Barber, D.L., Hieny, S., Feng, C.G., Caspar, P., Oland, S., Gordon, S., and Sher, A. (2011). Innate and adaptive interferons suppress IL-1 $\alpha$  and IL-1 $\beta$  production by distinct pulmonary myeloid subsets during *Mycobacterium tuberculosis* infection. *Immunity* **35**, 1023–1034.
- Mayer-Barber, K.D., Andrade, B.B., Oland, S.D., Amaral, E.P., Barber, D.L., Gonzales, J., Derrick, S.C., Shi, R., Kumar, N.P., Wei, W., et al. (2014). Host-directed therapy of tuberculosis based on interleukin-1 and type I interferon crosstalk. *Nature* **511**, 99–103.

- McNab, F.W., Ewbank, J., Howes, A., Moreira-Teixeira, L., Martirosyan, A., Ghilardi, N., Saraiva, M., and O'Garra, A. (2014). Type I IFN induces IL-10 production in an IL-27-independent manner and blocks responsiveness to IFN- $\gamma$  for production of IL-12 and bacterial killing in Mycobacterium tuberculosis-infected macrophages. *J. Immunol.* **193**, 3600–3612.
- Mishra, B.B., Moura-Alves, P., Sonawane, A., Hachon, N., Griffiths, G., Moita, L.F., and Anes, E. (2010). Mycobacterium tuberculosis protein ESAT-6 is a potent activator of the NLRP3/ASC inflammasome. *Cell. Microbiol.* **12**, 1046–1063.
- O'Garra, A., Redford, P.S., McNab, F.W., Bloom, C.I., Wilkinson, R.J., and Berry, M.P. (2013). The immune response in tuberculosis. *Annu. Rev. Immunol.* **31**, 475–527.
- Palanisamy, G.S., Smith, E.E., Shanley, C.A., Ordway, D.J., Orme, I.M., and Basaraba, R.J. (2008). Disseminated disease severity as a measure of virulence of Mycobacterium tuberculosis in the guinea pig model. *Tuberculosis (Edinb.)* **88**, 295–306.
- Pym, A.S., Brodin, P., Brosch, R., Huerre, M., and Cole, S.T. (2002). Loss of RD1 contributed to the attenuation of the live tuberculosis vaccines Mycobacterium bovis BCG and Mycobacterium microti. *Mol. Microbiol.* **46**, 709–717.
- Rao, F., See, R.Y., Zhang, D., Toh, D.C., Ji, Q., and Liang, Z.X. (2010). YybT is a signaling protein that contains a cyclic dinucleotide phosphodiesterase domain and a GGDEF domain with ATPase activity. *J. Biol. Chem.* **285**, 473–482.
- Reed, M.B., Gagneux, S., Deriemer, K., Small, P.M., and Barry, C.E., 3rd. (2007). The W-Beijing lineage of Mycobacterium tuberculosis overproduces triglycerides and has the DosR dormancy regulon constitutively upregulated. *J. Bacteriol.* **189**, 2583–2589.
- Rybniiker, J., Chen, J.M., Sala, C., Hartkoorn, R.C., Vocat, A., Benjak, A., Boy-Röttger, S., Zhang, M., Székely, R., Greff, Z., et al. (2014). Anticytolytic screen identifies inhibitors of mycobacterial virulence protein secretion. *Cell Host Microbe* **16**, 538–548.
- Saiga, H., Kitada, S., Shimada, Y., Kamiyama, N., Okuyama, M., Makino, M., Yamamoto, M., and Takeda, K. (2012). Critical role of AIM2 in Mycobacterium tuberculosis infection. *Int. Immunol.* **24**, 637–644.
- Schlee, M., Roth, A., Hornung, V., Hagmann, C.A., Wimmenauer, V., Barchet, W., Coch, C., Janke, M., Mihailovic, A., Wardle, G., et al. (2009). Recognition of 5' triphosphate by RIG-I helicase requires short blunt double-stranded RNA as contained in panhandle of negative-strand virus. *Immunity* **31**, 25–34.
- Schmid-Burgk, J.L., Schmidt, T., Gaidt, M.M., Pelka, K., Latz, E., Ebert, T.S., and Hornung, V. (2014). OutKnocker: a web tool for rapid and simple genotyping of designer nuclease edited cell lines. *Genome Res.* **24**, 1719–1723.
- Schoggins, J.W., MacDuff, D.A., Imanaka, N., Gainey, M.D., Shrestha, B., Eitson, J.L., Mar, K.B., Richardson, R.B., Ratushny, A.V., Litvak, V., et al. (2014). Pan-viral specificity of IFN-induced genes reveals new roles for cGAS in innate immunity. *Nature* **505**, 691–695.
- Solans, L., Aguiló, N., Samper, S., Pawlik, A., Frigui, W., Martín, C., Brosch, R., and Gonzalo-Asensio, J. (2014). A specific polymorphism in Mycobacterium tuberculosis H37Rv causes differential ESAT-6 expression and identifies WhiB6 as a novel ESX-1 component. *Infect. Immun.* **82**, 3446–3456.
- Stanley, S.A., Johndrow, J.E., Manzanillo, P., and Cox, J.S. (2007). The Type I IFN response to infection with Mycobacterium tuberculosis requires ESX-1-mediated secretion and contributes to pathogenesis. *J. Immunol.* **178**, 3143–3152.
- Stoop, E.J., Bitter, W., and van der Sar, A.M. (2012). Tubercle bacilli rely on a type VII army for pathogenicity. *Trends Microbiol.* **20**, 477–484.
- Sun, L., Wu, J., Du, F., Chen, X., and Chen, Z.J. (2013). Cyclic GMP-AMP synthase is a cytosolic DNA sensor that activates the type I interferon pathway. *Science* **339**, 786–791.
- Watson, R.O., Bell, S.L., MacDuff, D.A., Kimmey, J.M., Diner, E.J., Olivas, J., Vance, R.E., Stallings, C.L., Virgin, H.W., and Cox, J.S. (2015). The cytosolic sensor cGAS detects Mycobacterium tuberculosis DNA to induce type I interferons and activate autophagy. *Cell Host Microbe* **17**, this issue, 811–819.
- Westphalen, K., Gusarova, G.A., Islam, M.N., Subramanian, M., Cohen, T.S., Prince, A.S., and Bhattacharya, J. (2014). Sessile alveolar macrophages communicate with alveolar epithelium to modulate immunity. *Nature* **506**, 503–506.
- Woodward, J.J., Iavarone, A.T., and Portnoy, D.A. (2010). c-di-AMP secreted by intracellular Listeria monocytogenes activates a host type I interferon response. *Science* **328**, 1703–1705.





# Acknowledgement

I would like to take this opportunity to express my deepest gratitude to those who have given me help, advice, and those who have contributed to the realization of this thesis.

First of all, I thank my supervisor, Prof. Stewart Cole, who accepted me as a PhD student in his group to work on the challenging and exciting ESX-1 secretion system of *M. tb*. He discussed with me about the problems, inspired me and gave me enough freedom to try out my own ideas. He was particularly patient with me even when the progress was delayed. Without his guidance, encouragement and support, I would not have been able to complete my research. I also thank him for the time he spent correcting my research manuscript and PhD thesis.

I feel lucky that each time when I was frustrated and hesitated to give up, there was always a lab colleague to help me through the tough moment. I thank Dr. Jeffery Chen who sparked my interest on EspC. He showed me the potential significance of this protein to the ESX-1. When he left the lab, he provided me with some strains and plasmids which are useful throughout my project. His previous work on EspA/C/D also provided the insights into their roles in ESX-1, which has inspired me a lot. The cross-disciplinary nature of my work on *M. tb* could not be achieved without the help from Dr. Claudia Sala. When I fell into a difficulty of my first year's work on protein purification, she trained me in the basic skills of working with *M. tb*, a Biosafety 3 level pathogen. Since then my research scope has been much broadened, extended from protein chemistry to molecular microbiology. Dr. Jan Rybníček was the first person who questioned that EspC might be an outer membrane pore-forming protein, when I was still confused by the ladder-like bands on the western blot of culture filtrate sample. His insights and suggestions are critical for me to define a clear direction. I deeply thank him for sharing his knowledge and the guidance.

My research also benefitted immensely from the help of Dr. Andrej Benjak- the

bioinformatician from our lab, Prof. Graham Knott and Dr. Davide Demurtas from the EPFL Bioelectron Microscopy Core Facility, and Dr. Diego Chiappe from the EPFL Proteomics Core Facility. I am also grateful to Dr. Jérémie Piton, Dr. Florence Pojer and Dr. Andréanne Lupien for the discussions and help during troubleshooting. I thank Stefanie Boy-Röttger, Philippe Busso and Anthony Vocat for the technical assistance and lab maintenance. I would also like to express my gratitude to the former and present lab secretaries Suzanne Lamy and Cécile Prébandier.

Thanks to all UPCOLers, they make my time in the Cole's lab a pleasant experience. I also appreciate the thesis feedbacks, corrections and abstract translation by Andréanne, Andrej, Caroline, Charlotte, Claudia, Florence, Jérémie in the lab, as well as Dr. Alfred Chng from the Lemaitre lab.

Finally, despite being the only child in the family, I have decided to pursue science far away from home. Therefore, I give my heartily thanks to my parents, for their understanding, support, and love.

# Ye Lou

**Nationality:** China

**Gender:** Female

**Language:** Chinese, English, German (entry level)

**Mobile:** 41-786259219

**Email:** ye.lou@epfl.ch

## Education

**PhD candidate - École polytechnique fédérale de Lausanne (EPFL, Switzerland)**

Thesis topic: *Structural and functional of characterization of the mycobacterial ESX-1 secretion system*

Prof. Stewart.Cole's group, Global Health Institute, EPFL

05/2012 – 07/2016

**Master's Degree of Chemistry and Bioscience,  
Chalmers University of Technology (Sweden)**

Thesis topic: *Investigation of the cargo recognition step in peroxisomal import*

Prof. Matthias Wilmanns's group, **European Molecular Biology Laboratory (EMBL, Germany)**

Graduated: 11/2011

**Master's Degree of Microbiology minor in Biotechnology,  
Sun Yat-sen University (China)**

Thesis topic: *Isolation and screening of a marine strain 1701 and studies on its metabolite inhibiting multiple drug resistant bacteria*

Graduated: 06/2007

**Bachelor's Degree of Bioengineering,  
Hefei University of Technology (China)**

Graduated: 06/2005

## Employment History

**2007 – 2009    National Institutes for Food and Drug Control, China**

## **Publications**

Lou Y, Rybniker J, Sala C, Cole ST. EspC forms a filamentous structure in the cell envelope of *Mycobacterium tuberculosis* and effects ESX-1 secretion. Under submission.

Wassermann R, Gulen MF, Sala C, Perin SG, Lou Y, Rybniker J, Schmid-Burgk JL, Schmidt T, Hornung V, Cole ST, Ablasser A (2015), *Mycobacterium tuberculosis* Differentially Activates cGAS- and Inflammasome-Dependent Intracellular Immune Responses through ESX-1. ***Cell Host Microbe***. 17(6): 799-810.

Fodor K, Wolf J, Reglinski K, Passon DM, Lou Y, Schliebs W, Erdmann R, Wilmanns M (2015), Ligand-induced compaction of the PEX5 receptor-binding cavity impacts protein import efficiency into peroxisomes. ***Traffic***. 16(1): 85-98.

## **Conferences / Poster Presentations**

**2012** 26th Regio Meeting on Biocrystallography

**2014** 9th International Conference on the Pathogenesis of Mycobacterial Infections

**2015** EMBO symposia - New Approaches and Concepts in Microbiology

